

GLO1097

MAGNETOTELLURIC SURVEY

in the

SODA LAKE AREA

of

NEVADA

for

CHEVRON RESOURCES

GEOTRONICS CORPORATION

10317 McKalla Place

Austin, Texas 78758

Darrell R. Word, Chief Scientist

David Halpin, Senior Geophysicist

Ken Owens, Geologist

Report No.

TABLE OF CONTENTS

<u>Section</u>	<u>Page No.</u>
I. Introduction	I-1
II. Data Displays and Discussion of Results	II-1
A. Introduction	II-1
B. Data Displays	II-1
1. Site Location Map	II-1
2. Resistivity Cross Section Based on One- Dimensional Inversions; Dip-Axis Directions	II-1
3. Correlation Cross Section Based on One- Dimensional Inversion	II-3
4. Three Dimensionality Indices	II-5
5. Anisotropy Factor and Anisotropy Sense Cross Sections	II-6
C. Discussion of Results	II-7
1. Resistivity Cross Section Based on One- Dimensional Inversions; Dip-Axis Directions	II-7
2. Correlation Cross Section Based on One- Dimensional Inversions	II-9
3. Three Dimensionality Indices	II-9
4. Anisotropy Factor and Anisotropy Sense Cross Sections	II-9
III. Conclusions and Recommendations	III-1
A. Conclusions	III-1
B. Recommendations	III-3
 Selected Bibliography	

APPENDICES

Appendix A - Field Operations

Appendix B - Data Processing Procedure

Appendix C - MT Analysis -- Defining Equations and Glossary of
Computed Quantities

Appendix D - MT Interpretation -- Defining Equations and Glossary
of Computed Quantities

Appendix E - Resolution

Appendix F - Data Smoothing and Comments on Noise and Special
Conditions

LIST OF PLATES

- | | |
|-----------|---|
| Plate 1.1 | Site Location Map |
| Plate 2.1 | Resistivity Cross Section Based on One-Dimensional Inversions; Dip-Axis Direction |
| Plate 3.1 | Correlation Cross Section Based on One-Dimensional Inversions |
| Plate 4.1 | Three-Dimensionality Indices - Tensor Impedence, Skew and Ellipticity |
| Plate 5.1 | Anisotropy Factor and Anisotropy Sense Cross Section |

I. Introduction

In late March, 1977 Geotronics Corporation conducted a Magneto-telluric Survey near Soda Lake, Nevada for Chevron Resources Company. The magneto-telluric data were to be utilized to further delineate the subsurface resistivity structures seen on a previous survey performed in 1975. Data were acquired employing a Geotronics Corporation MT system utilizing field digital recording. A full five component electromagnetic field measurement was made at each site in the frequency range 0.002 Hz to 250 Hz, and the complete tensor MT analysis was used. Data were processed in Austin, Texas with computer processing utilizing the Houston Based CDC 6600 with a remote terminal. Various displays of the MT results were produced for presentation in this report. The MT results at various sites were subsequently correlated and interpreted. Discussions of these correlations are included, followed by a series of conclusions and recommendations based upon the results. Also included in this report are Appendices A through F, which present additional information on field operations, data processing and modeling procedures, the mathematical definitions of the Magnetotelluric parameters, and an assessment of the data quality. For more detail concerning these items the reader is referred to Word, et al, (1970) and other literature.

Data quality throughout the area ranged from fair to poor. Data at sites 2 and 3 were poor whereas data at sites 1 and 4 were fair below 0.5 Hz and .1Hz, respectively.

II. Data Displays and Discussion

A. Introduction

For this report Geotronics Corporation has prepared a series of displays containing parameters derived from the magnetotelluric data. These displays are composite presentations of single site information and provide the basis for establishing correlations along the traverses. Each display presents a different parameter, or a different aspect of a parameter, and provides input towards the final interpretation. The displays will be described first followed by a discussion of the results obtained from the survey.

B. Data Displays

1. Site Location Map

The site map (Plate 1) shows MT site locations on a topographic base map. Section lines are illustrated, along which the vertical cross section information is displayed on the following plates. All vertical cross sections are scaled to the site map.

2. Resistivity Cross Section Based on One-Dimensional Inversions; Dip-Axis Directions

Plate 2.1 displays an interpreted true resistivity structure. For each site, a one-dimensional model inversion was done for the

RTE (f) apparent resistivity-frequency function (E parallel to strike), to produce a resistivity-depth function $R(z)$. An adaption of the Bostick inversion method (see Appendix D) was used to produce $R(z)$ as a continuous function, employing the "amplitude inversion" mode in all cases. In Plate 2.1 the vertical cross section is constructed as a composite of the $R(z)$ functions. Resistivity values are tabulated at discrete points on the depth scale and contoured on constant resistivity.

The models presented in Plate 2.1 and all MT models derived as a composite of the 1D model inversions should be viewed as estimates of the volume averaged or smoothed electrical structures, where the dimensions of the averaging volume are approximately proportional to depth. The depth coordinate in the models represents mean depth of the averaging volume. The resistivity and dip-axis angle values result from the net influence of the structure within the averaging volume. This averaging concept is not mathematically precise but offers a reasonable intuitive view of the smoothing influence.

Dip-Axis directions versus depth are shown in plan view above the resistivity section. The dip-axis direction is given by the angle $A(YZ)$ (See Appendix C) determined from the vertical magnetic field. The dip-axis represents the direction of maximum gradient in the electrical structure, with 180 degree ambiguity

(i. e. the polarity of the gradient is not given by this quantity), and is a line normal to the apparent strike vs. frequency. Dip-axis information is displayed at each site location on a polar plot with a radial logarithmic depth scale. The computed frequency-domain functions are plotted on the depth scale via a pseudo depth-frequency relationship $z(f)$ produced by the RTE inversion process (there is no precise one-to-one depth-frequency correspondence). The unsmoothed $A(YZ)$ data points and the 180 degree complements are plotted so that directional trends may be deduced from patterns in the scattered data. The degree of scatter in the dip-axis data depends on the degree of directional preference caused by the electrical structure. Tighter grouping indicates a stronger directional trend, whereas the scatter approaches 360 degrees for data where the degree of directional preference is small.

3. Correlation Cross Section Based on One Dimensional Inversions

Plate 3.1 displays the correlation section with the same information shown on both logarithmic and linear depth scales. This display is derived by first plotting the continuous 1-D resistivity inversion $R(z)$ data for each site on a resistivity-depth scale at each corresponding site location (similar to a bore-hole log correlation display). The $R(z)$ curves for both the "amplitude inversion" mode

(solid curve) and the "phase inversion" mode (dotted curve) are plotted in the display. The "amplitude inversion" mode of $R(z)$ is used in the correlation process. A layered sequence is interpreted at each site by assuming interfaces at the inflection points in the $R(z)$ function. Correlation lines through the inflection points are drawn from site to site, connecting associated features and signatures of the $R(z)$ functions along the traverse. In this manner, even small features that are close to the noise level of the sounding may be interpreted when site to site correlation can establish sufficient credibility.

It is noteworthy that the process up to the act of correlating sequences along the traverse is a precisely defined, purely analytical procedure, and the results are stable and unique for each measuring site within noise limitations. The correlation process, however, is more subjective and a solution is not necessarily unique. The correlation process is done with learned discretion by the interpreter and is constrained by other known geological and geophysical information, and by the requirement of compatibility with the total observed MT response, including anisotropic effects.

The process used recognizes relatively resistive or conductive units between inflection points of $R(z)$. The absolute value of resistivity is also considered in the correlation process;

but due to the smoothing effect in the MT response, the $R(z)$ value for a given structure is affected by the relative thickness of the structure as well as its intrinsic resistivity. It is also true that the intrinsic resistivity of a given rock type can change from one point to another with a change in the local conditions. The resistivity is therefore not expected to necessarily remain constant along a correlated unit.

The logarithmic depth scale is used to facilitate the correlation process and to display the results on a constant resolution scale. Since the minimum dimensions of a detectable unit are approximately proportional to its depth, a given size plot feature in one place on the scale is of comparable resolution to a feature of the same size in another place on the scale.

The correlation results are also presented on a linear depth scale to facilitate the physical interpretation.

4. Three Dimensionality Indices

Plate 4 displays the skew and ellipticity (ALPHA and BETA in Appendix C) of the tensor impedance, both of which range in magnitude from 0 to 1.0 and indicate the degree of three dimensionality present in the MT response. ALPHA = 0 and BETA = 0 are necessary and sufficient conditions for two dimensionality (including one dimensionality). Two dimensionality in the MT response means that

the electrical structure is symmetrical about some vertical plane that passes through the measuring site (including a two-dimensional structure). The dip-axis would lie in that vertical plane of symmetry. A non-zero value for ALPHA or BETA indicates three dimensionality, meaning there is not vertical plane of symmetry for the structure. In such case, the dip-axis still defines the axis of maximum change. Certain qualitative aspects of the structure can be deduced from the nature of the 3D indices, as discussed briefly in Appendix B and more fully in Word, et (1970).

In the display, the unsmoothed estimates of ALPHA and BETA are shown in a vertical section with logarithmic depth plots superimposed at each corresponding site location. The frequency domain 3-D indices are related to depth via the pseudo-frequency relationship $z(f)$ produced by the RTE inversion process.

5. Anisotropy Factor and Anisotropy Sense Cross Section

Plates 5.1 displays the anisotropy factor and anisotropy sense values (AF and AS in Appendix D) contoured on vertical cross sections. The frequency domain functions are referred to the depth scale via the pseudo depth-frequency relationship $z(f)$ from the RTE inversion.

The anisotropy factor, $AF = RTM/RTE$, is an indicator of lateral change in the structure. $AF = 1$ for a one-dimensional structure, and $AF \neq 1$ where lateral inhomogeneity (apparent anisotropy) exists.

As the MT sounding depth increases, AF changes only through depth ranges where a laterally anomalous horizon is encountered, and it remains otherwise constant at the value imparted by any shallower anomalies. A change in AF along a traverse line indicates a change in the structure at or above the level for which the change in AF is observed. Abrupt lateral changes, such as near surface vertical contacts, are characterized by steep or near vertical contours in AF.

The anisotropy sense (AS) is based on the change in AF with frequency (or depth). By the convention used herein, $AS = 0$ indicates one dimensionality, $AS > 0$ indicates a dominant resistive anomaly, and $AS < 0$ indicates a dominant conductive anomaly, for the frequency or depth range that is effective.

(A study and further development of the anisotropy factor and sense parameters is one of the current Geotronics R & D efforts. Because of some obvious features of interest, the AF and AS results are presented here as an experimental display, but without exhaustive treatment in this report).

C. Discussion of Results

1. Resistivity Cross Section Based on One-Dimensional Inversions; Dip-Axis Directions (Plate 2.1)

Plate 2.1 illustrates the contoured Resistivity Cross Section based on One-Dimensional Inversions for the four sites recorded in March 1977. (For reference, Site 1-3 of the original 1975 survey

would lie halfway between sites 1 and 2 of this cross section). The section is characterized, in general, by zones of low resistivity materials. Near surface resistive zones are present at sites 4, 3 and 1. A shallow conductive zone, on the order of 1-3 ohm-meters is pervasive at +2200 to +2800 feet. Below this, a thick zone of varying resistivity is present. This zone varies from about 6000 feet to 14,000 feet thick. Resistivities within the zone vary from 5 to 14 ohm meters. The higher resistivities are present in the northern portion of the line where the zone appears to be thickest. Immediately beneath this broad zone is the "deep" conductor. Resistivities range from 0.2 to 1.6 ohm meters. The surface described by this zone appears to shallow from -29,000 feet beneath site 1 to -8000 feet beneath site 3. At depth, below site 1 (-34,000 feet), and site 2 (-26,000 feet), the section again starts to become slightly more resistive.

The new data fits well with the original survey data. If site 1-3 of the original survey were plotted, only minor contour adjustment would be needed. That information would cause a shallowing of the deeper conductive contours between sites 1 and 2.

Dip-axis data are consistent along the traverse. These data show a N-S to N20E strike direction. Data from sites 3 and 4 are quite tight. Data at site 1 are moderately scattered and data at site 2 are very scattered.

2. Correlation Cross Section Based on One-Dimensional Inversions

Plate 3.1 illustrates the correlation base on one-dimensional inversions. Correlations across the area are consistent with the resistor-conductor sequence readily trackable. Notable are (1) the near surface resistive "kick", (2) the pervasive shallow conductor which exhibits minor resistive kicks, (3) the thick "resistive" zone, and (4) the "deep" conductor.

Trends in the correlation data indicate an apparent deepening to the northeast.

3. Three-Dimensionality Indices

Tensor impedance skew and ellipticity data are presented on Plate 4.1. The data indicate that beneath sites 4 and 2 uncoupled anomalies exist below 8000 feet and 10,000 feet respectively. This type of anomaly indicates the coincidence of two or more anomalies in different directions from the site (as opposed to seeing one anomaly through another). Beneath site 1 uncoupled anomalies exist from 0 - 1200 feet, 4500 - 10,000 feet and from 13,000 - 30,000 feet. Data at site 3 indicate high levels of both skew and ellipticity, indicating high three dimensionality, from 8000 to 12,000 feet beneath the site.

4. Anisotropy Factor and Anisotropy Sense Cross Sections

Plate 5.1 illustrates the anisotropy factor and anisotropy

sense information. The anisotropy factor data indicate that moderate to high levels of anisotropy exist. Lowest anisotropy is exhibited beneath site 1. Beneath sites 2 and 4 anisotropies range from 3-4. High anisotropy exists at shallow levels beneath site 3. Anisotropy values of 10 are present at +1500 feet.

The anisotropy sense section depicts a general conductive nature to the Section. A strong conductive anomaly is indicated at -9000 feet beneath site 3. Scattered resistive anomalies are indicated at various levels beneath sites 4, 2 and 1.

III. Conclusions and Recommendations

A. Conclusions

As a result of the additional magneto-telluric sites in the Soda Lake area the following can be concluded:

(1) The shallow conductive zone, called the Lower Lahontan Valley Group in the earlier report, persists to the Southwest. The more conductive portion, less than 2 ohm meters, exists beneath sites 2, 3 and 4 of this survey and beneath sites 1-1 through 1-5 and sites 1-7 through 1-9 of the original survey. Therefore a northern and eastern limit can be established for this less than 2 ohm-meter zone.

(2) The second zone down, that referred to as Tertiary rhyolites and volcanics in the original report, exhibits resistive

and conductive trends. The more resistive portion of the zone lies beneath sites 1 and 4 and beneath sites 1-3, 1-4, and 1-5 through 1-10. The conductive portion lies beneath sites 2 and 3 beneath sites 1-1 and 1-2. Thus, a northeasterly trend for the conductive portion is established by the sites. This conductive trend appears to pass through Soda Lake. This conductive trend may represent intensely altered rhyolites and volcanics in the Trukee Formation (?) of the original report and/or a fracture zone. Lineations of contours to the northeast of the survey area have the same orientation.

(3) The "deep" conductive zone, referred to as the magma chamber in the original report, shallows from the north to the vicinity of site 3 and from west to east. Lowest resistivities at or near this interface exist beneath sites 3 and 4 and beneath sites 1-1, 1-2 and 1-5. Beneath sites 1 and 2, and perhaps site 4, the resistivities appear to begin rising again, possibly indicating a "bottom". Thus, the data begin to define a shape and trend to this important conductive anomaly. The dominant trend is northeasterly through sites 3, 4 and 1-1 and 1-2. To the north the conductor may have a bottom implying the existence of an arm.

(4) The magneto-telluric method appears well suited for tracking anomalies in the Soda Lake area.

B. Recommendations

As a result of this survey we would recommend the following:

(1) If interest is in the shallow conductor, additional sites should be placed to the west to define its western limits;

(2) If interest is in the conductive portion of the Tertiary rhyolite and volcanic section, sites should be placed to the west and east of Soda Lake, and

(3) If interest is in further delineation of the deep conductor, with the assumptions that (a) the "arm" is real and (b) resistivity value is related to temperature gradient, then additional sites should be established. Location of these sites would have to be to the west and east of Soda Lake. Additional sites in the vicinity of site 1-5 would be needed to solve the question of why it is so conductive and "off-trend". Attempts at all sites should be made to record long enough to penetrate the "arm" of the conductor as at several sites it appears that the conductor was penetrated. As sites are located closer to the conductive "core" of the anomaly, longer recording time would be needed to penetrate the conductive "arm".

Appendix A - Field Operation

Five orthogonal component, surface EM field measurements (E_x , E_y , H_x , H_y , H_z) are made of the micropulsation fields at each site in the overall frequency range of approximately 0.002 to 250 Hz. This range was covered by five overlapping bands as described in Table B-1.

Figure A-1 shows the field sensor configuration used. The positive x-axis is directed to magnetic north, in a right-hand coordinate system. The E-field sensors are electrode lines using Cd-CdCl₂ or Pb electrodes with a usual spacing of 300 feet. The H-field sensors are Geotronics induction magnetometers - Model MTC-4SS for H_x and H_y , and Model MTC - 6SS for H_z . A vertical axis air core loop is also available for H_z where needed.

The instrument van contains the recording system of Geotronics manufacture, consisting of the MTE-4 three-channel E-field preamplifier, the MTH-4 three-channel H-field preamplifier, the MTC-2 calibrator, the MTF-16 filter-post amplifier, and the MTDR-2 digital recorder. A six-channel Brush chart recorder is used for field monitoring of the signals.

A five-man crew is used, consisting of the crew chief and instrument man, alternate instrument man, and a three-man site layout team including a surveyor.

Proper field technique, which is of extreme importance in MT recording, has been developed by Geotronics personnel through 16 years of MT experience and is stressed throughout the survey. System noise and data quality checks are made routinely. All sensors are buried about 12 inches or more deep and all cables buried or weighted to reduce wind noise and improve thermal stability. While one site is

being recorded, an alternate set of sensors is installed at the next site, and an adequate time (a few hours) is allowed for stabilization, including thermal and magnetic stabilization of the magnetometers and contact potential stabilization of the electrodes.

Field tapes are sent back to Geotronics daily (when conditions permit) so that preliminary analysis can be done to assess signal quality while the field crew is still in the survey area.

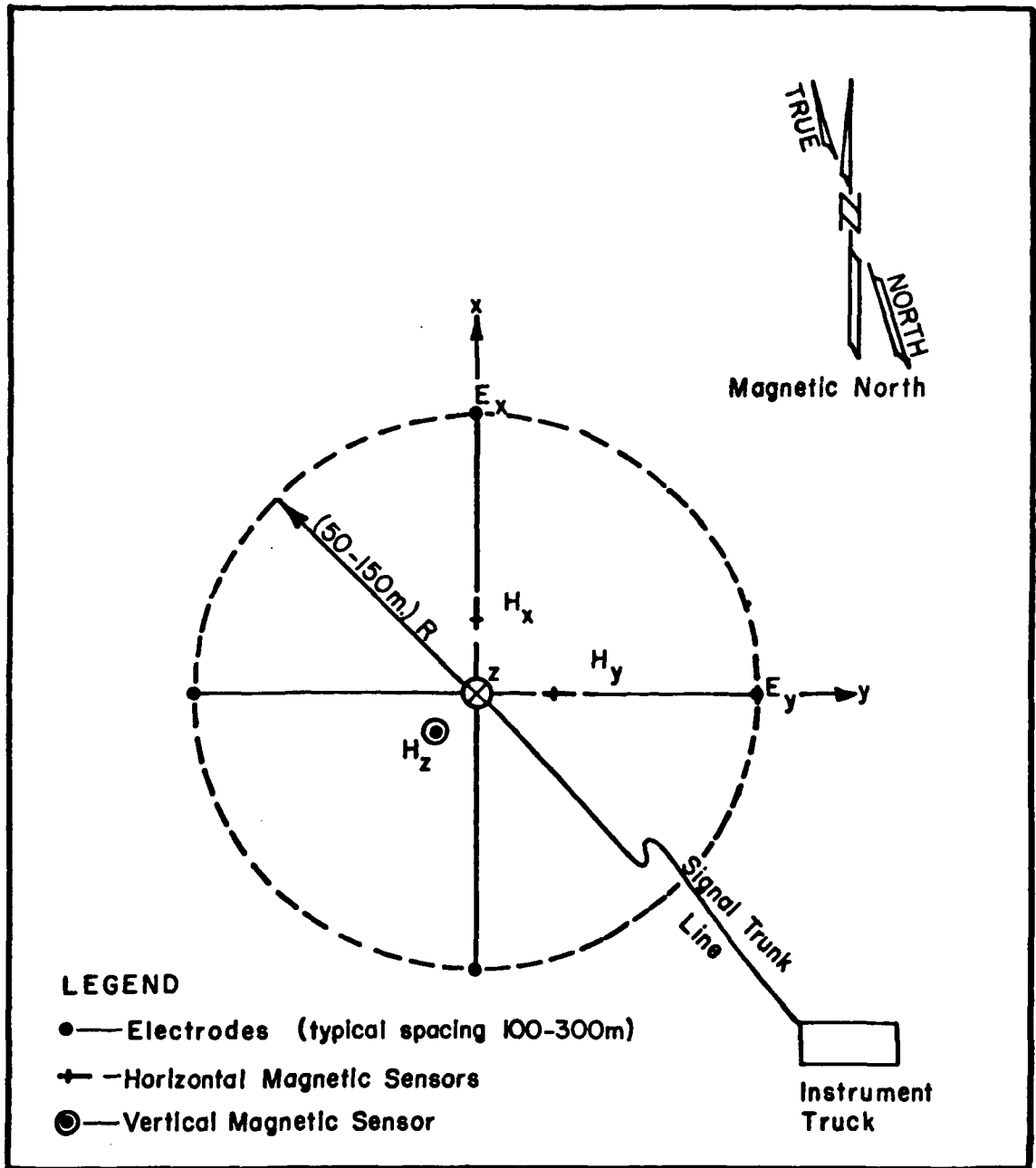


Fig. A-1: Magnetotelluric Field Sensor Layout.

PROPRIETARY INFORMATION NOTICE
 This document contains Geotronics Corporation proprietary and confidential information which is supplied for limited purposes only, and remains the property of Geotronics Corporation. This document may not be reproduced in whole or in part without written consent of Geotronics Corporation and the information therein must not be disclosed to persons not having need of such disclosure consistent with the License for which it is supplied. This document is to be returned to Geotronics Corporation upon termination of the License under which it is supplied.

Appendix B - Data Processing Procedure

The MT data processing, from field data through the final interpretation, is divided into two phases; (1) analysis and (2) interpretation. Mathematical definitions for the two phases are outlined in Appendices C and D respectively.

The field data represents a measurement of the total vector E and H fields (electric and magnetic fields respectively) on the surface at the measuring site. The basic output of phase (1) is a set of tensor quantities that totally and uniquely express the surface E and H field interrelationship at the point of the measuring site. With $[\bar{E}]$ and $[\bar{H}]$ representing horizontal vector fields (there is no vertical E at the surface), the basic field relationships can be expressed by the frequency domain matrix equations,

$$[\bar{E}] = [Z] [\bar{H}] \quad (B-1)$$

$$\text{and } [H_z] = [k_z] [\bar{H}] \quad (B-2)$$

where the tensors $[Z]$ (surface impedance) and $[k_z]$ are, within noise limitations, a function of only the subsurface electrical structure, and they contain all of the MT information available at the site. The same information is, however, expressed in other forms (see Appendix C) for convenience. The analysis results are obtained for all measuring sites, which should represent a spatial sampling of the structure being investigated.

The phase (2) objective is to interpret the set of $[Z]$ and $[k_z]$ functions for all sites (as sampled functions of frequency and space on the surface) in terms of the subsurface structure. The interpretation phase is essentially an open ended problem because of limitations

due to noise, finite sampling of the data, and lack of precise analytical solutions for 3-D geometry. The interpretation must be done by approximate modeling solutions and must deal with a certain degree of non-uniqueness imposed by the limitations mentioned. The non-uniqueness, which occurs in varying degrees depending on the problem, gives rise to the fact that the best interpretation is obtained by use of all available geological and geophysical information to constrain the process. Ideally, the approach is to choose the overlap or domain of compatibility between sets of acceptable models for the MT and other data, thereby reducing the number of possible models. In practice non-uniqueness does not uniformly affect all aspects of the model, which usually has some aspects that are well determined and some that are not. The 1-D resistivity-depth profile, for example, normally has a faithful stratigraphic sequence, while the depth and/or true resistivity of a given unit may be uncertain to some degree.

The standard modeling procedure (See Appendix D) produces for each site an estimate of the (1) continuous, one-dimensional, true resistivity-depth function $R(z)$ and a pseudo depth-frequency correspondence, $z(f)$, (2) the dip-axis direction $A(YZ)$ as a function of depth, z , (3) the anisotropy indices AF and AS as a function of depth, and (4) the 3-D indices, $ALPHA$ and $BETA$ as a function of depth. Assemblages of the one-dimensional functions are produced to represent the volume averaged or smoothed 3-D electrical structure. More complicated models are then applied to refine portions of the first model if justified by need and economics for a given case.

Finally, the geological interpretation is done, if requested, using all MT information and other control information available.

Computer processing is done on the Control Data Corporation Cybernet System. The Houston based CDC6600 is used and accessed

through the CDC-Austin user terminal. Field tapes are sent to Houston and stored in the CDC tape library in read-only mode for the duration of the survey and analysis.

The frequency bands used in the analysis are given in Table B-1, which includes the sampling parameters and the frequency range of results used for each band. The upper limit on the frequency range used is near the alias filter cut-off frequency, which is set to approximately half the Nyquist frequency. The lower three frequency points of the analysis results are omitted to avoid truncation aliasing error that is apt to be present. The analysis frequency bands overlap for redundancy.

Strip chart records and field logs are checked to select the best data recording runs for analysis. Initially, one run of each band for each site is processed and the results checked for several acceptance criteria. Additional runs are processed where needed to produce the best definition of the computed functions. Finally, all runs of the frequency domain results to be used are plotted for use in the subsequent interpretation. Averaged and smoothed functions are produced from the raw results for use in modeling and other interpretation. All data is corrected for local magnetic declination so that all subsequent results can be presented in geographic coordinates.

Table B-1 - Recording Frequency Bands

Band	Post Filter (Hz)	Sampling Rate (Hz)	Number Samples	Frequency Range Used (Hz)	No. Runs Recorded (Nominal)
B6	10-256	1000	4096	2.08-256	4
B5	1-25	100	4096	0.208-25.6	4
B4	0.1-5	20	4096	0.0415-5.12	4
B3	0.01-0.5	2	4096	0.00415-0.512	1-2
B2	0.002-0.125	.5	2048	0.00208-0.128	1

Appendix C

MT Analysis -- Defining Equations and Glossary of Computed Quantities

I. MT Model and Basic Relationships

The total electric and magnetic fields E and H in the frequency (f) domain at point '0' on the earth surface are related by

$$[\bar{E}] = [Z] [\bar{H}] \quad (C-1)$$

$$\text{and } [H_z] = [k_z] [\bar{H}] \quad (C-2)$$

$$\text{or } [H_z] = [Y_z] [\bar{E}] \quad (C-3)$$

(excluding $f = 0$), and where

- (1) $[\bar{E}]$, $[\bar{H}]$, and $[H_z]$ are column vectors representing the horizontal E and H field components (with bar) and the vertical H field ($E_z = 0$, due to surface boundary conditions),
- (2) $[Z]$ is a dyadic tensor representing the surface impedance, relating the horizontal E and H fields, and
- (3) $[k_z]$, $[Y_z]$ are tensors relating H_z to the horizontal E and H fields, respectively.

$[Z]$ and $[k_z]$ or $[Y_z]$ represent all information present in the MT response for a given site. For an essentially plane wave source, they are functions only of frequency and the earth parameters.

Coordinate System (See Fig. C-1) --

The coordinate system is a standard right hand rectangular (x, y, z - axes) with $+z$ -down (vertical axis) with the origin at point

'0'. The x-axis is rotated clockwise (looking in +z direction) by an angle 'A' from the reference axes xr and yr (normally north and east, respectively). In the rotated coordinate system, all fields and computed tensor quantities are functions of the rotation angle 'A'.

Model --

$z \geq 0$ - semi-infinite conductive half space (solid earth) with a generally 3-D distribution of properties

$z < 0$ - free space

Field Source --

EM plane wave propagating in +z direction (down) and incident on $z = 0$ surface. Any polarization is allowable except at least some degree of random polarization is required by the computation process.

Field Relations in Rectangular Coordinate System --

For the (x, y, z - axes) Equation (C-1), (C-2) and (C-3) become

$$E_x(A) = Z_{xx}(A) H_x(A) + Z_{xy}(A) H_y(A) \quad (C-4)$$

$$E_y(A) = Z_{yx}(A) H_x(A) + Z_{yy}(A) H_y(A) \quad (C-5)$$

$$H_z(A) = k_{zx}(A) H_x(A) + k_{zy}(A) H_y(A) \quad (C-6)$$

$$H_z(A) = Y_{zx}(A) E_x(A) + Y_{zy}(A) E_y(A) \quad (C-7)$$

Equations (C-6) and (C-7) are alternate expressions of H_z (e.g., k_{zx} and k_{zy} can be obtained by substituting (C-4) and (C-5) into (C-7).

Units Used - (MKS) --

E - mv/km

H - gamma

f - Hz

A - degrees

II. Rotated Quantities

Define: $Z1 = Z_{xy} - Z_{yx}$ (C-8)

$$Z2 = Z_{xx} + Z_{yy} \quad (C-9)$$

$$Z3 = Z_{xy} + Z_{yx} \quad (C-10)$$

$$Z4 = Z_{xx} - Z_{yy} \quad (C-11)$$

- A. Special values of the rotation angle 'A' for the principal axes of the tensor functions defined in Section I --

$$A(ZMX): |Z3(A(ZMX))| = |Z3(A)|_{mx} \quad (C-12)$$

$$A(KZ): |k_{zx}(A(KZ))| = |k_{zx}(A)|_{mx} \quad (C-13)$$

$$A(YZ): |Y_{zy}(A(YZ))| = |Y_{zy}(A)|_{mx} \quad (C-14)$$

$$A(Z) = \begin{cases} A(ZMX), & (A(YZ) - 45^\circ) \leq A(ZMX) \leq (A(YZ) + 45^\circ) \\ A(ZMX) \pm 90^\circ, & \text{otherwise} \end{cases} \quad (C-15)$$

- B. Rotated tensor components for principal axes.

$$ZTE = Z_{yx}(A(Z)) = |ZTE| / \underline{PTE} \quad (C-16)$$

$$ZTM = Z_{xy}(A(Z)) = |ZTM| / \underline{PTM} \quad (C-17)$$

$$RTE = (0.2/f) |ZTE|^2 \text{ (ohm-meters)} \quad (C-18)$$

$$RTM = (0.2/f) |ZTM|^2 \text{ (ohm-meters)} \quad (C-19)$$

$$KZTE = k_{zx}(A(KZ)), \quad (H_z / H \perp \text{ strike}) \quad (C-20)$$

- C. 3-D indices (skew and ellipticity)

$$\text{ALPHA} = |Z2/Z1|, \text{ (invariant with 'A')} \quad (C-21)$$

$$\text{BETA} = |Z4(A(ZMX)) / Z3(A(ZMX))| \quad (C-22)$$

III. Notes and Glossary of Terms

A. Notes

- 1) Principal values of the rotation angle 'A' for a given tensor function are indicated by a parenthetical suffix on A.

2) A "TE" or "TM" suffix is used on some variable names to indicate transverse electric (E parallel to strike) or transverse magnetic (H parallel to strike) components.

3) Refer to sections I and II for mathematical definitions of the terms described herein.

B. Glossary

1) Dip axis -- a straight line in the $z = 0$ plane, passing through the measuring point and normal to the apparent strike direction; axis of maximum change.

2) A(ZMX) -- principal rotation angle for the $[Z]$ tensor, placing the x-axis in the maximum impedance direction.

3) A(KZ) -- principal rotation angle for the $[k_z]$ tensor, such that H_z is most coherent with H_x ; x-axis is an estimate of the dip-axis.

4) A(YZ) -- principal rotation angle for the $[Y_z]$ tensor, such the H_z is most coherent with E_y ; x-axis is an estimate of the dip-axis.

5) A(Z) -- principal rotation angle for the $[Z]$ tensor, but adjusted by $\pm 90^\circ$ such that the x-axis angle is nearer A(YZ), the dip-axis angle; direction of the TM component of the electric field.

6) ZTE -- principal component of rotated $[Z]$ tensor, for E parallel to strike and H perpendicular to strike.

7) ZTM -- principal component of rotated $[Z]$ tensor, for E perpendicular to strike and H parallel to strike.

- 8) RTE -- apparent resistivity for ZTE
- 9) RTM -- apparent resistivity for ZTM
- 10) PTE -- phase of ZTE
- 11) PTM -- phase of ZTM
- 12) KZTE -- principal component of rotated $[k_z]$ tensor for x-axis aligned with dip-axis (equal to $H_z/H \perp \text{strike}$).
- 13) ALPHA -- skew of $[Z]$ tensor; ratio of magnitudes of phasor positions of the centers of the elliptical loci with rotation angle 'A' for Z_{xx} (numerator) and Z_{xy} (denominator); non-zero value indicates three-dimensionality.
- 14) BETA -- ellipticity of $[Z]$ tensor; ratio of minor to major axes of rotation angle loci ellipse; non-zero value indicates three-dimensionality.

IV. Reference

Word, D.R., H.W. Smith, F.X. Bostick, Jr., "An Investigation of the Magnetotelluric Tensor Impedance Method," Electrical Geophysics Research Lab., Tech. Report No. 82, Univ. of Texas, Austin, Texas, 1970.

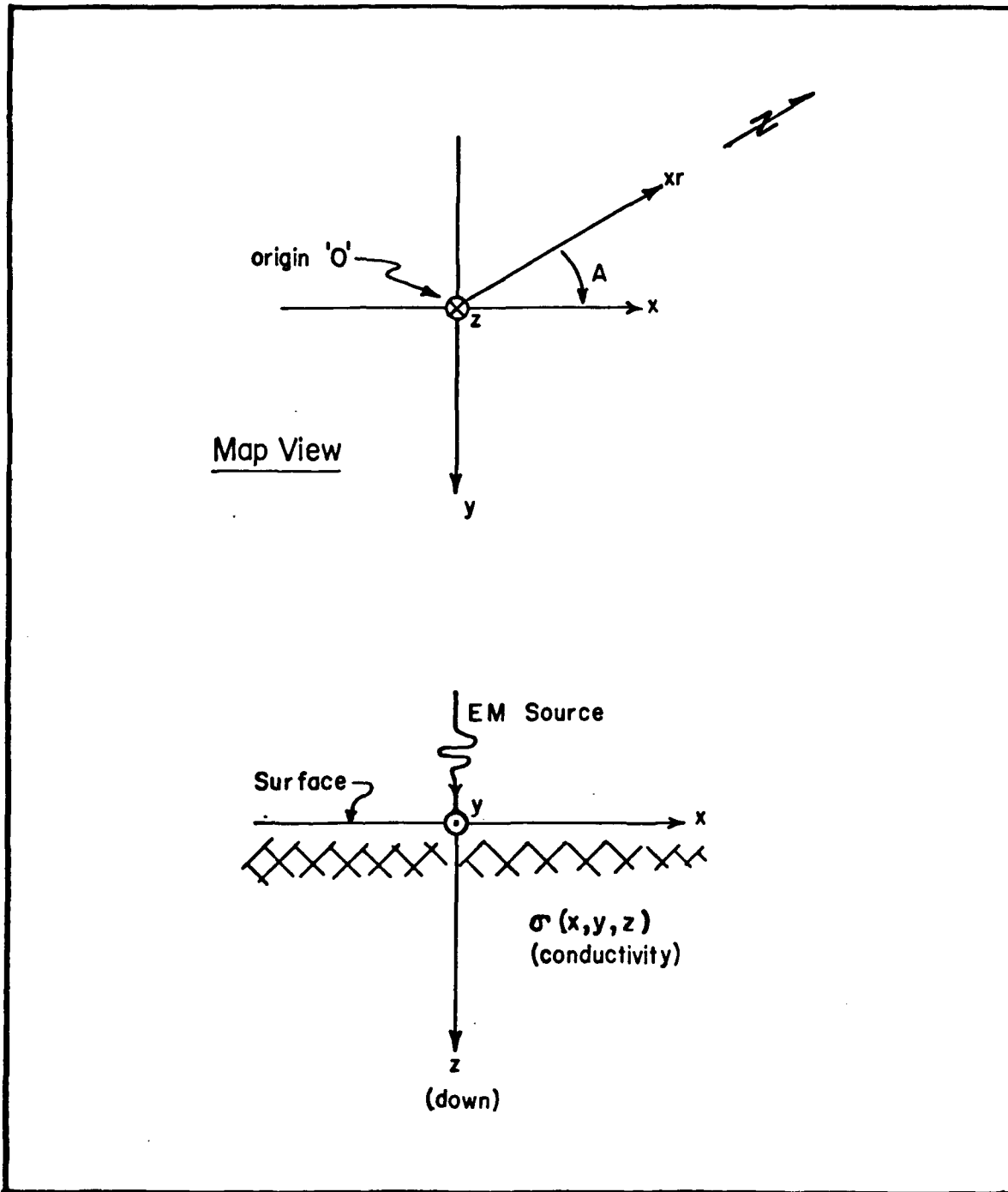


Fig. C-1: MT Co-ordinate System

PROPRIETARY INFORMATION NOTICE
 This document contains Geotronics Corporation proprietary and confidential information which is supplied for limited purposes only, and remains the property of Geotronics Corporation. This document may not be reproduced in whole or in part without written consent of Geotronics Corporation and the information therein must not be disclosed to persons not having need of such disclosure consistent with the License for which it is supplied. This document is to be returned to Geotronics Corporation upon termination of the License under which it is supplied.

Appendix D

MT Interpretation -- Defining Equations and Glossary of computed Quantities

(This appendix covers only the standard electrical interpretation process. See Appendix C for MT analysis information)

I. One-dimensional Inversion

The 1-D inversion process inputs ZTE(f) information (RTE and PTE are actually used) and produces a continuous resistivity-depth function, $R(z)$, that is an estimate of the smoothed true resistivity vs. depth under the measuring site. The algorithm used is an adaptation of a method devised by Dr. F. X. Bostick, Jr. at the University of Texas at Austin. The process, represented here by an operator 'B' is a forward going analytical approximation such that

$$R(z) = B \{ZTE(f)\} \quad (D-1)$$

The process produces two alternate models referred to as Amplitude Inversion (AI) and Phase Inversion (PI).

The AI version is used in the modeling and interpretation. The PI version, which has more inherent smoothing effect, is computed and used only for internal diagnostic purposes.

A pseudo depth-frequency correspondence, $z(f)$, is produced by the inversion process and can be used to relate other frequency domain functions to the depth scale in the model.

II. Anisotropy Factor and Anisotropy Sense

The anisotropy factor $AF(f)$ is defined by

$$AF(f) = RTM(f)/RTE(f) \quad (D-2)$$

and thus indicates the degree of separation between apparent resistivities parallel and normal to strike. $AF(f) = 1.0$ for a 1-D structure, and is in general non-unity if anisotropy or lateral inhomogeneity is present.

The anisotropy sense is derived from change in $AF(f)$ with frequency, or $AF'(f)$, which indicates whether an anomalous horizon is active at frequency f and whether it is apparently resistive or conductive. Because of the logarithmic depth nature of the MT response, the anisotropy sense is defined as the derivative in the log-log plane as

$$AS(f) = \frac{d(\log AF(f))}{d(\log f)} \quad (D-3)$$

The following rule applies to the structural horizon effective at frequency f :

$$AS(f) = 0, \text{ One-dimensional}$$

$$AS(f) > 0, \text{ Resistive anomaly}$$

$$AS(f) < 0, \text{ Conductive anomaly}$$

where "anomaly" refers to a reflector that is laterally anomalous. AF and AS are related to the depth scale in the electrical model by the pseudo depth-frequency function $z(f)$.

III. Notes and Glossary of Terms

A. Notes

- 1) Other frequency domain quantities, including the Dip-axis azimuth and the 3-D indices, (See Appendix C) are also related to depth by the pseudo depth-frequency function $z(f)$ for interpretational use.
- 2) One-dimensional refers to variation in z -direction only, and variation in more than one direction is referred to as an "anomaly".
- 3) Units are MKS.

B. Glossary

- 1) $R(z)$ -- true resistivity vs. depth estimate (as a continuous function) from inversion of RTE (f), where AI mode is "amplitude inversion" and PI mode is "phase inversion".
- 2) $z(f)$ -- pseudo depth-frequency correspondence from RTE(f) to $R(z)$ inversion.
- 3) AF(f) -- anisotropy factor
- 4) AS(f) -- anisotropy sense
- 5) Dip-axis plots -- dip-axis angle (normally A(YZ)) data plotted on a log-polar scale in map view, with angle on the azimuth scale and depth (interpreted through the $z(f)$ function) on a log-radial scale.
- 6) Resistivity Section -- refers to a display of the true resistivity estimates ($R(z)$ data) contoured in a cross section format (horizontal or vertical).
- 7) Correlation Section -- refers to a display of the $R(z)$ curves superimposed at site locations in vertical cross

section format, with site-to-site correlations drawn between like features and signatures in the $R(z)$ curves. Interfaces or boundaries are assumed at the inflection points of the $R(z)$ curves.

Appendex E - Resolution

A precise statement of MT resolution and accuracy is not presently practical, if possible at all, for generally 3-D geometry. Error estimates must be in large part empirical and in some cases qualitative. This section discusses some probable upper bounds on the errors. It does not attempt to deal with all possible sources of error and does not set absolute bounds.

The smoothing effects that exist for the overall model are likewise difficult to define in precise analytical terms because a precise 3-D solution does not exist. The smoothing is essentially a volume averaging of the conductivity distribution. The computed resistivity for a given point in the model is the result of an averaging of the conductivity in some volume about that point in the actual structure. The dimensions of the averaging volume, which are roughly proportional to depth, are a complicated function of the structure; but to the first order, one can assume a spherical averaging volume with a radius of about 30 percent or more of depth. The computed resistivity function is the reciprocal of the smoothed conductivity function.

For approximately 1-D results and mild anisotropy (say less than 0.3 decade split in RTE and RTM), and for normal measurement noise, the model conductivity should be within about ± 10 to 20 percent of the actual smoothed conductive structure. This assumes no severe 3-D effects are present. The mean depths to the various resistive units or features shown by the resistivity-depth function should be normally within ± 10 to 20 percent of actual depths.

When a high degree of anisotropy is present a greater possible error can be assumed, although the RTE inverse is still normally a

CA - actual intrinsic conductivity

f - frequency

z - depth

SD - skin depth

- 1) For a particular depth z_1 in the model find the corresponding frequency f , from the pseudo $z(f)$ relationship mentioned in Appendix D.
- 2) Features near depth z_1 will be averaged if their dimensions are less than about $0.5 SD(f_1)$, where $SD(f_1)$ is the skin depth at frequency f_1 in one of the following resistivities:
 - a) the resistivity $R(z_1)$ if the resistivity of the feature in question is greater than $R(z_1)$
 - or b) the resistivity of the feature in question itself if it is less than $R(z_1)$
- 3) The model conductivity $C(z_1)$ is the average of $CA(z)dz$ over an interval of about $z_1 \pm 0.5 SD(f_1)$.

The above criteria can be used to assess the possibility of the presence of thin conductive or resistive zones not shown explicitly in a given region of the model.

Appendix F - Data Smoothing and Comments on Noise and Special Conditions

The 1-D continuous inversion operator requires as input an impedance versus frequency function, $ZTE(f)$, that is compatible with a 1-D geometry. The RTE and PTE curves must be continuous and behave as a minimum phase function such that the slope of RTE(f) in the log-log plane is $(PTE/45^\circ) - 1$ to a first order approximation. The phase is bounded by $0^\circ \leq PTE \leq 90^\circ$ and the slope of RTE in the log-log plane is bounded by ± 1 .

Results computed from the field data are smoothed using the above constraints to produce a continuous, minimum phase function for the 1-D inversion. The field data are recorded in the presence of generally 3-D structures and a certain amount of noise, and the smooth functions are extrapolated through frequency bands of evident 3-D effects or excessive noise, using both amplitude and phase information in the process. This method results in a minimum phase best fit to the data, but due to the 3-D effects and noise, the smoothing operation is to a certain degree an interpretive process.

The noise level was generally high throughout the survey area, and the data quality was below normal for most sites. Most of the noise was probably due to cultural activity, including power lines and roadways which were especially difficult to avoid in the narrow valley area. A reasonable interpretation of the MT response was feasible at most sites over the frequency range from about 0.003 to 50 Hz with varying degrees of confidence. One exception is site 9 where excessive noise rendered the low frequency RTE data unuseable.

A "non-minimum phase" property is found to occur in the low frequency data for some sites, in that the slope of RTE in the log-log

plane exceeds one and the phase exceeds 90° . Theoretical work recently performed by Geotronics indicates that the observed behavior strongly suggests an extremely conductive anomaly with an abrupt upper horizon and a very high resistive to conductive contrast (probably 100:1 or more). MT responses of this type have been occasionally observed only in areas of recent magmatic activity and are probably of special significance in the geothermal survey, suggesting a zone of extremely conductive (possible semi-molten) rock.

Table F-1 lists several status codes pertaining to the data for certain frequency ranges and corresponding depth ranges. The status codes pertain to noise conditions, 3-D effects, and non-minimum phase conditions, showing categories of possible uncertainty due to noise. The main purpose of these codes is to show a relative indication of confidence level and to call attention to special conditions such as areas of greater 3-D influence and non-minimum phase. The error limits pertain to the uncertainty in depth and resistivity of a given feature in the 1-D inverse $R(z)$ and should not be taken as precise bounds on the errors, which in most cases should tend toward the low end of the range.

SLN-132

TABLE F-1

X-Y PLOT DATA QUALITY

SITE	FREQUENCY RANGE	BELOW SITE DEPTH RANGE METERS	BELOW SITE DEPTH RANGE FEET	STATUS CODE
1	3. -. 5 Whole Range	100-340	335-1110	2 (GAP) #
2	> .1 Whole Range	610	2000	2(GAP) #
3	TE: Whole Range TE > .1 TM4. -. 1 Whole Range	665 125-665	2190 410-2190	1(Noise) 3(GAP) 2(GAP) #
4	TE > .2 TM 6. -. 3 Whole Range	435 95-330	1425 310-1090	3(GAP) 1(Noise) #

Status Categories

- ‡ 3-D effects (e. g. RTE/RTM decision erratic)
- * NMP (significant non-minimum phase)
- 0 error less than 20% on R & z, second order features are significant
- 1 error 20% to 50% on R & z, second order features are significant but with greater variance in R & Z
- 2 error 50% to 100% on R & Z, second order feature are not dependable
- 3 error over 50% possible, only first order features are significant
- 4 first order features are not dependable

MAGNETO-TELLURIC SURVEY

SODA LAKE AREA
Churchill County, Nevada

1975

for

3-9-NV9 S230

CHEVRON OIL COMPANY

(MAP OPPOSITE ABSTRACT)
by

GEOTRONICS CORPORATION
Austin, Texas

Darrell R. Word, Chief Engineer
Ronald C. Petersen, Geophysicist

June, 1975

Table of Contents

Abstract

List of Figures

I. Introduction

II. Results

III. Geoelectrical Interpretation

IV. Geological Interpretation

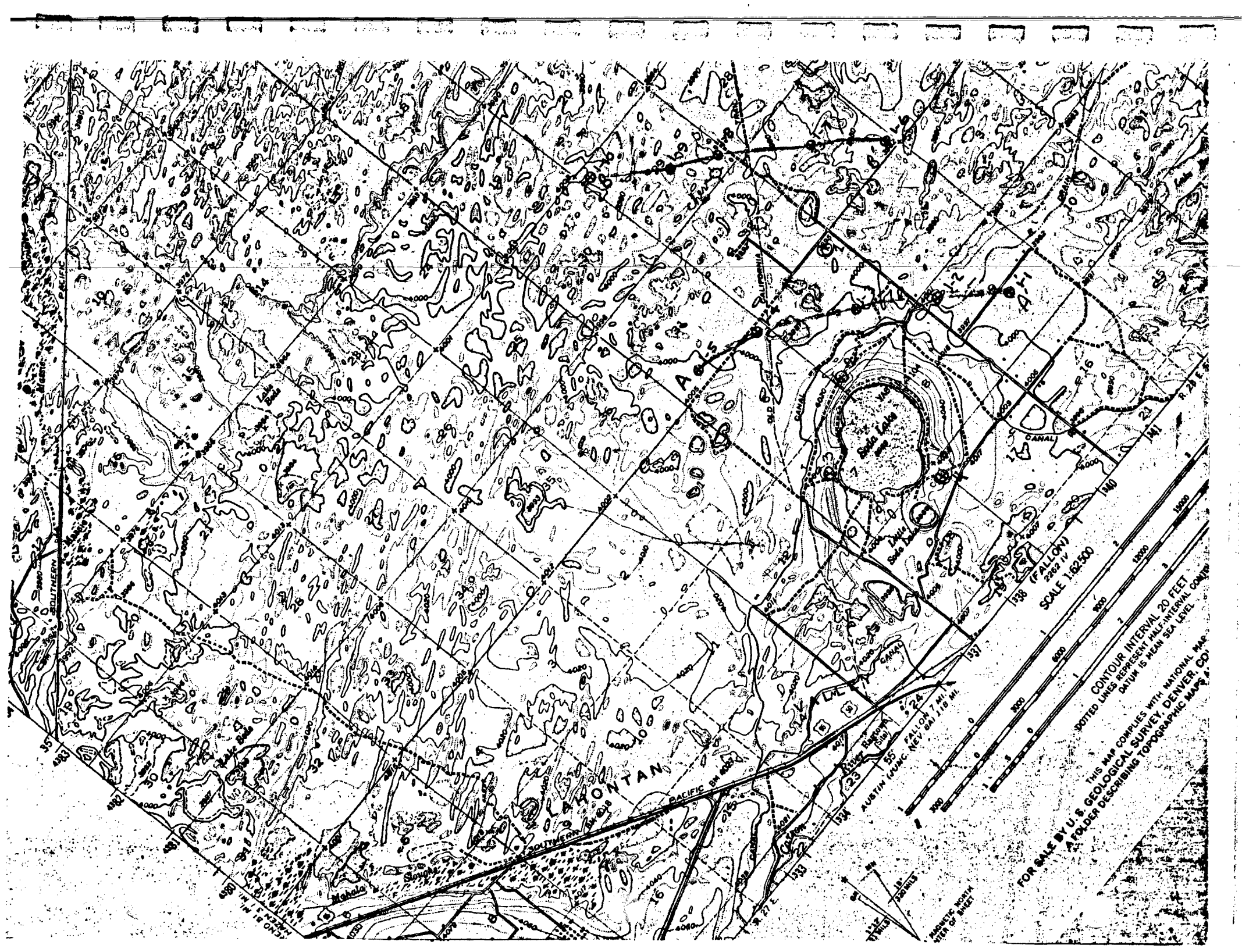
Bibliography

Appendix A - Field Operation

Appendix B - Data Processing Procedure

Appendix C - Computer Programs

Addendum



FOR SALE BY U.S. GEOLOGICAL SURVEY, DENVER CO.
A FOLDER DESCRIBING TOPOGRAPHIC MAPS

CONTOUR INTERVAL 20 FEET
DOTTED LINES REPRESENT HALF-INTERVAL CONTOUR
DAM IS MEAN SEA LEVEL

SCALE 1:62,500

528 (FALLOON)
2200 FT

1 MI

2 MI

3 MI

4 MI

5 MI

6 MI

7 MI

8 MI

9 MI

10 MI

1000
800
600
400
200
0

1000
800
600
400
200
0

1000
800
600
400
200
0

1000
800
600
400
200
0

1000
800
600
400
200
0

1000
800
600
400
200
0

1000
800
600
400
200
0

1000
800
600
400
200
0

1000
800
600
400
200
0

1000
800
600
400
200
0

1000
800
600
400
200
0

1000
800
600
400
200
0

1000
800
600
400
200
0

1000
800
600
400
200
0

1000
800
600
400
200
0

1000
800
600
400
200
0

1000
800
600
400
200
0

1000
800
600
400
200
0

1000
800
600
400
200
0

1000
800
600
400
200
0

1000
800
600
400
200
0

1000
800
600
400
200
0

1000
800
600
400
200
0

1000
800
600
400
200
0

1000
800
600
400
200
0

1000
800
600
400
200
0

1000
800
600
400
200
0

1000
800
600
400
200
0

1000
800
600
400
200
0

1000
800
600
400
200
0

1000
800
600
400
200
0

1000
800
600
400
200
0

1000
800
600
400
200
0

1000
800
600
400
200
0

1000
800
600
400
200
0

1000
800
600
400
200
0

1000
800
600
400
200
0

1000
800
600
400
200
0

1000
800
600
400
200
0

1000
800
600
400
200
0

1000
800
600
400
200
0

1000
800
600
400
200
0

1000
800
600
400
200
0

1000
800
600
400
200
0

1000
800
600
400
200
0

1000
800
600
400
200
0

1000
800
600
400
200
0

1000
800
600
400
200
0

1000
800
600
400
200
0

1000
800
600
400
200
0

1000
800
600
400
200
0

1000
800
600
400
200
0

1000
800
600
400
200
0

1000
800
600
400
200
0

1000
800
600
400
200
0

1000
800
600
400
200
0

1000
800
600
400
200
0

1000
800
600
400
200
0

1000
800
600
400
200
0

1000
800
600
400
200
0

1000
800
600
400
200
0

1000
800
600
400
200
0

1000
800
600
400
200
0

1000
800
600
400
200
0

1000
800
600
400
200
0

1000
800
600
400
200
0

1000
800
600
400
200
0

1000
800
600
400
200
0

1000
800
600
400
200
0

1000
800
600
400
200
0

1000
800
600
400
200
0

1000
800
600
400
200
0

1000
800
600
400
200
0

1000
800
600
400
200
0

1000
800
600
400
200
0

1000
800
600
400
200
0

1000
800
600
400
200
0

1000
800
600
400
200
0

1000
800
600
400
200
0

1000
800
600
400
200
0

1000
800
600
400
200
0

1000
800
600
400
200
0

1000
800
600
400
200
0

1000
800
600
400
200
0

1000
800
600
400
200
0

1000
800
600
400
200
0

1000
800
600
400
200
0

1000
800
600
400
200
0

1000
800
600
400
200
0

1000
800
600
400
200
0

1000
800
600
400
200
0

1000
800
600
400
200
0

1000
800
600
400
200
0

1000
800
600
400
200
0

1000
800
600
400
200
0

1000
800
600
400
200
0

1000
800
600
400
200
0

1000
800
600
400
200
0

1000
800
600
400
200
0

1000
800
600
400
200
0

1000
800
600
400
200
0

1000
800
600
400
200
0

1000
800
600
400
200
0

1000
800
600
400
200
0

1000
800
600
400
200
0

1000
800
600
400
200
0

1000
800
600
400
200
0

1000
800
600
400
200
0

1000
800
600
400
200
0

1000
800
600
400
200
0

1000
800
600
400
200
0

1000
800
600
400
200
0

1000
800
600
400
200
0

1000
800
600
400
200
0

1000
800
600
400
200
0

1000
800
600
400
200
0

1000
800
600
400
200
0

1000
800
600
400
200
0

1000
800
600
400
200
0

1000
800
600
400
200
0

1000
800
600
400
200
0

1000
800
600
400
200
0

1000
800
600
400
200
0

1000
800
600
400
200
0

1000
800
600
400
200
0

1000
800
600
400
200
0

1000
800
600
400
200
0

1000
800
600
400
200
0

1000
800
600
400
200
0

1000
800
600
400
200
0

1000
800
600
400
200
0

1000
800
600
400
200
0

1000
800
600
400
200
0

1000
800
600
400
200
0

1000
800
600
400
200
0

1000
800
600
400
200
0

1000
800
600
400
200
0

1000
800
600
400
200
0

1000
800
600
400
200
0

1000
800
600
400
200
0

1000
800
600
400
200
0

1000
800
600
400
200
0

1000
800
600
400
200
0

1000
800
600
400
200
0

1000
800
600
400
200
0

1000
800
600
400
200
0

1000
800
600
400
200
0

1000
800
600
400
200
0

1000
800
600
400
200
0

1000
800
600
400
200
0

1000
800
600
400
200
0

1000
800
600
400
200
0

1000
800
600
400
200
0

1000
800
600
400
200
0

1000
800
600
400
200
0

1000
800
600
400
200
0

1000
800
600
400
200
0

1000
800
600
400
200
0

1000
800
600
400
200
0

1000
800
600
400
200
0

1000
800
600
400
200
0

1000
800
600
400
200
0

1000
800
600
400
200
0

1000
800
600
400
200
0

1000
800
600
400
200
0

1000
800
600
400
200
0

1000
800
600
400
200
0

1000
800
600
400
200
0

1000
800
600
400
200
0

1000
800
600
400
200
0

1000
800
600
400
200
0

1000
800
600
400
200
0

1000
800
600
400
200
0

1000
800
600
400
200
0

1000
800
600
400
200
0

1000
800
600
400
200
0

1000
800
600
400
200
0

1000
800
600
400
200
0

1000
800
600
400
200
0

1000
800
600
400
200
0

1000
800
600
400
200
0

1000
800
600
400
200
0

1000
800
600
400
200
0

1000
800
600
400
200
0

1000
800
600
400
200
0

1000
800
600
400
200
0

1000
800
600
400
200
0

1000
800
600
400
200
0

1000
800
600
400
200
0

1000
800
600
400
200
0

1000
800
600
400
200
0

1000
800
600
400
200
0

1000
800
600
400
200
0

1000
800
600
400
200
0

1000
800
600
400
200
0

Abstract

This field report presents the results and conclusions of a magneto-tellurics survey in a suspected geothermal area. Two definite conductive zones are evident in the data. A third is postulated primarily on the basis of modeling studies performed on the data. All are of possible geothermal interest.

The zones are:

1) A low resistivity zone (approximately 1.5 to 2.5 ohm-meters) ranging from a few hundred feet to about 4000 feet in depth and approximately 1000 feet to 3000 feet in thickness under the two lines is readily evident in the data. This zone is likely a (hot?) saturated aquifer and may also be considerably altered.

2) A possible conductive zone centered under Site 1-2. Very little can be said about this zone, except that it might exist. Its size, conductivity, and depth are postulated primarily on the basis of geological reasonability -- they cannot be uniquely assigned from the data. The low conductivity might be due either to alteration or an isolated aquifer. The latter possibility is much the less likely of the two, but would be of more geothermal interest.

3) A deep conductive zone, the top of which varies from approximately 16,000 to 30,000 feet under the survey area. This zone is very conductive (averaging approximately 0.3 ohm-meters) and is quite likely a magma chamber.

List of Figures

<u>Figure Number</u>	<u>Title</u>
II-1 thru II-10	Resistivities and phase angles from data (Page 1); Smoothed version (Page 2); Tensor rotation angles (Page 3); and Smoothed version (Page 4) for each site.
II-11 thru II-20	OPTMOD and INVERT results for each site.
III-1	INVERT results - Line A
III-2	INVERT results - Line B
III-3A	Geoelectric cross-section, Line A
III-3B	Alternate Geoelectric cross-section, Line A.
III-4	Geoelectric cross-section, Line B.
III-5	Plan view of depth to surface of deep conductor and maximum impedance direction at that depth.
III-6	Plan view of depth to "basement" and maximum impedance direction at 3 kilometers.
IV-1A	Line A - Alteration Model
IV-1B	Line A - Buried Reservoir Model
IV-2	Line B - Geologic Model (common to both Alteration Model and Buried Reservoir Model)

I. Introduction

At the request of Mr. William E. Mero of the Chevron Oil Company, Minerals Staff, Geotronics Corporation conducted a magneto-tellurics survey near Soda Lake, Nevada, in March of 1975. The purpose of the survey was to attempt to detect, and if possible delineate, electrically conductive zones of geothermal interest in the subsurface of the area. The survey consisted of ten sites situated in two parallel lines just northeast of Soda Lake. Site locations are shown on the enclosed map.

The theory of magneto-telluric interpretation is presented in considerable detail in reference 2 of this report, along with the analysis and interpretation of a sample survey. For the sake of brevity, this theory has not been repeated extensively in this report, although it is the basis of most of the reasoning used in the interpretation.

Brief descriptions of the field operation, data processing procedure, and computer programs used in the interpretation are presented in the appendices.

II. Results

Figures II-1 through II-10 are plots of resistivity and phase, tensor rotation angles, and 3-D indices for sites 1-1 through 1-10. Final OPTMOD models are plotted over the data. The significance of these quantities, along with their acceptance criteria will be discussed in section III. Figures II-11 through II-20 are composite plots of the final layered models and the final INVERT models for each site. These models will also be discussed in more detail in section III.

The Chevron-Phillips 1-29 well log model is plotted along with the data from Site 1-8, which is only 400 feet away. The well log was modeled by inputting the resistivities and thicknesses on the log to the bottom of the drill hole (4310 feet). The bottom resistivity in the hole (28 ohm-meters) was then continued to a depth of approximately 32,000 feet, the point where the top of the lower conductor should be under this site. A resistivity of 1 ohm-meter was assumed for the lower conductor.

There is some discrepancy between the measured MT data and the modeled well log data at shallow depths. This is likely a real difference due to a difference in geology between MT Site 1-8 and the well site. It may also be partly attributable to the difference in measuring scale of the two methods and the fact that the local effects seen in the well log must be assumed to extend in infinite horizontal layers in order to compute the well log model.

Primarily, the well log appears to not be seeing as much of the shallow conductive zone as MT is. At greater depths, the two models begin to track each other somewhat better, indicating that the lower parts of the model are likely realistic.

III. Geoelectrical Interpretation

A. General Comments

The computed results used in the interpretation for this survey are contained in Section II, Figures II-1 through II-10. Refer to Appendices A, B, and C for more details regarding the measurements and data processing and for some description of the terminology used herein. The results used include the apparent resistivity (RTE and RTM) and associated phase functions, the tensor rotation angles for maximum impedance direction (A(Z)) and for maximum H_z admittance direction (A(YZ)), and the 3-D indices (ALPHA and BETA).

On the average, two or more recording runs were processed for each frequency band (except for B2) for each site. Data point acceptance criteria were based primarily on the levels of phasor coherency associated with the data points of each frequency. RTE and RTM data was passed for coherencies above 0.8. Rotation angle data and 3-D indices were passed only if both RTM and RTE values passed at a given frequency. For a coherency pass level of 0.8, the theoretical bands of $\pm 20\%$ of mean value should enclose about 90% of the data points for RTM and RTE from all individual data sets applying at a given frequency. The scatter in the computed results does appear to be about $\pm 20\%$ for most sites except for some cases where special noise influences came to bear in certain frequency regions (e. g., Site 1-8 between 0.1 and 1.0 Hz).

The results for each site tend to show a fairly low degree of apparent anisotropy. This applies generally over the entire survey area. The low apparent anisotropy (low degree of RTE-RTM separation) implies a low influence of lateral changes on the results for a given sounding and consequently favors an interpretation based upon 1-D inversions of the results for each site. The apparent anisotropy present at the lower frequency range appears to be due to anomalies in the resistive basement and the deep conductive zone. A discussion of this will follow. It should be noted at this point that the rotation angle results are well defined only for frequencies where the apparent anisotropy is significant compared to the measurement noise. The rotation angle data are consequently very scattered and essentially meaningless for most of the sites of this survey for frequencies above 0.1 to 1.0 Hz. The angles are reasonably well defined for lower frequencies where the RTE-RTM split begins to appear.

III. (continued...)

B. One-Dimensional Models

One dimensional models for each site were generated from the RTE and associated phase functions using both programs INVERT and OPTMOD (see Appendix C) and the resulting resistivity-depth functions are plotted in Section II, Figures II-11 - II-20, with both models for a given site plotted together for comparison. Both models reflect the same gross features of the resistivity profile and show essentially all of the detail that is warranted by the resolution for these results. The layered model provides a better means for estimating the bounds on the average resistivity for a given zone or layer, but the layered model does not imply that the resistivity values change abruptly at the interface shown. A given layer interface might fall near the center of a continuous transition between two values of resistivity at different depths. The INVERT model tends to smooth any abrupt changes that might actually exist. In a sense the two models tend to bracket the true model.

The estimated resistivity bounds or confidence limits are indicated on the model plots. These apply to the inverse of the average conductivity across a given zone indicated by a layer. Where no bounds are specified, the probable error in the parameter can be considered approximately ± 10 percent.

The ± 10 percent tolerance can be applied to layer interface depths while remembering that the interface might represent the mean depth for a smooth transition in the resistivity profile. It should be noted, too, that the specified parameter bounds are not meant to include all possibilities of error due to two- and three-dimensional anomalies. It can only be said that such effects are not apt to be large for these results.

The transition into the deep (lower) conductive zone of the model appears to be quite abrupt as evidenced by the rapid decrease in resistivity shown by the INVERT model at most sites. This zone is quite probably a magma chamber, since it is too shallow to be to upper mantle, and molten rock is the only material that deep in the earth likely to have such a high conductivity. It is very unlikely that any three-dimensional effects could cause more than 10 to 20 percent error in this depth determination.

The deep resistive zone (overlying the deep conductor) is electrically thin enough at sites 1-3, 1-4, 1-5, 1-6, 1-7, and 1-10 that

III. (continued...)

essentially only its thickness is defined by the sounding. The minimum values of resistivity allowed by the results are specified. For sites 1-1, 1-2, 1-8, and 1-9, the corresponding resistive zone is electrically thick enough (i. e. its conductivity-thickness product is great enough) that upper and lower limits on resistivity are indicated by the results. It is important to note that for sites 1-1 and 1-2 the deep resistive zone need only have an average conductivity across the zone of the range indicated. Another acceptable model for this zone would be to divide the layer (say resistivity ρ_0 and thickness T_0) into three zones with resistivities ρ_1 , ρ_2 , and ρ_3 and thicknesses T_1 , T_2 , and T_3 , where zone 2 is in the middle and situated in the mid to upper region of the original layer, and where ρ_2 is less than ρ_0 (say 1 to 2 ohm-m), and the condition $(T_1/\rho_1 + T_2/\rho_2 + T_3/\rho_3) = T_0/\rho_0$ is met. An alternate model is indicated in the model plot for Site 1-2.

C. Cross Sections from 1-D Models

Figures III-1 and III-2 show vertical geoelectric cross sections for the two traverse lines (A and B) produced from the INVERT models by contouring on constant resistivity. These models represent a smoothed version of the resistivity structure.

Figures III-3A and III-4 show vertical geoelectric cross sections for the two traverse lines (A and B) produced by a correlation of the OPTMOD models across the traverse. Resistivity bounds are indicated on the sections. Figure III-3B shows an alternate solution at sites 1-1 and 1-2 for traverse A.

The effects of lateral smoothing should be considered when interpreting the sections. For example, the transition in the surface depth of the deep conductive zone, in going from Site 1-8 to Site 1-6 might actually occur more abruptly near Site 1-7. Actual determination of this is beyond the resolution of the results.

The layers 3 and 4 at sites 1-6 and 1-7 possibly indicate a more gradual increase in resistivity with depth than at sites 1-8, 1-9, and 1-10, and do not necessarily imply a definite interface between layers 3 and 4.

D. Apparent Anisotropy and Rotation Angles

For the sake of discussion, it is convenient to define an anisotropy factor as

III. (continued...)

$$AF(f) = RTM/RTE \quad (1)$$

where f is frequency. Let $AF^1(f)$ be the first derivative of AF with respect to f . For one-dimensional results $AF(f) = 1$ and $AF^1(f) = 0$ for all f . For frequencies where a lateral anomaly (or apparent anisotropy) is sensed, the RTE and RTM functions separate and $AF(f) \neq 1$ and $AF^1(f) \neq 0$. It can be shown that the conductive or resistive nature of the anomaly is indicated by the polarity of $AF^1(f)$ as follows:

for $AF^1(f) \leq 0$, anomaly is conductive;
 $AF^1(f) > 0$, anomaly is resistive.

For the results of this survey, examination of the RTE and RTM functions shows that for sites 1-1 through 1-5 (traverse A) and 1-6 of the traverse B, as frequency is decreased, the first significant anomaly is a conductive one, as evidence by RTM rising above RTE for decreasing frequency ($AF^1(f) \leq 0$). For sites 1-7 through 1-10 the first significant anomaly is resistive and a deeper, conductive anomaly appears as it is further decreased.

This behavior is probably explained by the following two considerations:

1) For sites 1-3 through 1-6, the deep resistive zones are electrically thin and effects of the deep conductor surface appear for the same frequencies for which the resistor surface becomes effective. Consequently, anomalies in the conductor surface (perhaps the slope) dominate the effect. For sites 1-1 and 1-2, which are not considered electrically thin, the conductive anomaly might be an embedded conductor in the resistive zone, supporting the alternate model discussed in Section III-B.

2) For sites 1-7 through 1-10, the much thicker deep resistive zone (especially at sites 1-8 and 1-9) presents a resistive anomaly (perhaps its irregular surface) before the frequency is low enough to sense the effect of the deep conductor anomaly.

The foregoing is very speculative, but does seem to produce a rational agreement with the model structure. Figures III-5 and III-6

III. (continued...)

are plan views of the upper surfaces (obtained from OPTMOD models) of the deep resistor and deep conductor models, respectively. Rotation angles $A(YZ)$ corresponding to the two zones are plotted, indicating the apparent "dip axis" directions (direction of maximum change) which point normal to the apparent strike. The angles corresponding to the deep conductor were chosen as the values for the lowest frequency values computed. The $A(YZ)$ functions for all sites except 1-5 are still changing in the CCW direction at the lowest frequency value, implying that they have not reached final value and would swing further to the north with further decrease in frequency. This would perhaps cause better agreement with the average deep conductor surface contours. It is interesting to note that for the shallower rotation angles (which correspond to about 2 to 3 km depth, and consequently to the resistive zone) the directions tend to agree reasonably well with the surface contours for sites 1-7 through 1-10, showing a NE-SW strike, and the angles for sites 1-3 through 1-5 are close to the deep conductor angles for those sites. This behavior is in agreement with the earlier speculation regarding the anisotropy.

IV. Geologic Models of Soda Lake

The geologic models of Soda Lake are derived by correlating the magneto-telluric data with the published geology (Morrison, 1964), the well log of Chevron-Phillips 1-29, and a preliminary cross section provided by Chevron Oil.

Two possible models are herein proposed. The first one will be called the Alteration Model, and is the more likely of the two. The second will be called the Buried Reservoir Model, and although it is the more interesting geothermal model, it is not as easily justifiable geologically as is the Alteration Model.

The Alteration Model is shown by figures IV-1A and IV-2 for Lines A and B respectively. The Buried Reservoir Model is shown by figures IV-1B and IV-2, for lines A and B. Note that the single model for Line B is common to both the Alteration Model and the Buried Reservoir Model.

It should be kept in mind that these models are quite speculative. Lithologic units are proposed on the basis of the range of resistivities that they are likely to have. The models are subject to the error limits for both the depths to interfaces and resistivity ranges which were set down in Section III.

The Alteration Model assumes that unaltered Tertiary rocks, primarily rhyolites, have an average resistivity of about 40 to 70 ohm-meters, and that altered Tertiary rocks range in resistivity from possibly as low as one ohm-meter to about 25 ohm-meters -- the more intense the alteration, the lower the resistivity. If this assumption is valid, then the MT data is likely detecting alteration zones of the approximate dimensions and intensities shown on the model cross sections.

A low resistivity zone (approximately 1.5 to 2.5 ohm-meters) ranging from a few hundred feet to about 4000 feet in depth and approximately 1000 feet to 3000 feet in thickness under the two lines, is readily evident in the data. This zone likely lies in the Lower Lahontan Valley group (Wyemaha?). Since the Wyemaha apparently has fair potential as a reservoir (Morrison, 1964), and since 1.5 to 2.0 ohm-meters is a reasonable resistivity range for a saturated aquifer (especially if the

IV. (continued)

water is hot), one possibility is that this conductive zone is a saturated aquifer overlying the impermeable Tertiary basement. The other possibility is that this zone is not saturated, but that the alteration extends into it. A combination of saturation and alteration is also quite likely.

Above this is a thin layer (varying from approximately 300 to 1000 feet thick) of more resistive material (ranging from approximately 5 to 15 ohm-meters). This is likely unsaturated Sehoo or Wyemaha formation, with some interbedded volcanics. During the modeling phase, it was noted that the models for some sites required thin high resistivity layers in order to produce a good fit to the high frequency data.

The probable depth to the lower magma chamber varies from an average of about 20,000 feet under Line A to about 25 to 30,000 feet under Line B. Although these depths appear to be changing somewhat rapidly, they are probably quite representative, since 3-D effects would be relatively small, as per the discussion in section III.

The resistivity of the deep magma chamber cannot be precisely defined, but is likely in the range of 0.1 to 1.0 ohm meters, and appears to average about .30 ohm-meters.

The Buried Reservoir Model is similar to the Alteration Model in most respects. The major difference is the proposed cause of the conductive anomaly under Site 1-2. Modeling studies on the data show that a layer of approximately 1.23 ohm-meter resistivity and 1 kilometer thickness sandwiched within a layer of approximately 40 ohm-meters and 4.5 kilometers thick fits the data for Site 1-2 quite well. It should be noted that because of the restraints necessary in adjusting conductivity-thickness products for the model, we cannot unambiguously assign an exact depth to the layer, if it exists. Neither can we assign an exact resistivity or thickness to the layer -- only a conductivity-thickness product. For example, a layer twice as conductive, but only half as thick would produce the same results. Similarly, the conductive layer could lie anywhere between the upper and lower boundaries of the assumed 40 ohm-meter block, and the same data curve would result.

Geologically, this model is somewhat reasonable, if we assume that the conductive layer is possibly a saturated block of Truckee formation

IV. (continued)

overlain by younger volcanics. It is very speculative in that the exact sequence of geological events necessary for its existence are not immediately obvious, and open to more than one interpretation.

Finally, it should be noted that all faulting in the models is proposed primarily on the basis of geologic necessity, and is not necessarily indicated by MT data. The MT data shows little or no evidence of faulting. Any faulting in the area is probably on a scale too small to be within the resolution limits of the MT method.

Bibliography

1. Morrison, R. B. ; "Lake Lahontan: Geology of the Southern Carson Desert, Nevada," United States Geological Survey Professional Paper 401, 1964.
2. Word, D.R., H. W. Smith, and F.X. Bostick, Jr., "An Investigation of the Magnetotelluric Tensor Impedance Method," The University of Texas at Austin, Electrical Geophysics Research Lab., Report No. 82, 1970.

Appendix A - Field Operation

Five orthogonal component, surface EM field measurements (E_x , E_y , H_x , H_y , H_z) were made of the micropulsation fields of each site in the overall frequency range of approximately 0.002 to 100 Hz. This range was covered by four overlapping bands as described in Table B-1.

Figure A-1 shows the field sensor configuration used. The positive x axis is directed to magnetic north, which has an average declination of $18^\circ E$. The E-field sensors are electrode lines using 100 square inch lead electrodes with a spacing of 600 feet. The H-field sensors are Geotronics induction magnetometers - model MTC-4SS for H_x and H_y , and model MTC-6SS for H_z .

- The instrument van contains the recording system of Geotronics manufacture, consisting of the MTE-4 three-channel E-field preamplifier, the MTH-4 three-channel H-field preamplifier, the MTC-2 calibrator, the MTF-16 filter-post amplifier, and the MTDR-2 digital recorder. A 6-channel Brush chart recorder is used for field monitoring of the signals.

A five-man field crew is used, consisting of the crew chief and instrument man, alternate instrument man, and a three-man site layout team including a surveyor.

Proper field technique, which is of extreme importance in MT recording, has been developed by Geotronics personnel through 15 years of MT experience and is stressed throughout the survey. System noise and data quality checks are made routinely. All sensors are buried about 12 inches or more deep and all cables buried or weighted to reduce wind noise and improve thermal stability. While one site is being recorded, an alternate set of sensors is installed at the next site, and an adequate time (a few hours) is allowed for stabilization, including thermal and magnetic stabilization of the magnetometers and contact potential stabilization of the electrodes.

Field tapes are sent back to Geotronics daily (when conditions permit) so that preliminary analysis can be done to assess signal quality while the field crew is still in the survey area.

The Soda Lake survey consists of 2 traverse lines containing a total of 10 sites. Data bands B6, B5, B4, and B3 were recorded at sites 1-2,

Appendix A, Field Operation, continued...

1-3, 1-4, 1-7, 1-8, and 1-9. Bands B6, B5, B4, and B2 were recorded at sites 1-1, 1 5, 1-6, and 1-7 (end sites of each line). Multiple recordings of bands B3 through B6 were made to assure data quality; multiple recordings were not routinely made of band B2 because of the recording time involved.

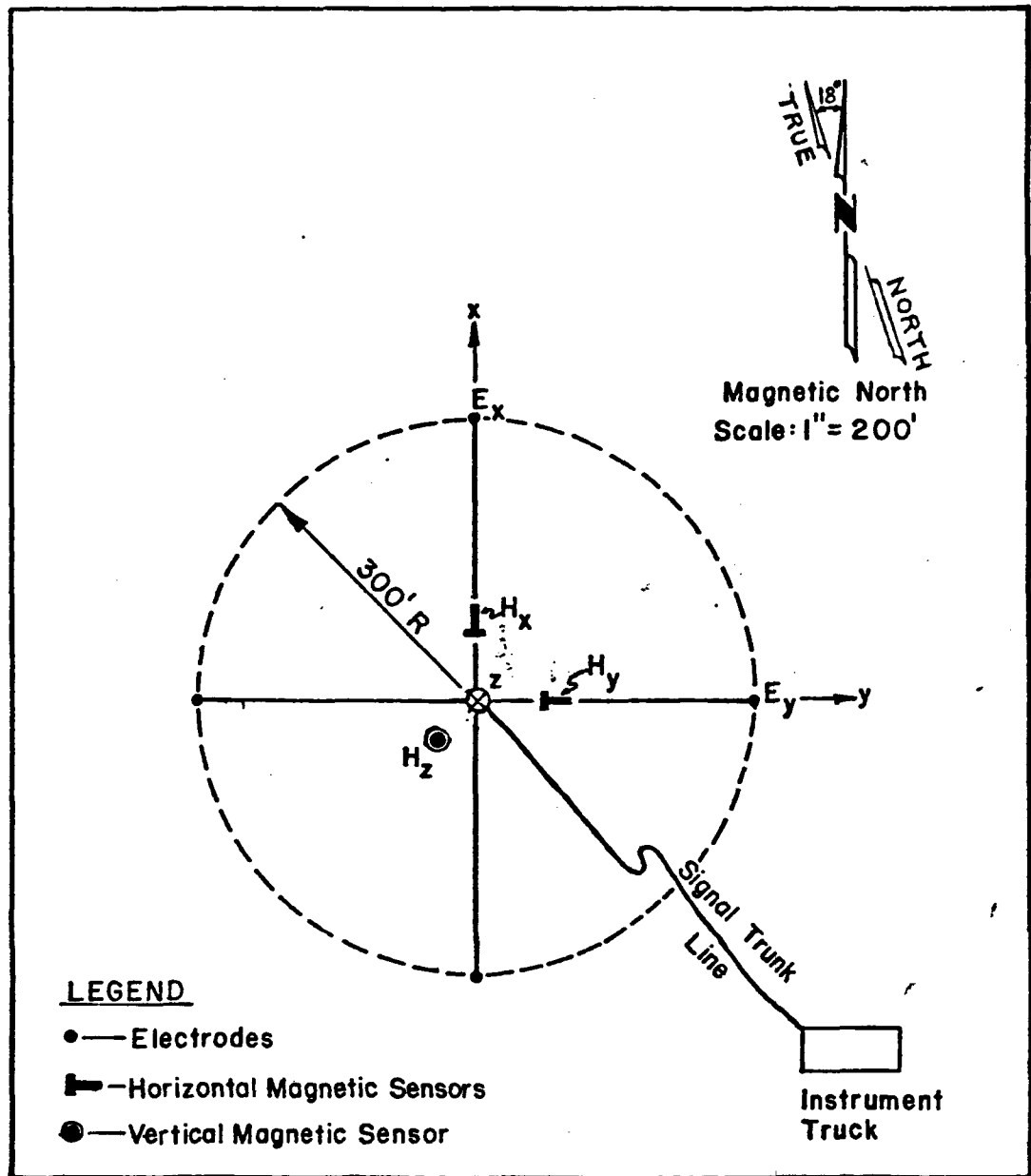


FIGURE #1. Magneto-Telluric Field Sensor Layout.

Appendix B - Data Processing Procedure

Computer processing was done on the Control Data Corporation Cybernet System. The Houston based CDC 6600 was used and accessed through the CDC-Austin 200 series user terminal. Field tapes were sent to Houston and stored in the CDC tape library in read-only mode for the duration of the survey and analysis.

The analysis phase of the processing was done by program MAGTAN2, which performs a tensor MT analysis. A description of the program functions and output results is given in Appendix C. The frequency domain results used in the interpretation of this survey are:

- (1) Rotated apparent resistivity and phase functions (RTE and RTM and related phase functions) for E-parallel to strike and E-perpendicular to strike respectively.
- (2) Rotation angle (A(YZ)) for the apparent "dip-axis" direction determined from H_z , the vertical magnetic field, and is the direction of maximum gradient.
- (3) Rotation angle (A(Z)) for maximum impedance.
- (4) Three-dimensionality indices (ALPHA and BETA) which are the "skew" and "ellipticity" of the impedance tensor. Zero value for both of these quantities constitutes the necessary and sufficient condition for two-dimensionality.

The frequency bands used in the analysis are given in Table B-1, which includes the sampling parameters and the frequency range of results used for each band. The upper limit on the frequency range used is near the alias filter cut-off frequency, which is set to approximately half the Nyquist frequency. The lower three frequency points of the analysis results are omitted to avoid truncation aliasing error that is apt to be present. The analysis frequency bands overlap for redundancy.

Strip chart records and field logs were checked to select the best data recording runs for analysis. Initially, one run of each band for each site was processed and the results checked for several acceptance

Appendix B, Data Processing Procedure, continued...

criteria. Additional runs were processed where needed to produce the best definition of the computed functions. Finally, all runs of the frequency domain results to be used were plotted for use in the subsequent interpretation. Averaged and smoothed functions were produced from the raw results for use in modeling and other interpretation.

One-dimensional models were fit to the RTE and phase functions at each site using two different methods and employing computer programs described briefly in Appendix C. In the first method, 1-D inversions were made by program INVERT, which analytically produces a continuous smoothed function of intrinsic resistivity vs. depth. In the second method, best fit 1-D N-layered models were produced by program OPTMOD. These 1-D models were correlated or contoured to produce laterally and vertically smoothed versions of the vertical cross-sections along the survey traverses.

The 1-D models are considered as estimates of the resistivity-depth, vertical profile under a given site. The 1-D inversion of the RTE function produces the best estimate of the 1-D vertical profile, but it must be kept in mind, when interpreting the model, that any neighboring lateral variations in the conductivity structure have some degree of influence on the profile, depending upon the distance to and magnitude of the anomaly. Normally, the influence is such as to produce a lateral smoothing effect on the cross section. Consequently, it must be considered that a change in any direction in the structure may, in reality, be more abrupt than reflected in the interpreted cross section. When a low degree of two- and three-dimensionality is indicated in the MT results the lateral structural variations (electrical parameters) are usually gradual enough to yield a reasonably faithful interpreted cross section.

Two-dimensional modeling is often useful for verifying the response to an anomaly in a particular region of the structure, but, because of the large number of degrees of freedom in the model, it is not usually practical to attempt a precise fit to the measured results. Two-dimensional modeling was not applied in the interpretation of this survey, primarily because of lack of time to produce a meaningful test. In any case, it was considered of lesser importance because of the fairly low degree of two- and three-dimensionality present.

Appendix B, Data Processing Procedure, continued...

After producing 1-D models, model parameter-tests were made using program LAYERPXY, which solves the forward MT solution, to estimate parameter tolerances or confidence limits.

Finally, a study was made to correlate the two- and three-dimensional properties of some of the computed MT results with the interpreted geoelectric cross sections. This includes the apparent anisotropy evidenced in the RTE and RTM functions, the rotation angles, $A(YZ)$, and the 3-D indicators ALPHA and BETA.

Table B-1 - Recording Frequency Bands

Band	Post Filter (Hz)	Sampling Rate (Hz)	Number Samples	Frequency Range Used (Hz)	No. Runs Recorded (Nominal)
B6	10-256	1000	4096	2.08-256	8
B5	1-25	100	4096	0.208-25.6	4
B4	.1-5	20	4096	0.0415-5.12	4
B3	.01-.5	2	4096	0.00415-0.512	2
B2	.002-.125	.5	2048	0.00208-0.128	1

Appendix C - Computer Programs

This section gives a brief description of programs:

- (1) MAGTAN2
- (2) INVERT
- (3) OPTMOD
- (4) LAYERPXY

Additional information on program functions, data tape formats, etc., are available on request.

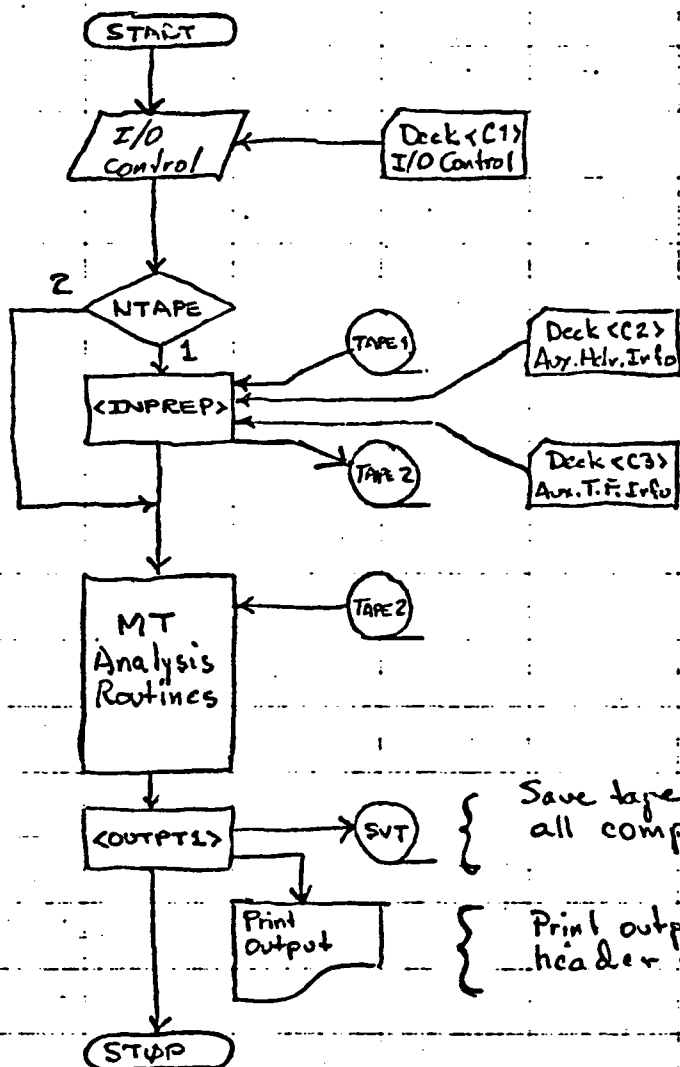
(1) MAGTAN MT ANALYSIS

Program Introduction

& Description of Transfer function form used to represent system

MAGTAN2

(Simplified Flow Diagram)



Save tape - header info, all computed MT Results.

Print output - Title page, header info, MT results

- Notes:
- 1) TAPE 1 - Packed binary field tape - Header - Site, system, sampling parameters
Data - N channels, time multiplexed
 - 2) TAPE 2 - Unpacked BCD tape - Header - TAPE 1 Header info & system polynomial coefficients
Data - N channels demultiplexed
 - 3) Card Deck C1 - Input/Output control parameters -
 - 4) Card Deck C2 - Auxilliary Header information -
 - 5) Card Deck C3 - Auxilliary Transfer function info. -
 - 6) Subroutine INPREP - controls unpacking of TAPE 1 & generation of TAPE 2. Info. from Decks C2 and C3 is included in TAPE 2.

28 May 74

PROGRAM MAGTANI (INPUT, OUTPUT, TAPE1, TAPE2, TAPE3, TAPE4, TAPE5,
TAPE6, TAPE7, PUNCH)

••• GEOTRONICS CORP - AUSTIN, TEXAS USA •••

••• PROGRAM <MAGTANI> ••• - FORTRAN IV ••• DRW5001X001

• MAGNETOTELLURIC (MT) ANALYSIS PROGRAM • GEOTRONICS CORPORATION
• FOR TENSOR SURFACE IMPEDANCE METHOD • AUSTIN, TEXAS - U.S.A.

PURPOSE: <MAGTANI> COMPUTES TENSOR IMPEDANCE METHOD MT RESULTS
FOR 5-COMPONENT E AND H FIELD MEASUREMENTS IN RECTANGULAR
COORDINATES.

COMPUTER ADAPTATION: CDC-6600

SOURCE LANGUAGE: FORTRAN IV
COMPASS

NO. OF SUBROUTINES: 43

CORE STORAGE REQMT: LOAD-155000 BASE-8
RUN -145000 BASE-8

PERIPHERAL STORAGE AND I/O:

TAPE UNITS- 1 ; FILE <TAPE1> (INPUT DATA - PACKED BINARY)
DISK UNITS- 6 ; FILE <TAPE2-7> (2-UNPKD DATA, 3-7-SCRATCH)
CARD HEADER
LINE PRINTER
OPTIONAL I/O -
TAPE UNITS- 2 ; FILE <TAPE2,8> (2-UNPKD DATA, 4-OUTPUT)
CARD PUNCH (SEE NOTE)
PLOTTER (SEE NOTE)

NOTE- DUMMY SUBROUTINES ARE INCLUDED FOR USER IMPLEMENTATION
OF TAPE, PUNCH, AND PLOT OUTPUT. ALL OUTPUT IS
CONTROLLED BY SUBROUTINE <OUTPT1>. COMPUTED RESULTS ARE
AVAILABLE TO OUTPUT ROUTINES VIA COMMON BLOCK <SPEC>.

SPECIAL CORE STORAGE AREAS:
COMMON BLOCK <SPEC> - 25000 WORDS

ROUTINES CALLED BY <MAGTANI>: <TITLE1>
<INPREP>
<POST2>
<XFURMK>
<IPSPEC>
<APSPEC>
<TITLE2>
<MAGTEL>
<SPECVAV>
<OUTPT1>

SPECIAL PROGRAM VARIABLES :

<TAPEID> - INPUT TAPE ID - FOR <TAPE> AND/OR <TAPE-2>.
 <TITLE> - TAPE FILE (DATA SET) TITLE.
 <TITLEA> - TITLE FOR AVERAGED RESULTS.
 <A,B,C,D,E,H> - SRATCH ARRAYS
 <NFREQ> - NO. OF OUTPUT FREQUENCIES.
 <FR(I)> - OUTPUT FREQ ARRAY- FREQ OF I TH WORD IN OUTPUT ARRAYS.
 <P(K,I)> - SIGNAL POWER SPECTRA ARRAY- K TH COMPONENT, I TH FREQ.
 <NSP(I)> - NO. OF INCREMENTAL SPECTRAL HARMONICS AVERAGED
 IN EACH P(K,I).

GENERAL: MOST PROGRAM VARIABLES AND PARAMETERS ARE DEFINED IN THE
 SECTIONS THAT DESCRIBE THEIR USE.

INDIVIDUAL SUBROUTINE HEADERS DESCRIBE THE PROGRAM FUNCTIONS
 AND THE ASSOCIATED PARAMETERS.

1. --- SCOPE ---

A. MT MODEL AND BASIC RELATIONSHIPS:

THE TOTAL ELECTRIC AND MAGNETIC FIELDS <E> AND <H> (FREQ (F) DOMAIN)
 AT POINT <O> ON THE EARTH SURFACE ARE CONSIDERED TO BE RELATED BY

$$(I-1,2) \quad \langle E \rangle = \langle Z \rangle \langle H \rangle \quad \text{OR} \quad \langle H \rangle = \langle Y \rangle \langle E \rangle \quad (\text{EXCLUDING } F=0);$$

WHERE <E>, <H> ARE VECTORS AND <Z>, <Y> ARE DYADIC TENSORS REPRESENTING
 THE SURFACE IMPEDANCE AND ADMITTANCE RESPECTIVELY. <Z> AND <Y> ARE
 FUNCTIONS OF FREQ, THE FIELD SOURCE AND THE EARTH PARAMETERS.

COORDINATE SYSTEM ---

STANDARD RIGHT HAND RECTANGULAR COORD SYSTEM (X,Y,Z-AXES) WITH
 +Z-DOWN (VERTICAL AXIS) AND THE ORIGIN AT POINT <O>. THE X-AXIS
 IS IN GENERAL ROTATED CLOCKWISE (LOOKING IN +Z-DIRECTION) BY AN
 ANGLE (A) FROM THE REFERENCE XR-AXIS, WHERE +XR-NORTH, +YR-EAST.
 IN THE ROTATED COORD SYSTEM <E(A)>=<Z(A)><H(A)>, ETC.

MODEL ---

Z ≥ 0 - SEMI-INFINITE CONDUCTIVE HALF-SPACE (SOLID EARTH) WITH
 GENERALLY 3-DIMENSIONAL INTRINSIC PROPERTIES.
 Z < 0 - FREE SPACE

FIELD SOURCE ---

EM PLANE WAVE PROPAGATING IN +Z-DIRECTION (DOWN) AND INCIDENT
 ON Z=0 SURFACE. ANY POLARIZATION IS ALLOWABLE EXCEPT AT LEAST SOME
 DEGREE OF RANDOM POLARIZATION IS REQUIRED BY THE COMPUTATION PROCESS.

<Z> AND <Y> ARE INDEPENDENT OF PLANE WAVE SOURCE CONDITIONS.

FIELD RELATIONS IN RECTANGULAR COORD SYSTEM ---

FOR THE (X,Y,Z-AXES) EQUATIONS (I-1) AND (I-2) BECOME

$$(I-3) \quad EX(A) = ZXX(A) HX(A) + ZXY(A) HY(A)$$

$$(I-4) \quad EY(A) = ZYX(A) HX(A) + ZYY(A) HY(A)$$

$$(I-5) \quad HX(A) = YXX(A) EX(A) + YXY(A) EY(A)$$

$$(I-6) \quad HY(A) = YYX(A) EX(A) + YYY(A) EY(A)$$

$$(I-7) \quad HZ(A) = YZX(A) EX(A) + YZY(A) EY(A)$$

ANOTHER MT RELATIONSHIP TO CONSIDER IS OBTAINED BY SUBSTITUTING (I-3), (I-4) INTO (I-7)

$$(I-8) \quad HZ(A) = KZX(A) HX(A) + KZY(A) HY(A)$$

REFERENCE INFO ---

WORD, D.R., M.W. SMITH, F.X. BOSTICK, JR., "AN INVESTIGATION OF THE MAGNETOTELLURIC TENSOR IMPEDANCE METHOD", ELECTRICAL GEOPHYSICS RESEARCH LAB., TECH REPT NO. 82, UNIV. OF TEXAS, AUSTIN, TEX., 1970.

B. PROGRAM FUNCTION:

<MAGTANI> PERFORMS THE FOLLOWING FUNCTIONS (IN ORDER SHOWN)---

- 0- INPUT I/O CONTROL PARAMETERS AND DATA ACQUISITION SYS. INFO.
- 1- INPUT TIME DOMAIN SAMPLED DATA REPRESENTING ALL RECTANGULAR COMPONENTS OF <E> AND <H> FOR THE REF COORD DIRECTIONS XR, YR, AND Z.
- 2- FOURIER TRANSFORM ALL SIGNAL COMPONENTS.
- 3- MODIFY SPECTRAL WINDOW TO REDUCE SIGNAL TRUNCATION ALIASING.
- 4- SCALE DATA WITH GENERALIZED FREQ FUNCTIONS - TO CORRECT FOR DATA ACQUISITION TRANSFER FUNCTIONS, ETC.
- 5- COMPUTE INCREMENTAL AUTO- AND CROSS-POWER SPECTRA FOR ALL FIELD COMPONENTS.
- 6- COMPUTE FREQ BAND AVERAGE OF INCR AUTO- AND CROSS-POWER SPECTRA AND ASSOCIATED FREQ ARRAY FOR AVERAGED SPECTRA.
- 7- COMPUTE <E> AND <H> POLARIZATION PROPERTIES.
- 8- COMPUTE <Z(A)> AND <Y(A)> ELEMENTS (AMPL AND PHASE) FOR A=0 AND FOR THE VARIOUS PRINCIPAL VALUES OF (A). COHERENCIES, DIMENSIONAL PROPERTIES (SKEW AND ELLIPTICITY); AND INDICATORS OF COMPUTATIONAL STABILITY ARE ALSO COMPUTED. <ZIF(A)> IS ALSO COMPUTED FOR 10 DEGREE INCREMENTS IN (A).
- 9- OUTPUT RESULTS PER OUTPUT OPTION SELECT ARRAY (I/O CONTROL).

NOTE - THE FREQ RANGE OF COMPUTATION FOR ITEMS 2-8 IS THE ENTIRE RANGE ALLOWED BY SAMPLING COND.

I. --- PROGRAM OPERATION ---

A. INPUT :

- 1- I/O CONTROL - <C1> DATA CARD DECK

(A)

2- DATA - <TAPE1> PACKED BINARY TAPE (BMR FORMAT) (1 5-CH DATA)
OR <TAPE2> UNPACKED BCD TAPE (BC FORMAT) (SET/FILE)

3- AUX TAPE1
HEADER INFO - <C2> DATA CARD DECK (OPTIONAL)

4- AUX SYSTEM
TRANSFER FN - <C3> DATA CARD DECK (OPTIONAL)

<MAGTAN1> HAS A NUMBER OF BASIC INPUT OPTIONS. A PRECISE DEFINITION
OF THE OPTIONS AND THE VARIOUS CONTROLLING PARAMETERS IS PROVIDED IN
THE DESCRIPTION OF CARD DECK <C1>. THE MAIN OPTIONS ARE:

- (1) <TAPE1> OR <TAPE2> MAY BE USED AS INPUT.
- (2) <TAPE1> MAY BE UNPACKED WITH OR WITHOUT FULL EXEC OF <MAGTAN1>
- (3) <TAPE1> HEADER INFO MAY BE INPUT FROM <TAPE1>, <C2>, OR A MIXTURE.
- (4) AUXILIARY TRANSFER FUNCTION INFO MAY BE INPUT FROM <C3> FOR
ANY FREQ DOMAIN SCALING OF THE DATA.
- (5) <TAPE1> FILES MAY BE SELECTED IN ANY ORDER. DATA RECORDS
WITHIN A FILE MAY BE SKIPPED PRIOR TO READ. THIS FILE AND
RECORD SELECT DETERMINES THE ORDER IN WHICH DATA IS PLACED
ON <TAPE2> (WHICH MAY BE EITHER A DISK OR TAPE UNIT).
- (6) <TAPE2> FILES MAY BE SELECTED IN ANY ORDER.
- (7) DATA SETS ARE PROCESSED INDIVIDUALLY. THE POWER SPECTRAL AVERAGE
OF SPECIFIED GROUPS OF COMPATIBLE DATA SETS MAY BE COMPUTED
AND PROCESSED.

DATA CARD DECK STRUCTURE:

READ ORDER -- 1- DECK <C1> I/O CONTROL READ BY <MAGTAN1>
2- DECK <C2(N)> (FOR DATA SET N), READ BY <MOMCROS>
3- DECK <C3(N)> (FOR DATA SET N), READ BY <AUXMOD>

- REPEAT THE <C2>, <C3> GROUP FOR EACH DATA FILE
READ AND PROCESSED FROM <TAPE1> IN THE ORDER (N)
SELECTED FROM <TAPE1>. EITHER OR BOTH <C2> AND
<C3> MUST BE OMITTED IF THE CORRESPONDING AUX
INPUT IS NOT OPTED BY <C1>. FOR <TAPE2> DATA
INPUT ONLY <C1> IS REQUIRED.

SYSTEM FUNCTION ---

A STANDARDIZED FUNCTIONAL FORM IS USED TO REPRESENT A SYSTEM CHANNELS AND THE NOS. OF POLES AND ZEROS ARE FIXED. A FIXED NO. OF ZEROS IS PLACED AT THE ORIGIN AND CERTAIN POLE ALLOCATIONS ARE COMMITTED TO LO-CUT USE WITH THE ORIGIN ZEROS. LO-CUT POLES NOT USED ARE TO BE PLACED AT THE ORIGIN. OTHER POLES AND ZEROS ARE TO BE PLACED AT A HIGH ENOUGH FREQ TO BE INEFFECTIVE IN THE PASS BAND. THE FOLLOWING NOTATION WILL USE: <J> - SYSTEM CHAN NO.

<I> - POLE OR ZERO INDEX.
<AP(J)> - PREAMP GAIN - CHAN J.
<AFO(J)> - POSTAMP GAIN - CHAN J.
<KX(J)> - SENSOR GAIN FACTOR.
<KP(J)> - POLE-ZERO NORMALIZING FACTOR - PREAMP.
<KI(J)> - POLE-ZERO NORMALIZING FACTOR - PLUG-IN FILTER.
<KF(J)> - POLE-ZERO NORMALIZING FACTOR - POST FILTER.
<S> - COMPLEX FREQ.
<P(I,J)> - SYSTEM POLE.
<Z(I,J)> - SYSTEM ZERO.

7
<DF(J)> = E-LINE LENGTH (METERS)
<GA(J)> = AUX TRANSFER FN GAIN FACTOR.
<PA(I,J)> = AUX TRANSFER FN POLE.
<ZA(I,J)> = AUX TRANSFER FN ZERO.
<NPA(J)> = NO. AUX TF POLES - CH J
<NZA(J)> = NO. AUX TF ZEROS - CH J

PRD <X(I)>, I=1, N = X(1)*X(2)*...*X(N)

SENSOR-PREAMP FN -

$$GP(J) = \frac{AP(J) \cdot KX(J) \cdot KP(J) \cdot (S)}{\text{PRD } \langle S-P(I,J) \rangle, I=1,6} \cdot KX(J) = (1.E-6) \cdot DE(J), J=1,2$$

= 1.0, J=3,5

WHERE KP(J) = CABS(PRD <P(I,J)>, I=2,6)

P(1,J) = LO-CUT POLE.

PLUG-IN FILTER FN -

$$GI(J) = K1(J) \cdot \frac{\text{PRD } \langle S-Z(I,J) \rangle, I=1,4}{\text{PRD } \langle S-P(I,J) \rangle, I=7,10}$$

WHERE K1(J) = CABS((PRD <P(I,J)>, I=7,10) / (PRD <Z(I,J)>, I=1,4))

POST AMP-FILTER FN -

$$GF(J) = \frac{AFD(J) \cdot KF(J) \cdot (S^3)}{\text{PRD } \langle S-P(I,J) \rangle, I=11,19}$$

WHERE KF(J) = CABS(PRD <P(I,J)>, I=14,19)

P(I,J), I=11,13 = LO-CUT POLES.

SYSTEM TRANSFER FN -

$$GO(J) = GP(J) \cdot GI(J) \cdot GF(J)$$

AUXILIARY TRANSFER FN --- SEE <AUXMOD> FOR INPUT DETAILS.

$$G(J) = GA(J) \cdot \frac{\text{PRD } \langle S-ZA(I,J) \rangle, I=1, NZA(J)}{\text{PRD } \langle S-PA(I,J) \rangle, I=1, NPA(J)}$$

TOTAL TRANSFER FUNCTION REMOVED FROM DATA ---

$$GOX(J) = GO(J) \cdot G(J)$$

SEE <POLYCO> FOR THE POLYNOMIAL REPRESENTATION OF <GOX> AS
IT IS USED FOR RESPONSE CORRECTION IN <FILTER>.

C. OUTPUT I

6/8

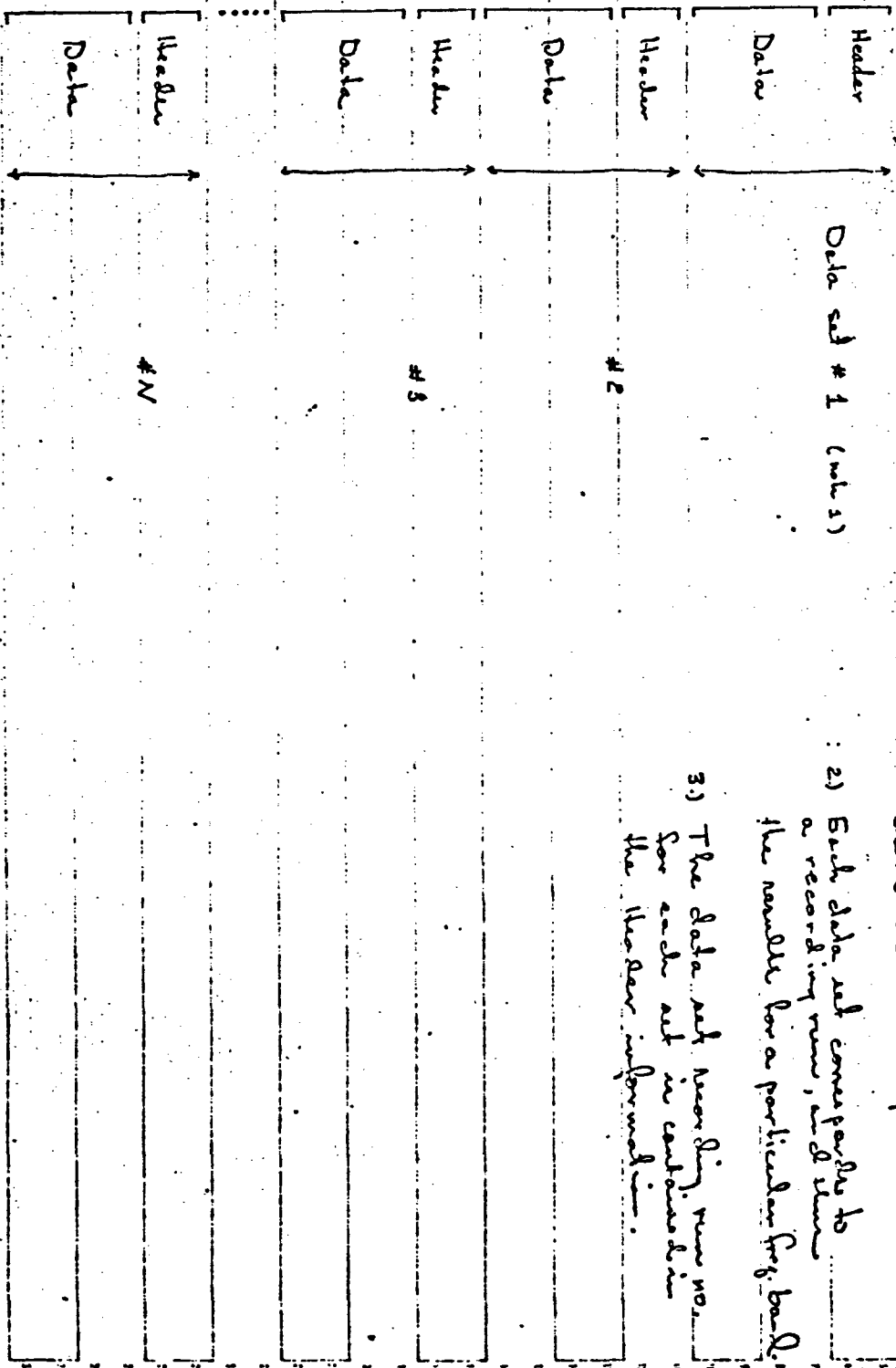
OTHER SPECIAL OUTPUT ROUTINES. THE OUTPUT OPTION SELECT ARRAY <IOS>
(READ IN VIA DECK <C1>) IS CHECKED TO DETERMINE THE OUTPUT STATUS.
ALL COMPUTED RESULTS ARE MADE AVAILABLE TO <C1> W/ COMMON <SPEC>.

SUBROUTINE <OUTPRT> FOR LINE PRINTER OUTPUT IS PRESENTLY INCLUDED.
SUBR<OUTCARD>,<OUTTAPE>,<OUTPLOT> ARE INSERTED AS BLANK ROUTINES FOR
THE USER TO IMPLEMENT WITH HIS DESIRED FORMAT.

SEE SUBROUTINES <MAGTEL>,<ZFIT>,<OUTPT1> FOR OUTPUT PARAM DETAILS.

Save Tape (Merge Tapes) Format

BPT Beg of Tape reflecting work



Notes:

- 1) See SAVE TAPE FORMAT and send for detail of format of individual data sets on tape.
- 2) Each data set corresponds to a recording run, and items the number for a particular freq band.
- 3) The data set recording run no. for each set is contained in the header information.

~~1/6~~

SUBROUTINE OUTTAPE (TITLE,IOS,I1,I2,I3)

```

C
C SAVE TAPE FORMAT
C
C ---HEADER RECORD---
C
C VARIABLE OR ARRAY          WORD NUMBER
C   FLAG1                    1
C   NFREQ                    2
C   IOS                      3--82
C   I1                       R3
C   I2                       R4
C   I3                       R5
C   DATE                     R6
C   HOUR                     R7
C   MIN                      R8
C   SEC                      R9
C   HEAD2(1-500)            90--589
    
```

---DATA RECORD---

```

C
C VARIABLE OR ARRAY          WORD NUMBER
C   FLAG2                    1
C   NFREQ                    2
C   PASSLVLS                 3--27
C   FR                       23--22*NREQ
C   NSP                      23*NREQ--22*2*NREQ
C   PP                       23*2*NREQ--22*27*NREQ
C   DFPC                     23*27*NREQ--22*29*NREQ
C   ELIPC                    23*29*NREQ--22*31*NREQ
C   IANC                     23*31*NREQ--22*33*NREQ
C   RHOC                     23*33*NREQ--22*35*NREQ
C   IAC                      23*35*NREQ--22*37*NREQ
C   COR                      23*37*NREQ--22*4 *NFR58
C   RC                      23*41*NREQ--22*45*NREQ
C   IPC                      23*45*NREQ--22*49*NREQ
C   COC                      23*49*NREQ--22*53*NREQ
C   PRC                      23*53*NREQ--22*58*NREQ
C   ANC                      23*58*NREQ--22*63*NREQ
C   COHC                    23*63*NREQ--22*68*NREQ
C   ANGC                    23*68*NREQ--11*71*NREQ
C   KMMC                    23*71*NREQ--22*73*NREQ
C   ALPC                    23*73*NREQ--22*75*NREQ
C   RTAC                    23*75*NREQ--22*78*NREQ
C   DELC                    23*78*NREQ--22*80*NREQ
C   KZF                     23*80*NREQ--22*82*NREQ
C   AKZ                     23*82*NREQ--22*84*NREQ
C   COK                     23*84*NREQ--22*85*NREQ
C   ANK                     23*85*NREQ--22*86*NREQ
C   RTAK                    23*86*NREQ--22*87*NREQ
C   IXXC                    23*87*NREQ--22*105*NREQ
C   IXYC                    23*105*NFR50--22*123*NFR58
C   IEXXC                   23*123*NREQ--22*124*NREQ
    
```

```

OUTTAPE 2
OUTTAPE 3
OUTTAPE 4
OUTTAPE 5
OUTTAPE 6
OUTTAPE 7
OUTTAPE 8
OUTTAPE 9
OUTTAPE 10
OUTTAPE 11
OUTTAPE 12
OUTTAPE 13
OUTTAPE 14
OUTTAPE 15
OUTTAPE 16
OUTTAPE 17
OUTTAPE 18
OUTTAPE 19
OUTTAPE 20
OUTTAPE 21
OUTTAPE 22
OUTTAPE 23
OUTTAPE 24
OUTTAPE 25
OUTTAPE 26
OUTTAPE 27
OUTTAPE 28
OUTTAPE 29
OUTTAPE 30
OUTTAPE 31
OUTTAPE 32
OUTTAPE 33
OUTTAPE 34
OUTTAPE 35
OUTTAPE 36
OUTTAPE 37
OUTTAPE 38
OUTTAPE 39
OUTTAPE 40
OUTTAPE 41
OUTTAPE 42
OUTTAPE 43
OUTTAPE 44
OUTTAPE 45
OUTTAPE 46
OUTTAPE 47
OUTTAPE 48
OUTTAPE 49
OUTTAPE 50
OUTTAPE 51
OUTTAPE 52
OUTTAPE 53
OUTTAPE 54
OUTTAPE 55
    
```

Notes:

- Header Record flag, FLAG1 = 1
 - NREQ = 27 (for all runs up through
 APPROX. May 1975)

- TAPE 2 header words in order - see
 TAPE 2 specs.

- Data Record flag, FLAG2 = 0

- not currently used

VERSION 2.3 --PSR LEVEL 363--

03/09/75

C	TEXYC	23*124*NFREQ--22*125*NFREQ	OUTTAPE	56
C	EPDCOH	23*125*NFREQ--22*126*NFREQ	OUTTAPE	57 -
C	HPDCOH	23*126*NFREQ--22*127*NFREQ	OUTTAPE	58 -
C			OUTTAPE	59
C			OUTTAPE	60
10	* COMMON /SPEC/SP(8193),	FR(100),RNSP(100),P(25,140),PP(100,25)	OUTTAPE	61
	1,DEPC(100,2),ELIPC(100,2),RIANC(100,2),RHOC(100,2),RIAC(100,2),		OUTTAPE	62
	2COR(100,2),RC(100,4),RIPC(100,4),COC(100,4),RRC(100,5),ANC(100,5),		OUTTAPE	63
	3 COMC(100,5),ANGC(100,3),RKMMC(100,2),ALPC(100,2),RTAC(100,3),DELC		OUTTAPE	64
	4(100,2),RKZE(100,2),AKZ(100,2),COK(100),ANK(100),RTAK(100),		OUTTAPE	65
	5PIXXC(100,18),RIXYC(100,18),RIEXXC(100),RIEXYC(100),EPDCOH(100),		OUTTAPE	66
	6HPDCOH(100)		OUTTAPE	67
110	COMMON /HEADER/ HEAD2(500)		OUTTAPE	68
110	COMMON /PASSLVL/ ARRAY(20)		OUTTAPE	69
110	DIMENSION TITLE(A),RIOS(80),IOS(1)		OUTTAPE	70
110	INTEGER DATE,CLOCK		OUTTAPE	71

* See subsequent description of variable names in
the enclosed documentation section for Subroutine MACTEL.

Header and Data records each written by FORTRAN III WRITE statement
of form:

WRITE (i) l , where i - unit number
l - variable list

SUBROUTINE MAGTEL (P,F,NSP,TITLE,NFREQ,NBIAS)

 ** GEOTRONICS CORP - AUSTIN, TEXAS USA **

SUBROUTINE *MAGTEL* - FORTPAN IV DRW5022X001

USEO CALL MAGTEL (P,F,NSP,TITLE,NFREQ,NBIAS)

MAGTEL COMPUTES MAGNETOTELLURIC (MT) RESULTS FROM THE POWER SPECTRA MATRIX *P*. QUANTITIES COMPUTED ARE DESCRIBED BELOW IN THE NOTATION GIVEN IN THE *MAGTANI* HEADER. ALL OUTPUT QUANTITIES ARE STORED IN COMMON *SPEC* FOR FURTHER ACCESS BY OUTPUT ROUTINES.

PARAMETERS:

P(J,I) - AUTO- AND CROSS-POWER SPECTRA MATRIX FOR FIELD COMPONENTS *EX,EY,HX,HY,HZ*.

I- FREQ INDEX
 J- COMPONENT INDEX

SPEC COMPONENT LOCATIONS -

J= 1-PEXEX 10-PEYEX 18,19-PHXHY
 2,3-PEXEY 11,12-PEYHX 20,21-PHXHZ
 4,5-PFXHX 13,14-PEYHY 22-PHYHY
 6,7-PEXHY 15,16-PEYHZ 23,24-PHYHZ
 8,9-PEXHZ 17-PHXHX 25-PHZHZ

(CROSS-POWERS ARE STORED WITH REAL AND IMAG PARTS ADJACENT WORDS IN ORDER)

NOTE 1-E-POWER UNITS - (MV/KM)**2/HZ
 H-POWER UNITS - GAMMA**2/HZ
 E-H-POWER UNITS - (MV/KM)*GAMMA/HZ

NOTE 2-THE COMPONENT ORDER GIVEN IS FOR *P* UPON INPUT TO *MAGTEL*. THE *P* ORDER IS MODIFIED IN *MAGTEL* AFTER CALL OF *ZFIT* AND SOME INFO IS DISCARDED. THE UNMODIFIED *P(J,I)* INFO IS SAVED IN *PP(I,J)*. BOTH ARE STORED IN *SPEC*.

F(I) - FREQ OF ITH WORD IN ALL OUTPUT ARRAYS (HZ).
 NSP(I) - NO. OF INCREMENTAL HARM ASSOC WITH *FR(I)*.
 TITLE - TITLE OF DATA SET.
 NFREQ - NO. OF WORDS IN *FR(I)* (I=1,NFREQ).
 NBIAS - NO. OF COMPONENTS IN *P(J,I)* (J=1,NBIAS)

ROUTINES CALLED *ZFIT*
 IDATAN

SPECIAL STORAGE AREAS
 COMMON BLOCK *SPEC* - 25000 WORDS

MT RESULTS COMPUTED (ARRAYS IN COMMON *SPEC*)
 NOTE 1-SFE *MAGTANI* FOR NOTATION.
 NOTE 2-I - FREQ INDEX (I=1,NFREQ).
 J - CONTENTS INDEX

MAGTEL	2
MAGTEL	3
MAGTEL	4
MAGTEL	5
MAGTEL	6
MAGTEL	7
MAGTEL	8
MAGTEL	9
MAGTEL	10
MAGTEL	11
MAGTEL	12
MAGTEL	13
MAGTEL	14
MAGTEL	15
MAGTEL	16
MAGTEL	17
MAGTEL	18
MAGTEL	19
MAGTEL	20
MAGTEL	21
MAGTEL	22
MAGTEL	23
MAGTEL	24
MAGTEL	25
MAGTEL	26
MAGTEL	27
MAGTEL	28
MAGTEL	29
MAGTEL	30
MAGTEL	31
MAGTEL	32
MAGTEL	33
MAGTEL	34
MAGTEL	35
MAGTEL	36
MAGTEL	37
MAGTEL	38
MAGTEL	39
MAGTEL	40
MAGTEL	41
MAGTEL	42
MAGTEL	43
MAGTEL	44
MAGTEL	45
MAGTEL	46
MAGTEL	47
MAGTEL	48
MAGTEL	49
MAGTEL	50
MAGTEL	51
MAGTEL	52
MAGTEL	53
MAGTEL	54
MAGTEL	55

* * *
 * * * +NFREQ> - NO. OF FREQS.
 * * * +FR(I)> - FREQ. - I=1,NFREQ - (HZ)
 * * * +NSP(I)> - NO. INCREMENTAL HARM AVGD FOR +FR(I)>.
 * * *
 * * * +P(J,I)> - POWER SPECTRA MATRIX - SEE ABOVE DESCR.
 * * * +PP(I,J)> - = +P(J,I)> PRIOR TO ANY MOD OF +P>.
 * * *
 * * * +DEPC(I,J)> - J=1,2 - RATIO OF UNPOLARIZED POWER TO TOTAL
 * * * POWER OF E AND H FIELDS RESPECTIVELY.
 * * *
 * * * +ELIPC(I,J)> - J=1,2 - RATIO OF MINOR TO MAJOR AXIS OF
 * * * POLARIZATION ELLIPSE FOR POLARIZED COMPONENTS
 * * * OF E AND H(HORIZ) FIELDS RESPECTIVELY.
 * * * (+ FOR RT HAND POLARIZ - CLOCKWISE WHEN
 * * * LOOKING IN +Z-AXIS DIRECTION)
 * * *
 * * * +IANG(I,J)> - AZIMUTH ANGLE (DEGREES) OF MAJOR AXIS OF
 * * * POLARIZ ELLIPSE FOR E AND H(HORIZ) FIELDS.
 * * *
 * * * 0 +RHOC(I,J)> - J=1,2- APPARENT RESISTIVITY (APP RES) FOR
 * * * 0 ZX AND ZY RESPECTIVELY (OHM-METERS).
 * * * 0 +IAC(I,J)> - J=1,2- PHASE OF ZX AND ZY (DEGREES).
 * * * 0 +COR(I,J)> - COHERENCY FOR (EX-HY) AND (EY-HX).
 * * * 0
 * * * 0 WHERE ZX = EX/HY AND ZY = EY/HX (UNROTATED CAGNIARD Z).
 * * *
 * * * +RC(I,J)> - J=1,4- APP RES FOR TENSOR +Z> ELEMENTS
 * * * ZXX,ZYY,ZXY,ZYX IN ORDER (OHM-METERS).
 * * * +IPC(I,J)> - J=1,4- PHASE OF ZXX,ZYY,ZXY,ZYX (DEGREES)
 * * * +COC(I,J)> - J=1,4- PHASOR COHERENCY FOR ZXX,ZYY,ZXY,ZYX.
 * * *
 * * * NOTE--ROTATED +Z> AND +Y> RESULTS --- IN THE FOLLOWING THE
 * * * XY-AXES ARE ROTATED AT EACH FREQ TO ANGLE +A>=+A(Z)>
 * * * FOR +Z> AND INVERTED +Y> TENSORS SO THAT
 * * * CAHS+ZXY(A)+ZYX(A)> IS MAX FOR +A>=+A(Z)>. THE XY-AXES
 * * * ARE ROTATED FOR +YZ> (EQUATION I-7 OF +MAGTAN)> TO
 * * * ANGLE +A>=+A(YZ)> SO THAT CAHS+YZY(A)> IS MAX (HZ IS
 * * * MOST COHERENT WITH EY). THE XY-AXES ARE ROTATED FOR
 * * * +KZ> (EQUATION I-8 OF +MAGTAN)> TO +A>=+A(KZ)> SO THAT
 * * * CAHS+KZX(A)> IS MAX (HZ IS MOST COHERENT WITH HX).
 * * * FINALLY THE IMPEDANCES +ZTE> (E PARALLEL TO STRIKE)
 * * * AND +ZTM> (H PARALLEL TO STRIKE) ARE SELECTED FROM
 * * * +ZXY(A(Z))> AND +ZYX(A(Z))> ON THE BASIS OF THE
 * * * 1ST AN 4TH QUADRANT PRINCIPLE VALUES OF +A(Z)> AND
 * * * +A(YZ)> -
 * * * IF (ABS+A(Z)-A(YZ))>.LE.45 DEGR) --+ZTE>=+ZYX(A(Z))>
 * * * +ZTM>=+ZXY(A(Z))>
 * * * IF (ABS+A(Z)-A(YZ))>.GT.45 DEGR) --+ZTE>=+ZXY(A(Z))>
 * * * +ZTM>=+ZYX(A(Z))>
 * * *
 * * * +RRC(I,J)> - J=1,2- APP RES - +ZTE>,+ZTM> - +Z> TENSOR
 * * * 3,4- APP RES - +ZTE>,+ZTM> - +Y> TENSOR
 * * * 5- APP RES - +YZY(A(YZ))>- +Y> TENSOR
 * * * (I.E.- APP RES FOR EY/HZ AT +A(YZ)>.)

MAGTEL 56
 MAGTEL 57
 MAGTEL 58
 MAGTEL 59
 MAGTEL 60
 MAGTEL 61
 MAGTEL 62
 MAGTEL 63
 MAGTEL 64
 MAGTEL 65
 MAGTEL 66
 MAGTEL 67
 MAGTEL 68
 MAGTEL 69
 MAGTEL 70
 MAGTEL 71
 MAGTEL 72
 MAGTEL 73
 MAGTEL 74
 MAGTEL 75
 MAGTEL 76
 MAGTEL 77
 MAGTEL 78
 MAGTEL 79
 MAGTEL 80
 MAGTEL 81
 MAGTEL 82
 MAGTEL 83
 MAGTEL 84
 MAGTEL 85
 MAGTEL 86
 MAGTEL 87
 MAGTEL 88
 MAGTEL 89
 MAGTEL 90
 MAGTEL 91
 MAGTEL 92
 MAGTEL 93
 MAGTEL 94
 MAGTEL 95
 MAGTEL 96
 MAGTEL 97
 MAGTEL 98
 MAGTEL 99
 MAGTEL 100
 MAGTEL 101
 MAGTEL 102
 MAGTEL 103
 MAGTEL 104
 MAGTEL 105
 MAGTEL 106
 MAGTEL 107
 MAGTEL 108
 MAGTEL 109
 MAGTEL 110

* +AMC(I,J)> - J=1,2- PHASE - +ZTE>,+ZTM> - +Z> TENSOR	* MAGTEL	111
3,4- PHASE - +ZTE>,+ZTM> - +Y> TENSOR	* MAGTEL	112
5- PHASE - +YZY(A(YZ))> - +Y> TENSOR	* MAGTEL	113
* +COMC(I,J)> - J=1,2- PHASOR COH - +ZTE>,+ZTM> - +Z> TENSOR	* MAGTEL	114
3,4- PHASOR COH - +ZTE>,+ZTM> - +Y> TENSOR	* MAGTEL	115
5- PHASOR COH - +YZY(A(YZ))> - +Y> TENSOR	* MAGTEL	116
* +ANGC(I,J)> - J=1,2- +A(Z)>-+Z> TENSOR, +A(Y)>-+Y> TENSOR	* MAGTEL	117
3- +A(YZ)> - +Y> TENSOR	* MAGTEL	118
* +DFLC(I,J)> - J=1,2- NORMALIZED DENOMINATOR TERMS ASSOC	* MAGTEL	119
WITH SOLUTIONS FOR +Z> AND +Y> RESP.	* MAGTEL	120
(USED TO ASSESS COMPUTATIONAL	* MAGTEL	121
STABILITY, +Z> OR +Y> ESTIMATE IS	* MAGTEL	122
ACCEPTED IF +DFLC>.GE.+0.1>).	* MAGTEL	123
* +ALPC(I,J)> - J=1,2- TENSOR SKEW FOR +Z> AND +Y> RESP.	* MAGTEL	124
DEFN	* MAGTEL	125
+ALPC>=+ZXX+ZYY>/+ZXY-ZYX>	* MAGTEL	126
(INDEPENDENT OF +A>).	* MAGTEL	127
* +RTAC(I,J)> - J=1,3- TENSOR ELLIPTICITY FOR +Z>,+Y>,+YZ>	* MAGTEL	128
RESP. DEFN	* MAGTEL	129
+RTAC>=+YZX(A)>/+YZY(A)>,+A>=+A(YZ)>	* MAGTEL	130
* +KMMC(I,J)> - J=1,2- NO.OF INDEPENDENT SOLUTIONS OF	* MAGTEL	131
+Z> AND +Y> RESP ACCEPTED AND AVGD	* MAGTEL	132
TOGETHER - USING +DFLC> ACCEPTANCE TEST	* MAGTEL	133
* +KZX(A)>,+KZY(A)> RESP FOR +A>=+A(KZ)>	* MAGTEL	134
(EQUATION I-A OF +MAGTANI>)	* MAGTEL	135
* +AKE(I,J)> - J=1,2- PHASE FOR +KZX(A)>,+KZY(A)>,+A>=+A(KZ)>	* MAGTEL	136
+COK(I)> - (HZ-HX) COHERENCY FOR +A>=+A(KZ)>	* MAGTEL	137
+ANK(I)> - +A(KZ)> FOR +KZ> TENSOR	* MAGTEL	138
+RTAK(I)> - +KZ> TENSOR ELLIPTICITY.	* MAGTEL	139
DEFN +RTAK> = +KZY(A)>/+KZX(A)>.	* MAGTEL	140
+A>=+A(KZ)>	* MAGTEL	141
	* MAGTEL	142
	* MAGTEL	143
NOTE--THE FOLLOWING ARRAYS PERTAIN TO ROTATION OF +ZXX>	* MAGTEL	144
AND +ZXY> BY 10 DEGREE INCREMENTS FROM +A>=-90 DEG	* MAGTEL	145
TO +A>=+90 DEG FOR EACH FREQ VALUE.	* MAGTEL	146
	* MAGTEL	147
* +IXXC(I,J)> - J=1,18- APP RES FOR +ZXX(A)>, -90<A<+90 DEGR	* MAGTEL	148
IN 10 DEGR INCR. (DIVIDED BY 10**IXXC)>	* MAGTEL	149
* +IXYC(I,J)> - J=1,18- APP RES FOR +ZXY(A)>, -90<A<+90 DEGR	* MAGTEL	150
IN 10 DEGR INCR. (DIVIDED BY 10**IXYC)>	* MAGTEL	151
* +IEXXC(I)> - DECIMAL EXPONENT FOR +IXXC>.	* MAGTEL	152
* +IEXYC(I)> - DECIMAL EXPONENT FOR +IXYC>.	* MAGTEL	153
	* MAGTEL	154
NOTE--REFER TO REFERENCE(S) GIVEN IN +MAGTANI> FOR MORE	* MAGTEL	155
DETAILED DESCRIPTION OF THE MT THEORY AND COMPUTATIONS	* MAGTEL	156
	* MAGTEL	157
	* MAGTEL	158
	* MAGTEL	159

MAGTAN 2 - Line Printer Output
Specific

```

SURROUTINE OUTPT1 (TITLE,IOS,I1,I2,I3)
*****
** GEOTRONICS CORP - AUSTIN, TEXAS USA **
*
SUBROUTINE +OUTPT1> - FORTRAN IV          DRW5014X001
*
USE0 CALL OUTPUT1 (TITLE,IOS,I1,I2,I3)
*
OUTPUT1 CONTROLS THE OUTPUT OF +MAGTAN1>. ARRAYS TO BE
OUTPUT ARE TAKEN FROM COMMON BLOCK +SPEC>. OUTPUT
OPTIONS ARE CONTROLLED BY THE I/O SELECT ARRAY +IOS>.
+IOS> ALLOWS SELECTION OF ANY OR ALL OF A NUMBER
OF PRINTED OUTPUT SUBSETS PER SUBR+OUTPRNT>, PUNCH
CARD OUTPUT PER SUBR+OUTCARD>, AND MAG TAPE OUTPUT
PER SUBR+OUTTAPE>. THE FLAG PARAMETERS +I1>,+I2>,+I3>
ARE PASSED TO INDICATE THE IDENTITY AND STATUS OF
THE DATA SET BEING PROCESSED. THESE MAY BE USED WITH
+IOS> IN SELECTION OF THE OUTPUT OPTIONS WITH LOGIC
ADDED BY THE USER.
(PLOT OUTPUT BY SUBR+OUTPLOT> MAY BE EASILY INCLUDED
BY ADDING THE PROPER CALLING LOGIC TO +OUTPT1>, USING
BLANK ELEMENTS OF +IOS>.)
*
PARAMETERS0
+TITLE> - DATA SET TITLE.
+IOS(N)> - I/O SELECT ARRAY - (80 SINGL CHAR ELEMENTS).
          IOS(N)=1 - ENABLE CONDX FOR ITEM N
          =0 - DISABLE CONDX FOR ITEM N
---TABLE OF PRESENT IMPLEMENTATION OF +IOS> OPTIONS.
N#1 - TITLE PAGE 1 - PER SUBR+TITLE1>.
  2 - TITLE PAGE 2 - PER SUBR+TITLE2>.
  3 - DECODED TAPE1 HEADER INFO - PER SUBR+TFOUT>.
  4 - BLANK
  5 - ENABLE CALL SUBR+OUTPRNT> - CK IOS(N),N= 6,19.
  6 - E-H FIELD AUTO-POWER SPECTRA. --+OUTPRNT>.
  7 - E-H FIELD POLARIZATION PROPERTIES. --+OUTPRNT>.
  8 - Z-SCALAR RESULTS - UNROTATED. --+OUTPRNT>.
  9 - Z-TENSOR RESULTS - UNROTATED. --+OUTPRNT>.
 10 - Z-TENSOR RESULTS - ROTATED. --+OUTPRNT>.
 11 - Y-TENSOR RESULTS - ROTATED. --+OUTPRNT>.
 12 - HZ-RELATIONS - ROTATED. --+OUTPRNT>.
 13 - Z-TENSOR AXIS ROTATION - FREQ MAP.--+OUTPRNT>.
 14 - PRINT SETS 5,13 FOR AVG RESULTS ONLY.
 15-19 - BLANK
 20 - ENABLE CALL SUBR+OUTCARD> - CK IOS(N),N=21,29.
 21-29 - BLANK
 30 - ENABLE CALL SUBR+OUTTAPE> - CK IOS(N),N=31,39.
 31-39 - BLANK
 40-80 - BLANK (MAY BE USED FOR ADDED OPTIONS).
NOTE- IN PRESENT USE +IOS> ELEMENTS HAVE ONLY 2 STATES
+0> AND +1>. THE USER MAY INTRODUCE STILL MORE
FLEXIBILITY BY IMPLEMENTING THE USE OF MORE
STATES. ANY OR ALL OF THE ALPHANUMERIC CHARACTER
SET MAY BE USED.
    
```

OUTPT1	2
OUTPT1	3
OUTPT1	4
OUTPT1	5
OUTPT1	6
OUTPT1	7
OUTPT1	8
OUTPT1	9
OUTPT1	10
OUTPT1	11
OUTPT1	12
OUTPT1	13
OUTPT1	14
OUTPT1	15
OUTPT1	16
OUTPT1	17
OUTPT1	18
OUTPT1	19
OUTPT1	20
OUTPT1	21
OUTPT1	22
OUTPT1	23
OUTPT1	24
OUTPT1	25
OUTPT1	26
OUTPT1	27
OUTPT1	28
OUTPT1	29
OUTPT1	30
OUTPT1	31
OUTPT1	32
OUTPT1	33
OUTPT1	34
OUTPT1	35
OUTPT1	36
OUTPT1	37
OUTPT1	38
OUTPT1	39
OUTPT1	40
OUTPT1	41
OUTPT1	42
OUTPT1	43
OUTPT1	44
OUTPT1	45
OUTPT1	46
OUTPT1	47
OUTPT1	48
OUTPT1	49
OUTPT1	50
OUTPT1	51
OUTPT1	52
OUTPT1	53
OUTPT1	54
OUTPT1	55

Note: Punch code incompatibility
causes some special symbols
to print incorrectly:

< -> +
: -> 0
≤ -> ≠

and a few others

Note: 1) I/O(S(N)) is printed
in upper right corner of
each standard output page

2) For non-standard, special
printouts, example output
pages are provided marked
to identify the output

```

*      +I1> - OUTPUT DATA SET STATUS --+0>--SINGLE DATA SET. *
*      +I2> - DATA SET GROUP INDEX (+J> IN +MAGTAN1>). *
*      +I3> - DATA SET INDEX IN GROUP+I2> (+I> IN +MAGTAN1>). *
*
*  ROUTINES CALLED +OUTPRNT> *
*      +OUTCARD> *
*      +OUTTAPE> *
*
*  SPECIAL STORAGE AREAS *
*  COMMON BLOCK +SPEC> - 24828 WORDS *
*  NOTE - SEE SUBR+MAGTEL> AND SURR+ZFIT> FOR *
*  DEFINITION OF OUTPUT ARRAYS IN +SPEC>. *
*
*.....*

```

```

OUTPT1 56
OUTPT1 57
OUTPT1 58
OUTPT1 59
OUTPT1 60
OUTPT1 61
OUTPT1 62
OUTPT1 63
OUTPT1 64
OUTPT1 65
OUTPT1 66
OUTPT1 67
OUTPT1 68
OUTPT1 69
OUTPT1 70

```

SUBROUTINE OUTPRNT(TITLE,IOS,I1,I2,I3)

 ** GEOTRONICS COPP - AUSTIN, TEXAS USA **

SUBROUTINE <OUTPRNT> - FORTRAN IV DSR1025X001

USED CALL OUTPRNT(TITLE,IOS,I1,I2,I3)

THIS ROUTINE PRODUCES LINE PRINTER OUTPUT FOR RESULTS FROM <MAGTEL> AND <ZFIT>, WITH APPROPRIATE TITLES AND COLUMN HEADINGS.

PARAMETERS

<TITLE> - TITLE OF DATA SET - FORMAT(8A10).
 <IOS> - OUTPUT OPTION SELECT ARRAY.
 (SEE HEADER FOR <MAGTAN1> OR <OUTPT1> FOR CURRENT IMPLEMENTATION OF OPTIONS)
 <I1> - TYPE OF DATA BEING CURRENTLY PROCESSED
 0-SINGLE DATA SET
 1-AVERAGED RESULTS
 <I2> - NOT USED.
 <I3> - NOT USED.

ROUTINES CALLED NONE

SPECIAL STORAGE AREAS
 COMMON BLOCK <SPEC> - 22993 WORDS

DESCRIPTION OF OUTPUT BY HEADINGS

ALL PRINTER OUTPUT

NO. - THE LINE NUMBER, CORRESPONDING TO THE ITH FREQ.
 FREQ - FR(I) - FREQUENCY (HZ).
 NHARM - NSP(I) - INCREMENTAL HARMONICS AVERAGED.

E-H FIELD AUTO-POWER SPECTRA

PEXEX - PP(I,1) - EX - AUTO-POWER-(MV/KM)**2/HZ.
 PEYEX - PP(I,10) - EY - AUTO-POWER-(MV/KM)**2/HZ.
 PHXHX - PP(I,17) - HX - AUTO-POWER- GAMMA**2/HZ.
 PHYHY - PP(I,22) - HY - AUTO-POWER- GAMMA**2/HZ.
 PHZHZ - PP(I,25) - HZ - AUTO-POWER- GAMMA**2/HZ.

E-H FIELD POLARIZATION PROPERTIES

EDEP - DEPC(I,1) - E-FIELD DEPOLARIZATION - RATIO OF UNPOLARIZED TO TOTAL POWER
 EELIP - ELIPC(I,1) - E-FIELD ELLIPTICITY OF POLARIZED POWER COMPONENT
 EA - IANC(I,1) - E-FIELD POLARIZATION ANGLE (DEGR)
 HDEP - DEPC(I,2) - H-FIELD DEPOLARIZATION - RATIO OF UNPOLARIZED TO TOTAL POWER
 HELIP - ELIPC(I,2) - H-FIELD ELLIPTICITY OF POLARIZED POWER COMPONENT
 HA - IANC(I,2) - H-FIELD POLARIZATION ANGLE (DEGR)

OUTPRNT 2
 OUTPRNT 3
 OUTPRNT 4
 OUTPRNT 5
 OUTPRNT 6
 OUTPRNT 7
 OUTPRNT 8
 OUTPRNT 9
 OUTPRNT 10
 OUTPRNT 11
 OUTPRNT 12
 OUTPRNT 13
 OUTPRNT 14
 OUTPRNT 15
 OUTPRNT 16
 OUTPRNT 17
 OUTPRNT 18
 OUTPRNT 19
 OUTPRNT 20
 OUTPRNT 21
 OUTPRNT 22
 OUTPRNT 23
 OUTPRNT 24
 OUTPRNT 25
 OUTPRNT 26
 OUTPRNT 27
 OUTPRNT 28
 OUTPRNT 29
 OUTPRNT 30
 OUTPRNT 31
 OUTPRNT 32
 OUTPRNT 33
 OUTPRNT 34
 OUTPRNT 35
 OUTPRNT 36
 OUTPRNT 37
 OUTPRNT 38
 OUTPRNT 39
 OUTPRNT 40
 OUTPRNT 41
 OUTPRNT 42
 OUTPRNT 43
 OUTPRNT 44
 OUTPRNT 45
 OUTPRNT 46
 OUTPRNT 47
 OUTPRNT 48
 OUTPRNT 49
 OUTPRNT 50
 OUTPRNT 51
 OUTPRNT 52
 OUTPRNT 53
 OUTPRNT 54
 OUTPRNT 55

* SCALAR RESULTS - UNROTATED	* 56
* RX(PH)COH - RHOC(I,1),IAC(I,1),COR(I,1) - APP RES ,	* 57
* PHASE, AND COHERENCY FOR ZX = EX/HY.	* 58
* (CAGNIARD SOLUTION)	* 59
* RY(PH)COH - RHOC(I,2),IAC(I,2),COP(I,2) - APP RES ,	* 60
* PHASE, AND COHERENCY FOR ZY = EY/HX.	* 61
* (CAGNIARD SOLUTION)	* 62
* Z-TENSOR RESULTS - UNROTATED	* 63
* RXX(PH)COZ - RC(I,1),IPC(I,1),COC(I,1) - APP RES ,	* 64
* PHASE, AND PHASOR COH FOR ZX ELEMENT	* 65
* OF +Z> TENSOR (UNROTATED)	* 66
* RYY(PH)COZ - RC(I,2),IPC(I,2),COC(I,2) - APP RES ,	* 67
* PHASE, AND PHASOR COH FOR ZYY ELEMENT	* 68
* OF +Z> TENSOR (UNROTATED)	* 69
* RXY(PH)COZ - RC(I,3),IPC(I,2),COC(I,2) - APP RES ,	* 70
* PHASE, AND PHASOR COH FOR ZXY ELEMENT	* 71
* OF +Z> TENSOR (UNROTATED)	* 72
* RYX(PH)COZ - RC(I,4),IPC(I,4),COC(I,4) - APP RES ,	* 73
* PHASE, AND PHASOR COH FOR ZYX ELEMENT	* 74
* OF +Z> TENSOR (UNROTATED)	* 75
* Z-TENSOR RESULTS - ROTATED	* 76
* RTM(PH)COZ - RRC(I,1),ANC(I,1),COHC(I,1) - APP RES ,	* 77
* PHASE, PHASOR COH - E PERP TO STRIKE	* 78
* RTE(PH)COZ - RRC(I,2),ANC(I,2),COHC(I,2) - APP RES ,	* 79
* PHASE, PHASOR COH - E PARAL TO STRIKE	* 80
* A(Z) - ANGC(I,1) - ROTATION ANGLE FOR PRINCIPLE AXES	* 81
* OF +Z> TENSOR (DEGREES)	* 82
* N - KMMC(I,1) - NO. OF INDEPENDENT +Z> SOLUTIONS	* 83
* AVERAGED	* 84
* ALPHA - ALPC(I,1) - +Z> TENSOR SKEW	* 85
* BETA - BTAC(I,1) - +Z> TENSOR ELLIPTICITY	* 86
* DEN - DELC(I,1) - NORM DENOM DETERMINANT FOR	* 87
* +Z> SOLUTIONS	* 88
* Y-TENSOR RESULTS - ROTATED	* 89
* RTM(PH)COZ - RRC(I,3),ANC(I,3),COHC(I,3) - APP RES ,	* 90
* PHASE, PHASOR COH - E PERP TO STRIKE	* 91
* RTE(PH)COZ - RRC(I,4),ANC(I,4),COHC(I,4) - APP RES ,	* 92
* PHASE, PHASOR COH - E PARAL TO STRIKE	* 93
* A(Z) - ANGC(I,2) - ROTATION ANGLE FOR PRINCIPLE AXES	* 94
* OF +Y> TENSOR (DEGREES)	* 95
* N - KMMC(I,2) - NO. OF INDEPENDENT +Y> SOLUTIONS	* 96
* AVERAGED	* 97
* ALPHA - ALPC(I,2) - +Y> TENSOR SKEW	* 98
* BETA - BTAC(I,2) - +Y> TENSOR ELLIPTICITY	* 99
* DEN - DELC(I,2) - NORM DENOM DETERMINANT FOR	* 100
* +Y> SOLUTIONS	* 101
* HZ-RELATIONS - ROTATED	* 102
* RZTE(PH)COY - RRC(I,5),ANC(I,5),COHC(I,5) - APP RES ,	* 103
* PHASE, PHASOR COH FOR YZY(A(YZ)).	* 104
* A(YZ) - ANGC(I,3) - PRINCIPLE ROTATION ANGLE FOR +YZ>	* 105
* BETA + BTAC(I,3) - ELLIPTICITY OF +YZ>	* 106
	* 107
	* 108
	* 109
	* 110

RUN VERSION 2.3 --PSR LEVEL 363--

03/09/75

* KZTE (PHI)COK - KZE(I,1),AKZ(I,1),COK(I) - KZX(A(KZ)), *
* PHASE, AND (HZ-HX) COH FOR +KZ> TENSOR *
* A(KZ) - ANK(I) - PRINCIPLE ROTATION ANGLE FOR +KZ> *
* BETA - RTAK(I) - ELLIPTICITY OF +KZ> *
* *
* Z-TENSOR AXIS ROTATION-FREQ MAP0 PLOT OF RXX (TOP LINE)*
* AND RXY (BOT LINE) VS. A (DEGR) AND FREQ (HZ). *
* DECIMAL ASSUMED AT LEFT OF 3 DIGITS (LEADING *
* ZEROS OMITTED) FOR EACH R VALUE . MULTIPLY EACH *
* VALUE BY 10 TO EXPONENT AT END OF ROW. *
* *****

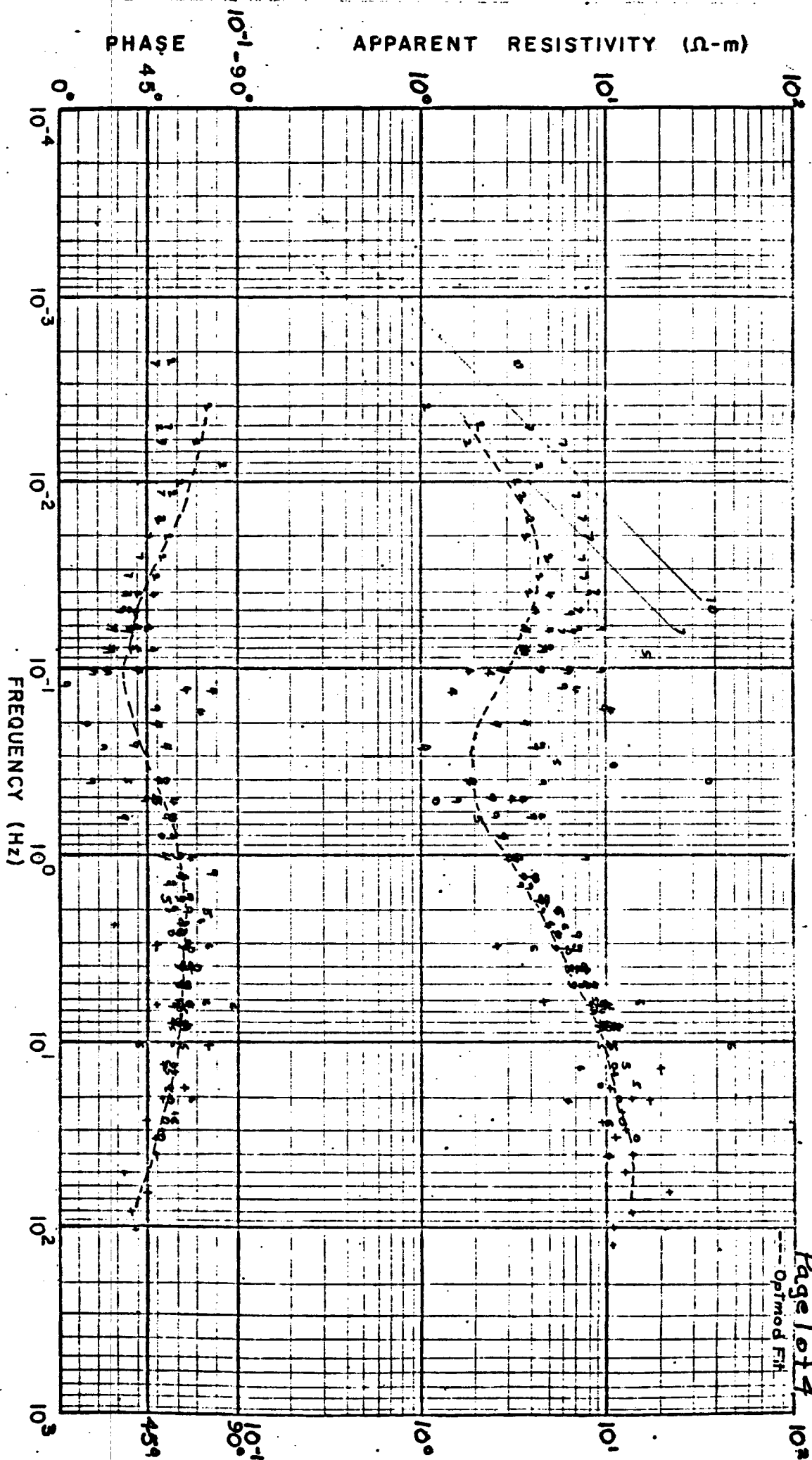
OUTPRNT 111
OUTPRNT 112
OUTPRNT 113
OUTPRNT 114
OUTPRNT 115
OUTPRNT 116
OUTPRNT 117
OUTPRNT 118
OUTPRNT 119
OUTPRNT 120
OUTPRNT 121
OUTPRNT 122

Appendix C, Computer Programs, continued...

(2) INVERT - produces an approximate one-dimensional inversion of an apparent resistivity and associated phase function, using an analytical approach. The output is a continuous function of intrinsic resistivity vs. depth and represents a vertically smoothed version of the real vertical profile. This, like any MT inversion is more sensitive to conductive zones and will tend to underestimate or ignore electrically thin resistive zones.

(3) OPTMOD - produces a one-dimensional N-layered model by least squares fitting the complex impedance functions for the model and the measured data, with respect to all model parameters, for up to N = 10 layers.

(4) LAYERPXY - produces the forward MT solution for a one-dimensional layered model and plots the model apparent resistivity and phase with the like measured functions for comparison. Results for permutations of a number of values for one or two model parameters can be produced to examine the effect of a parameter change.



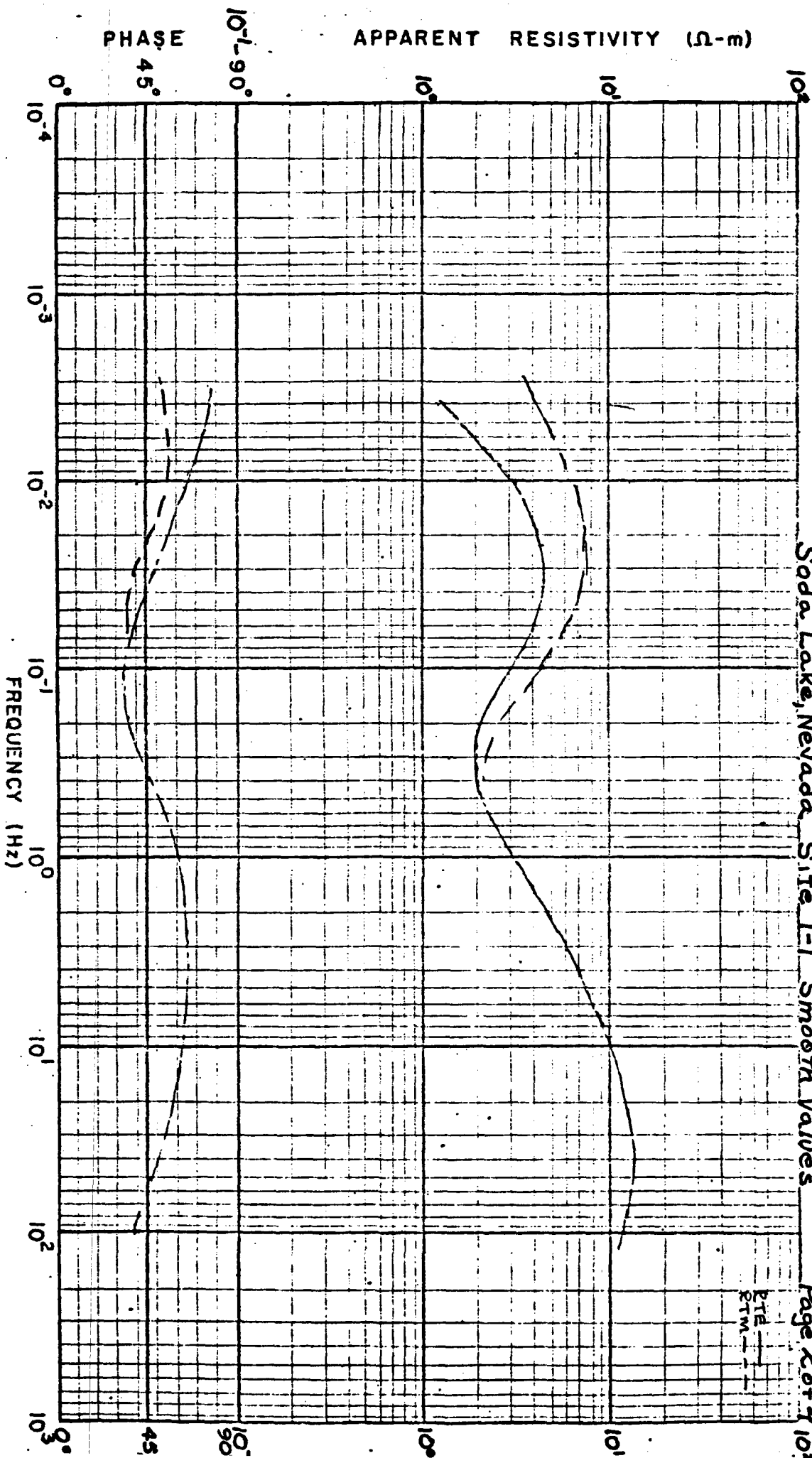
Soda Lake, Nevada Site 1-1

Figure II-1

Page 1 of 4

PHASE

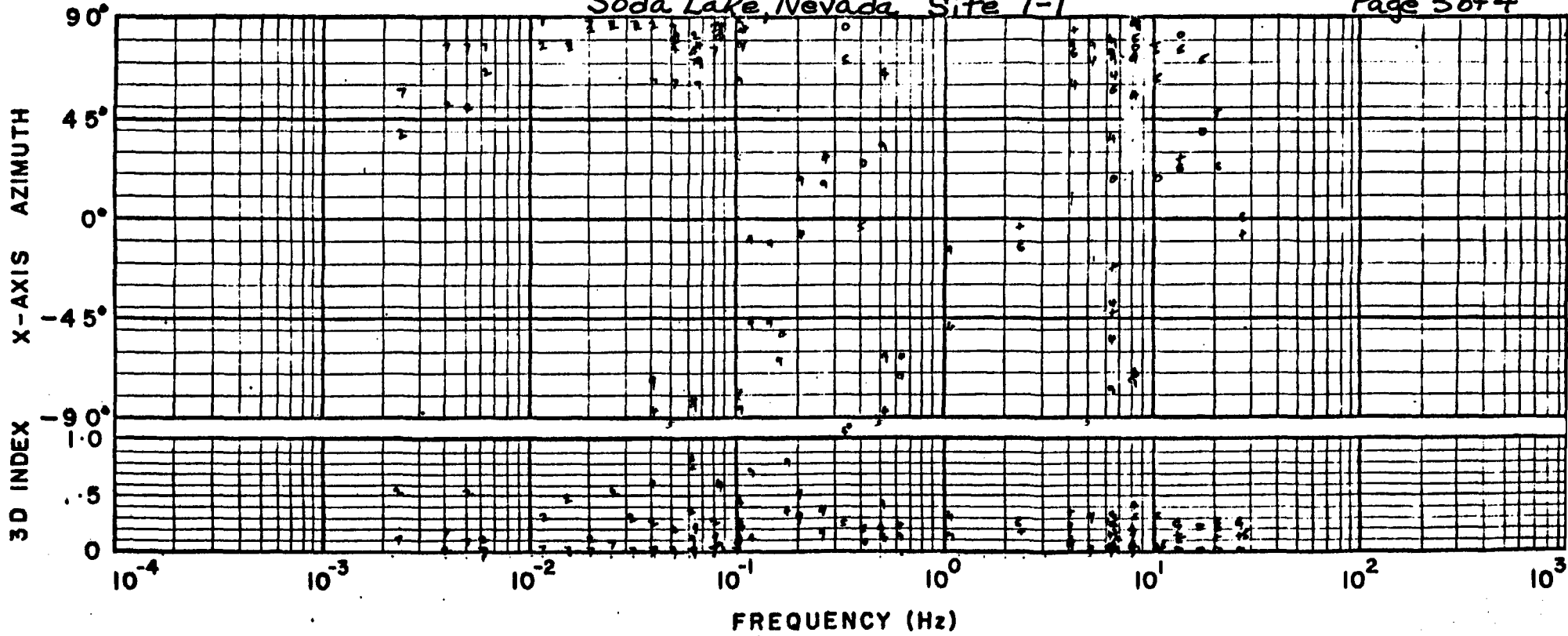
APPARENT RESISTIVITY (Ω -m)

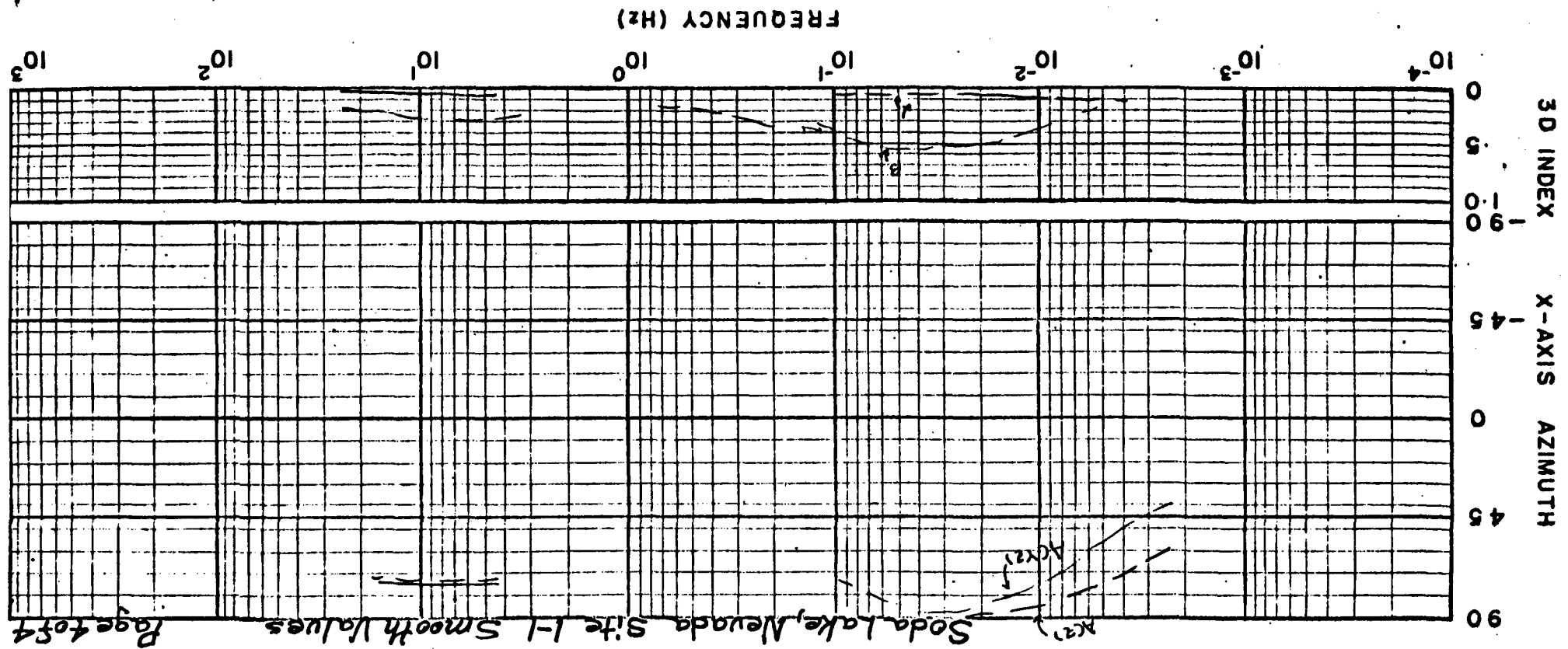


Soda Lake, Nevada Site 1-1 Smooth Values

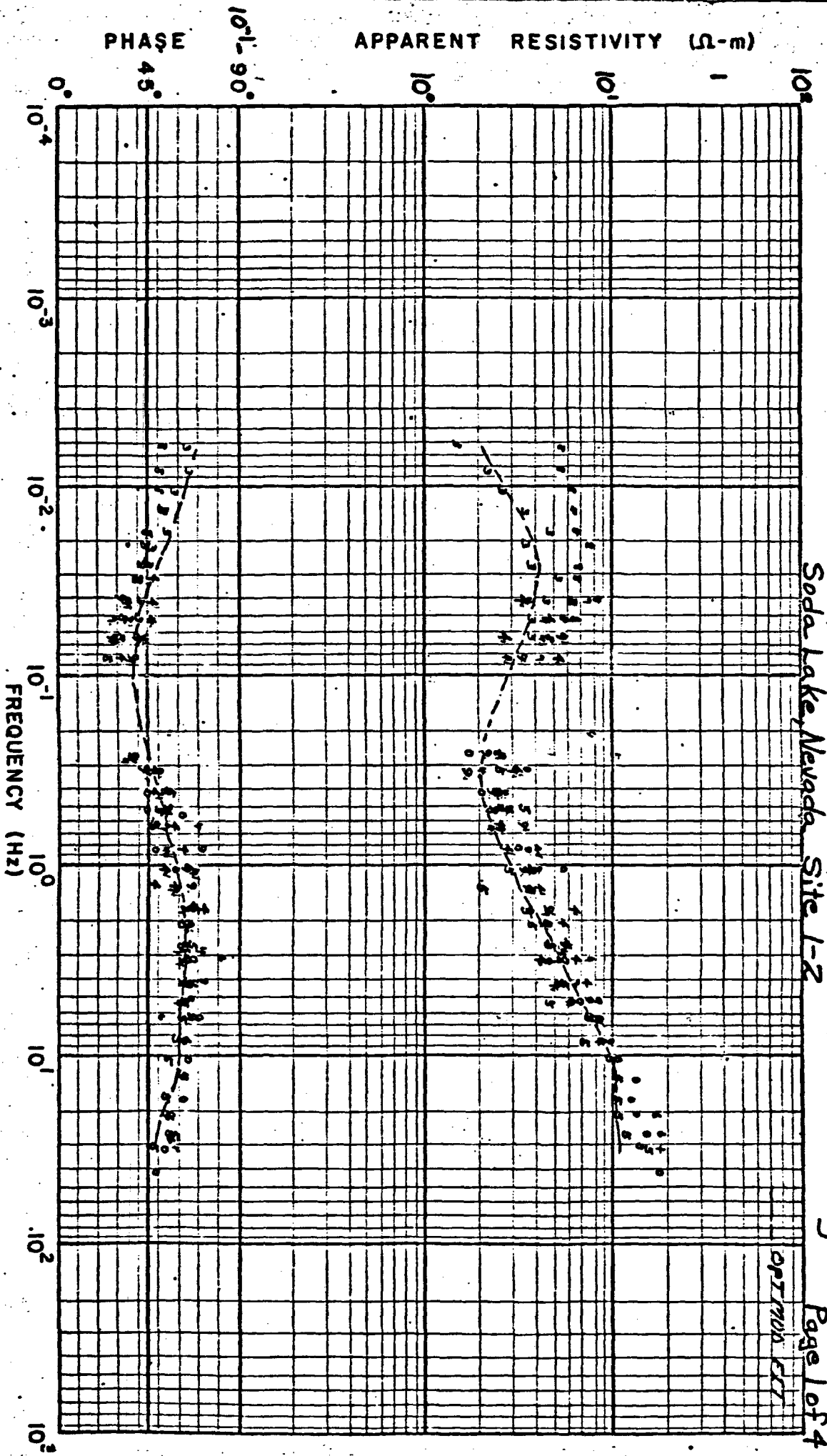
Page 2 of 4

RTD
PTM





Soda Lake, Nevada Site I-1 Smooth Values



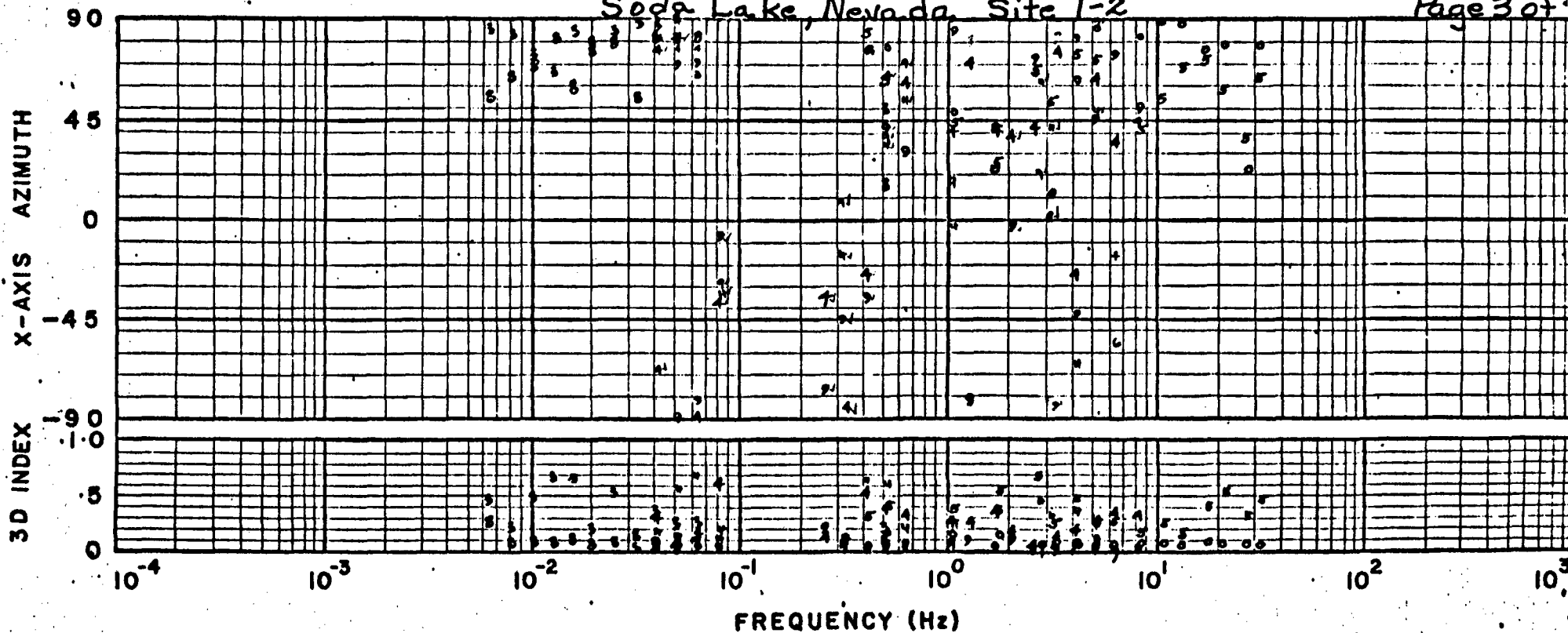
Soda Lake, Nevada Site L-2

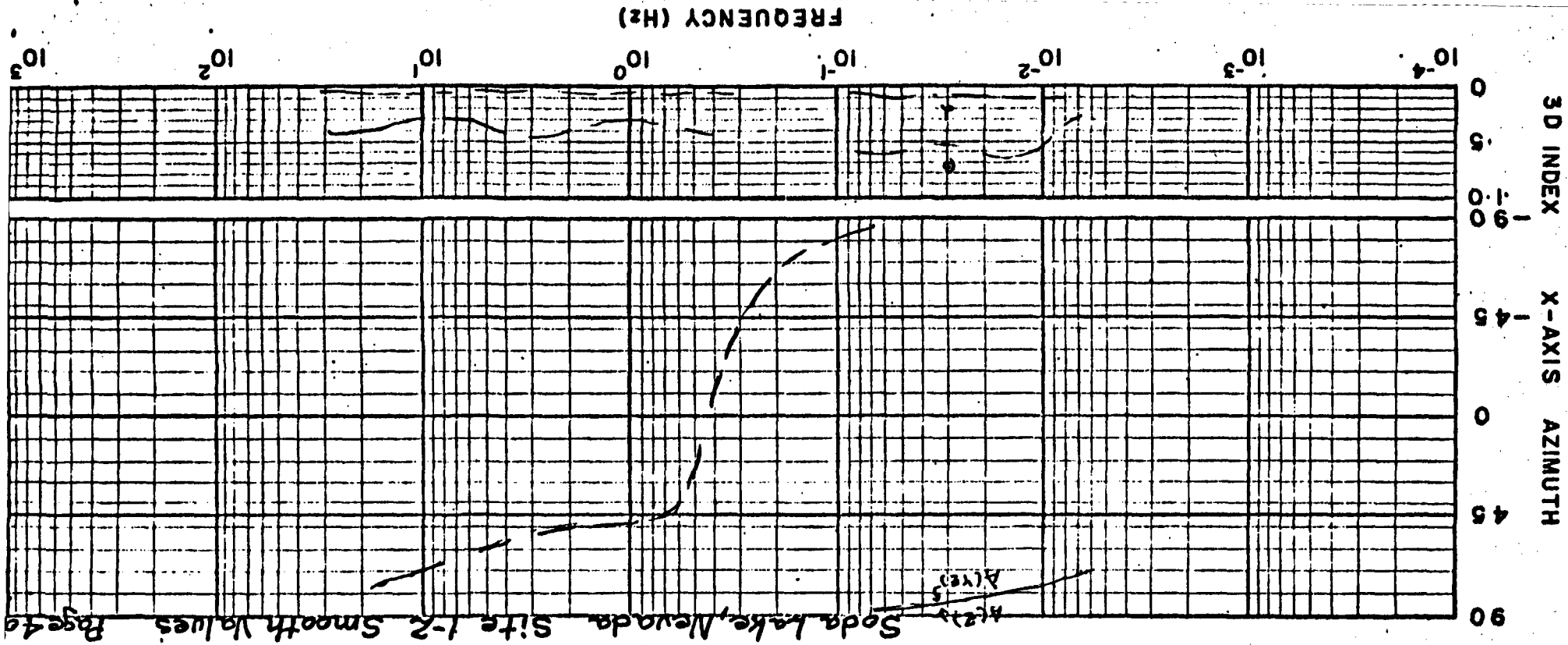
Figure II-2
Page 1 of 4

OPTIMUS CRT

Soda Lake, Nevada, Site 1-2

Page 3 of 3





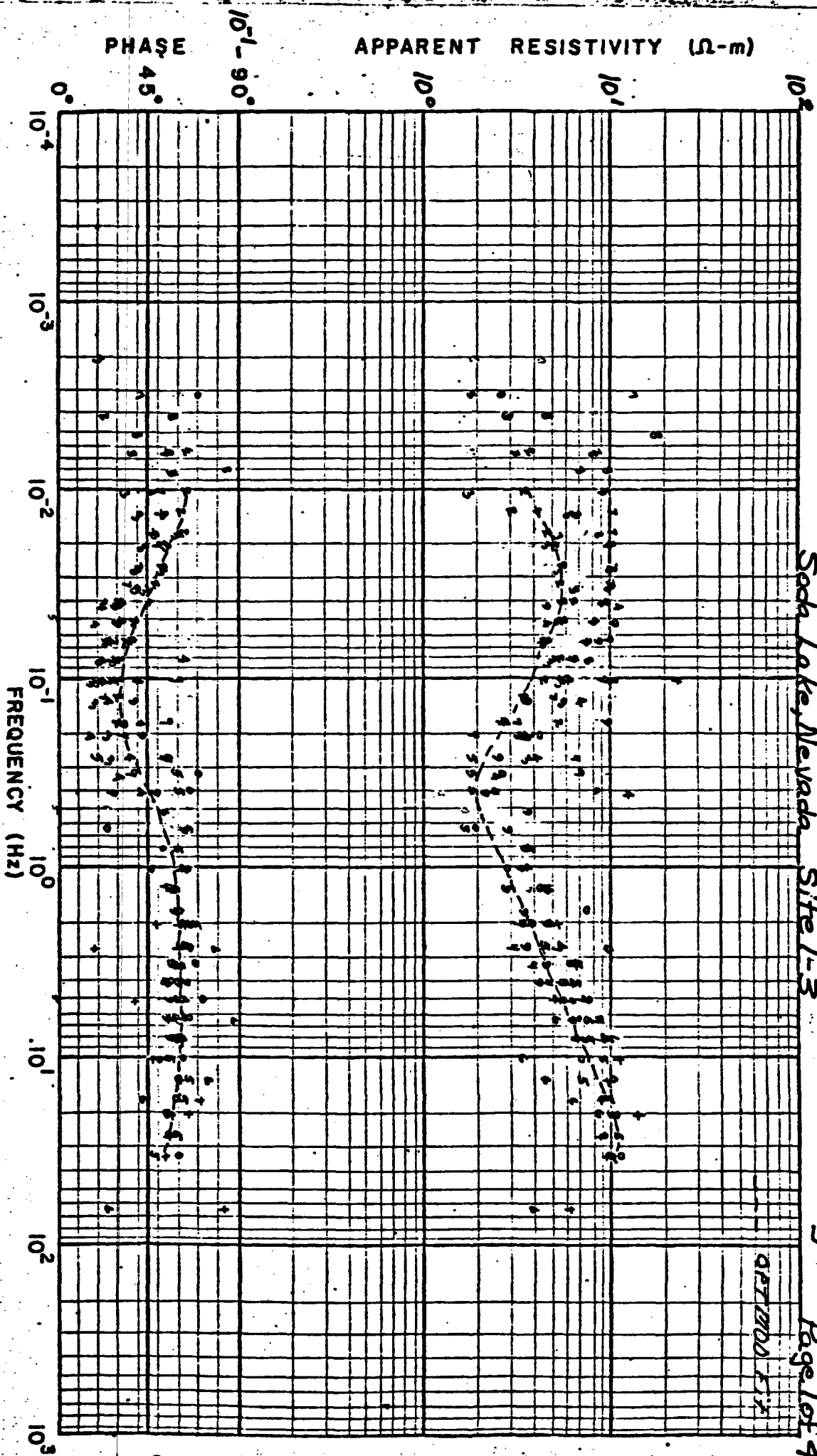
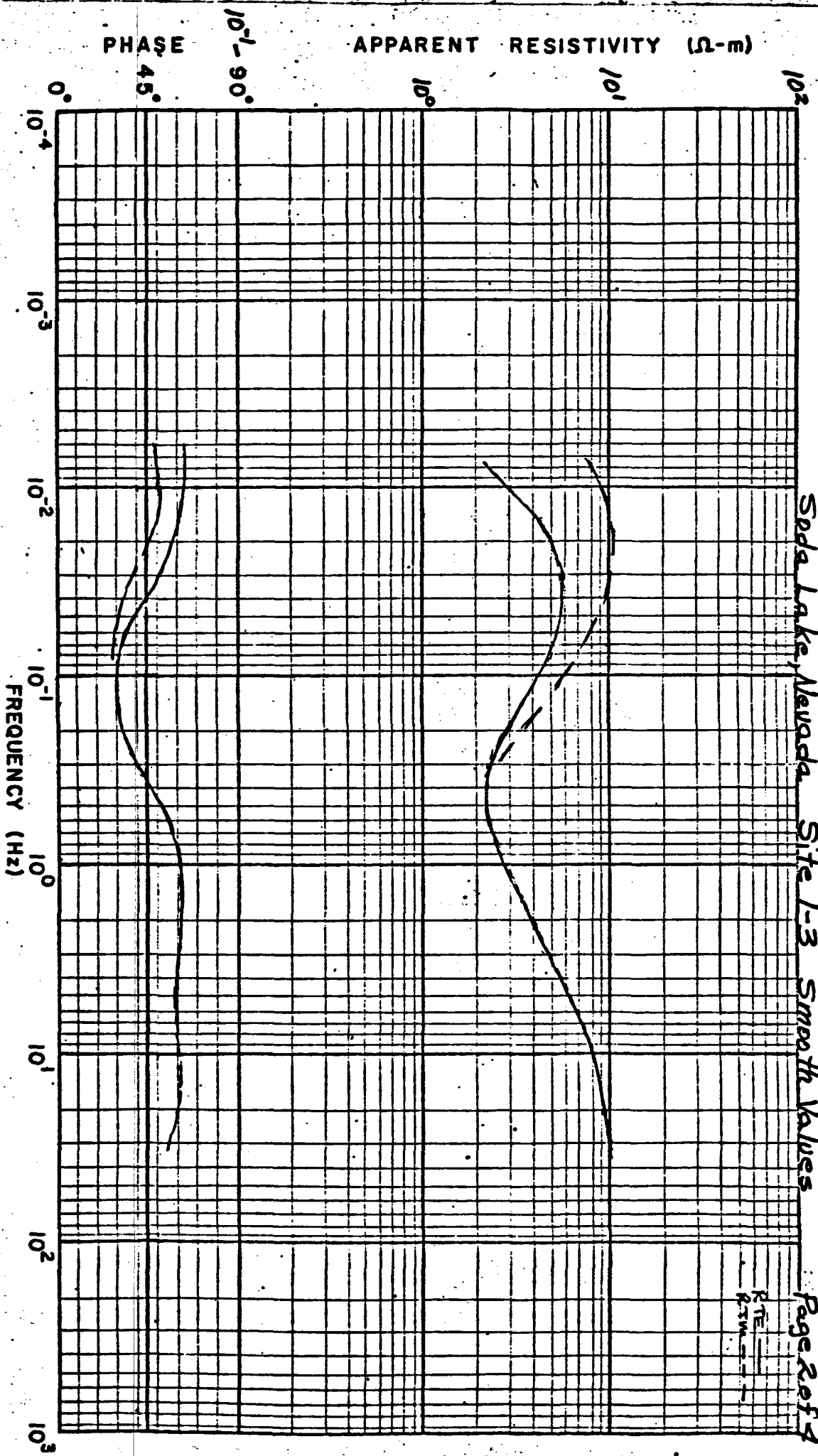
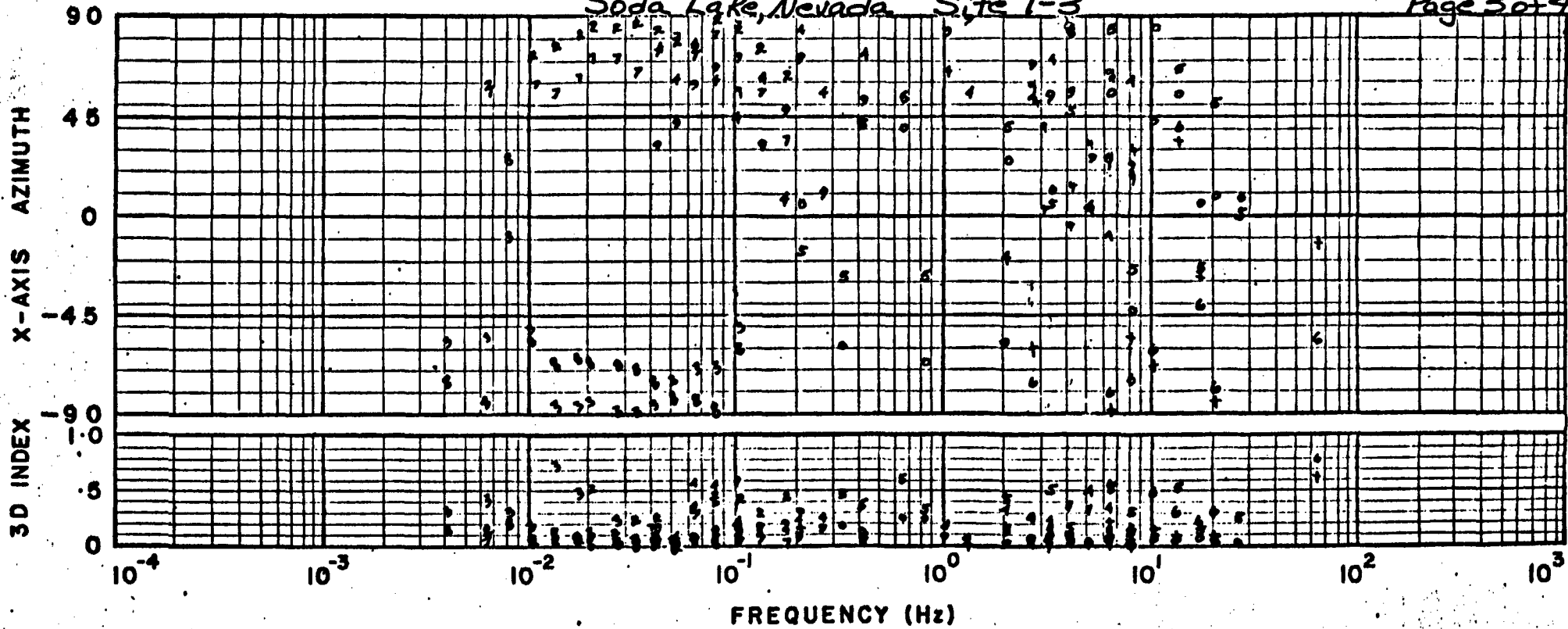


Figure II-3

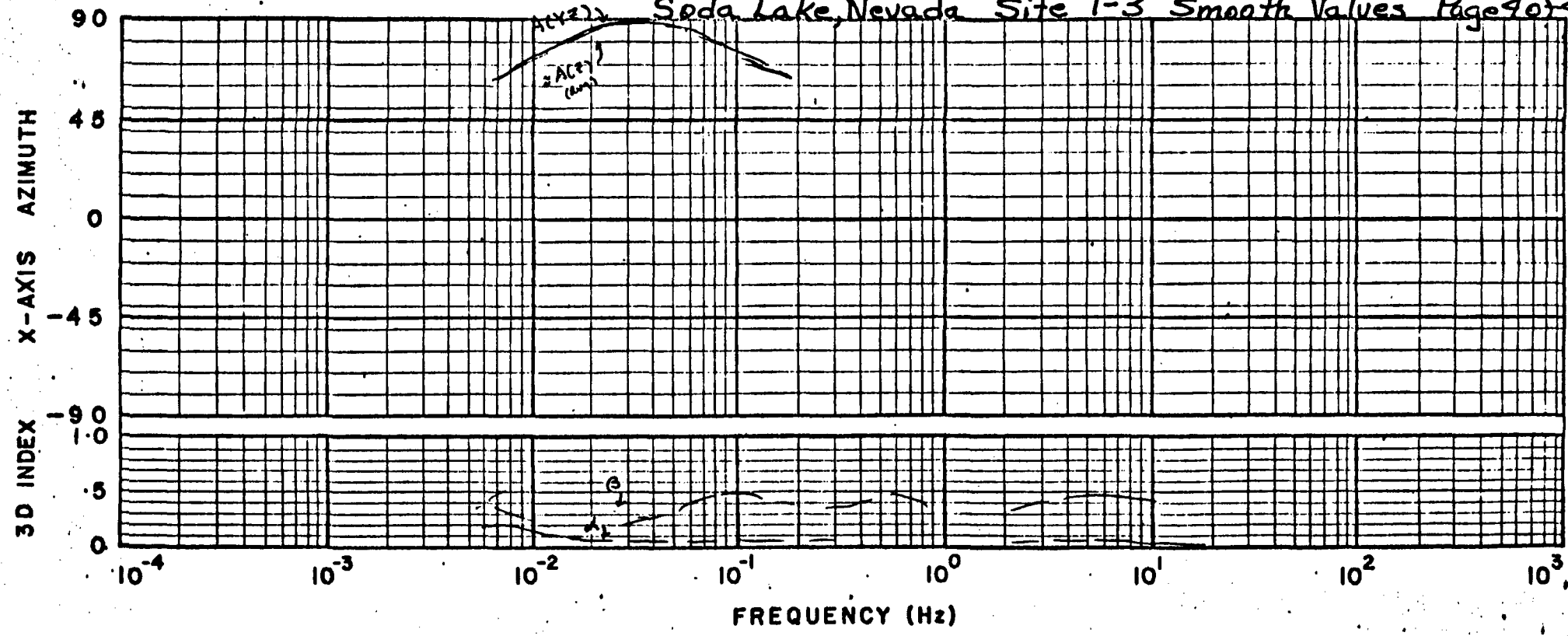


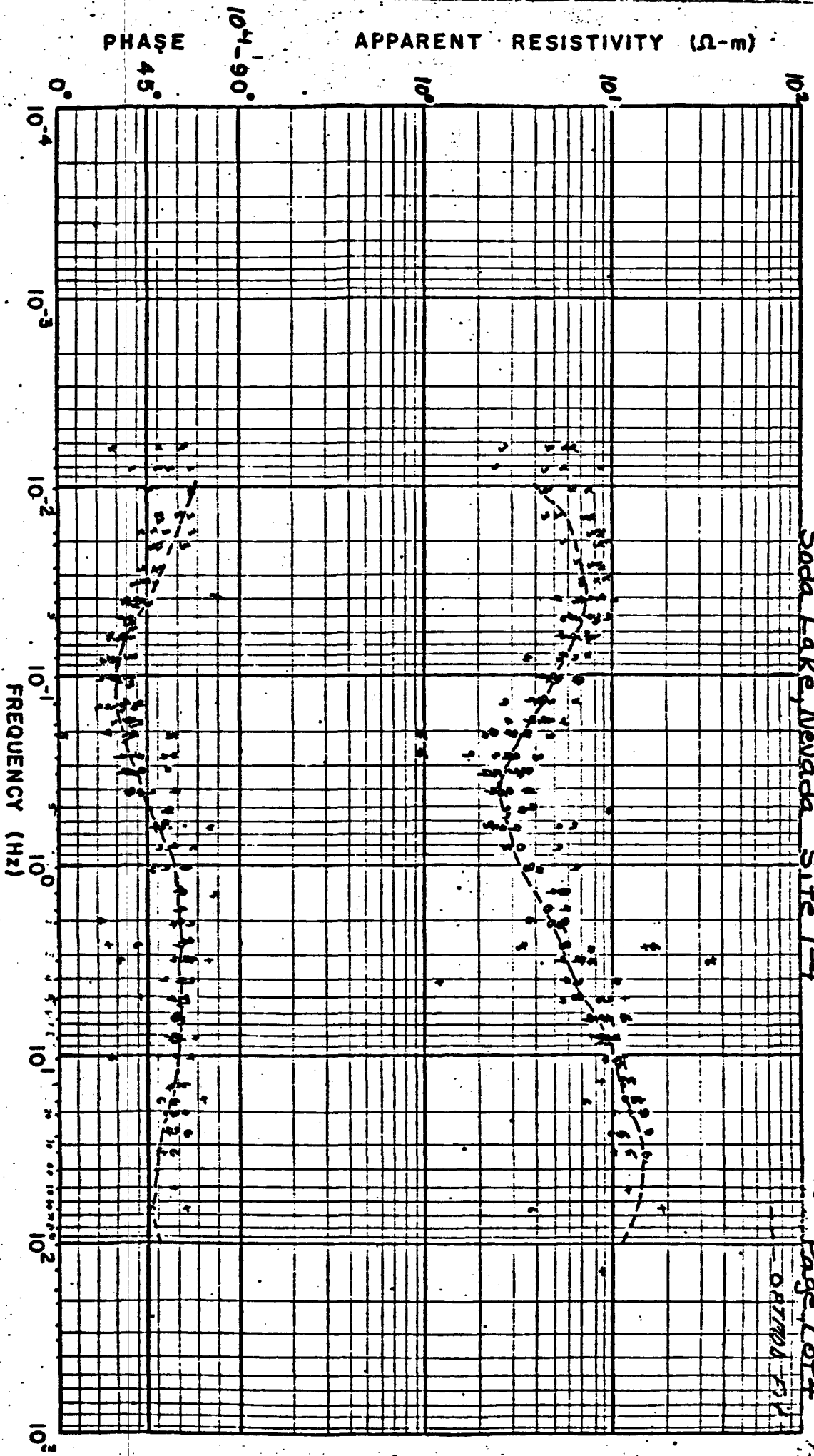
Soda Lake, Nevada Site 1-3

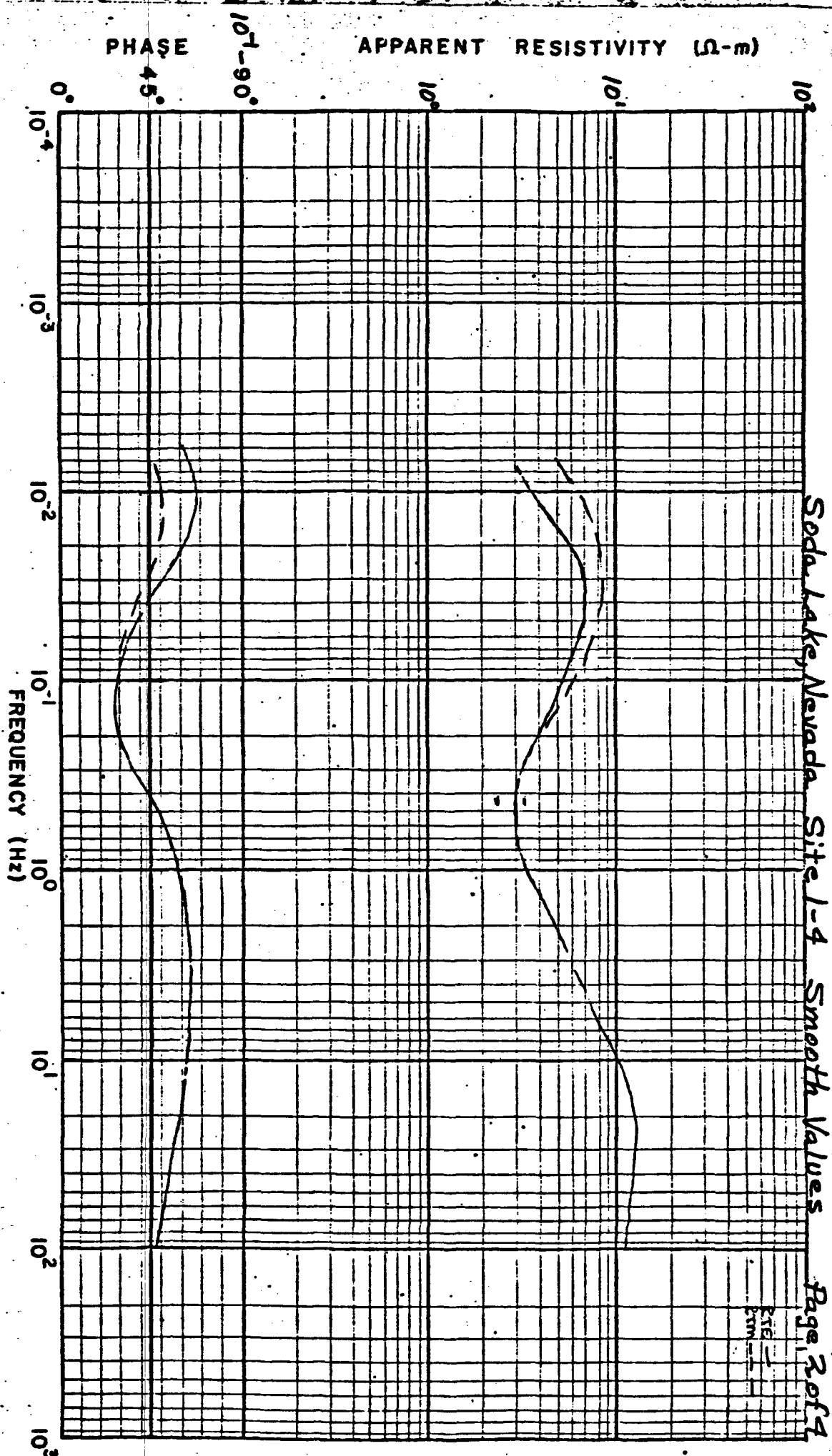
Page 3 of 4



Soda Lake, Nevada Site 1-3 Smooth Values Page 4 of 4

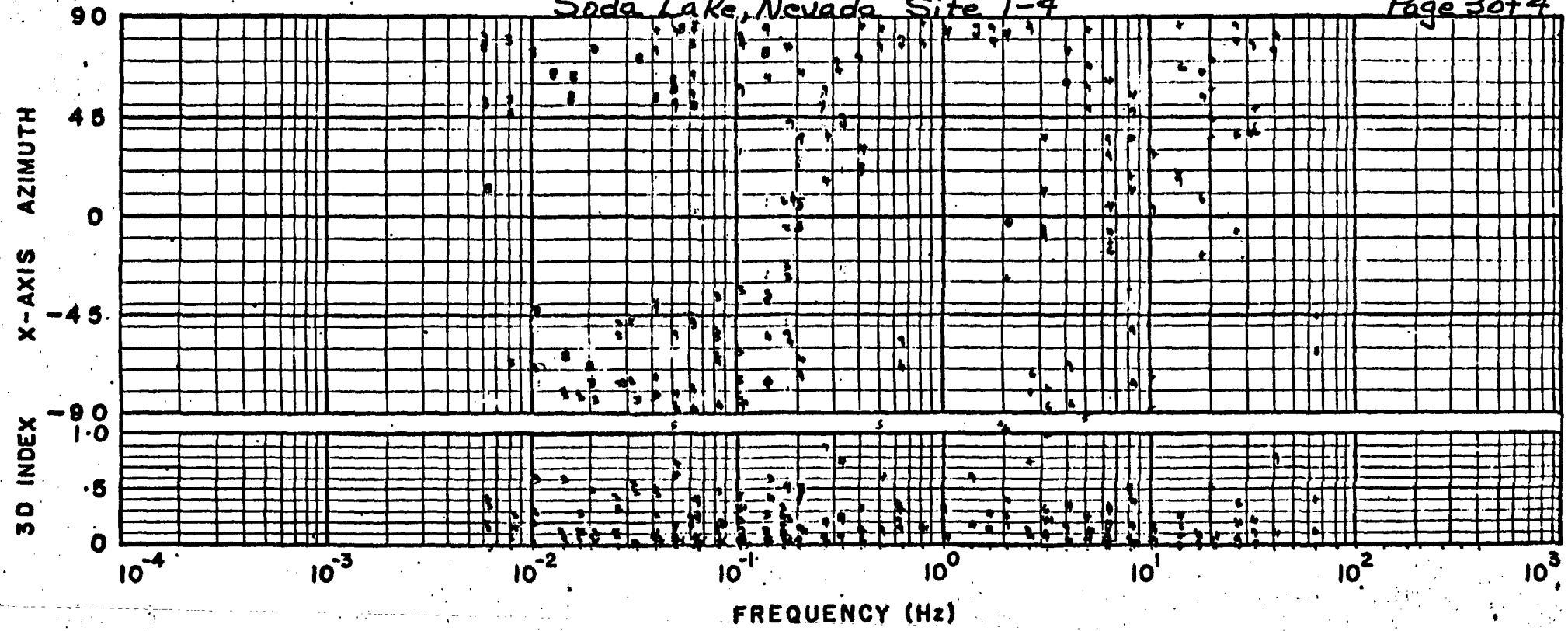


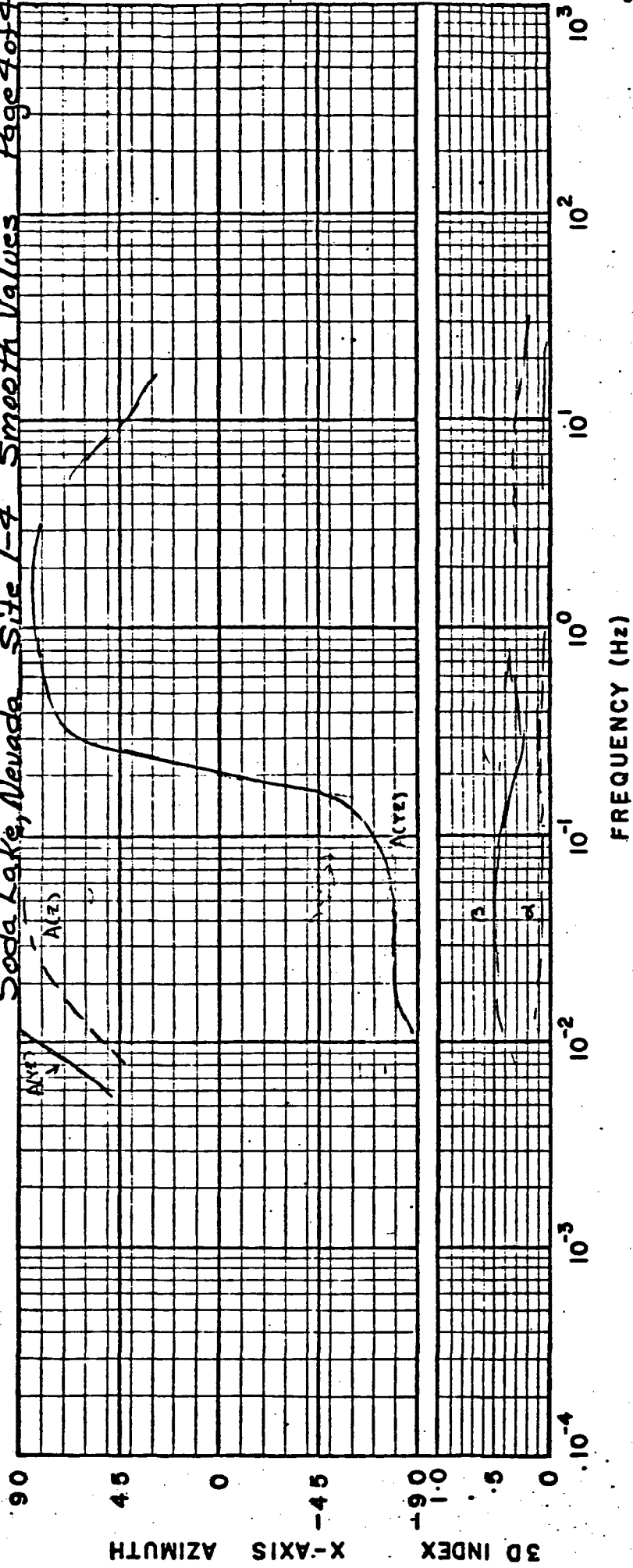


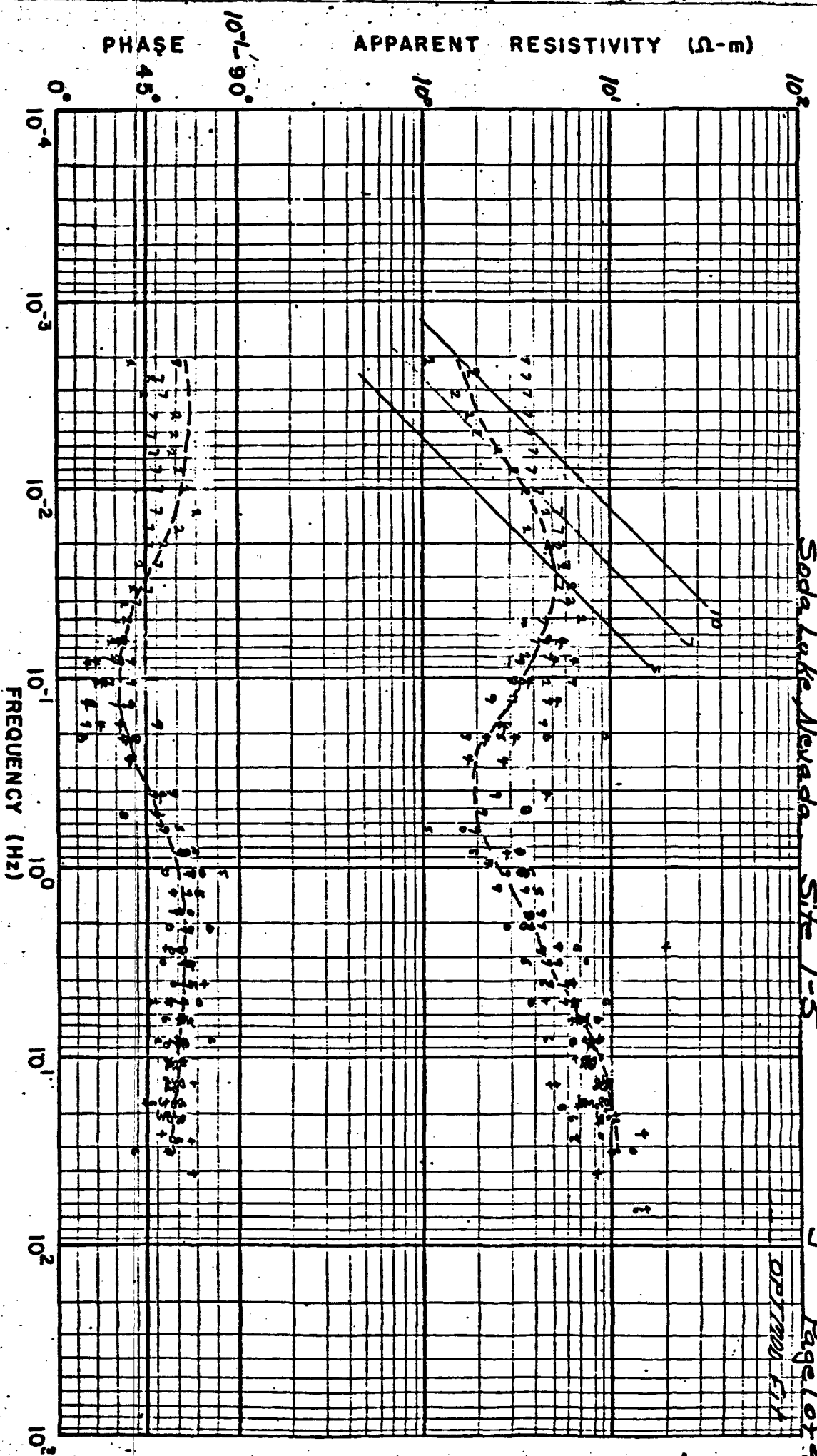


Soda Lake, Nevada Site 1-4

Page 3 of 4







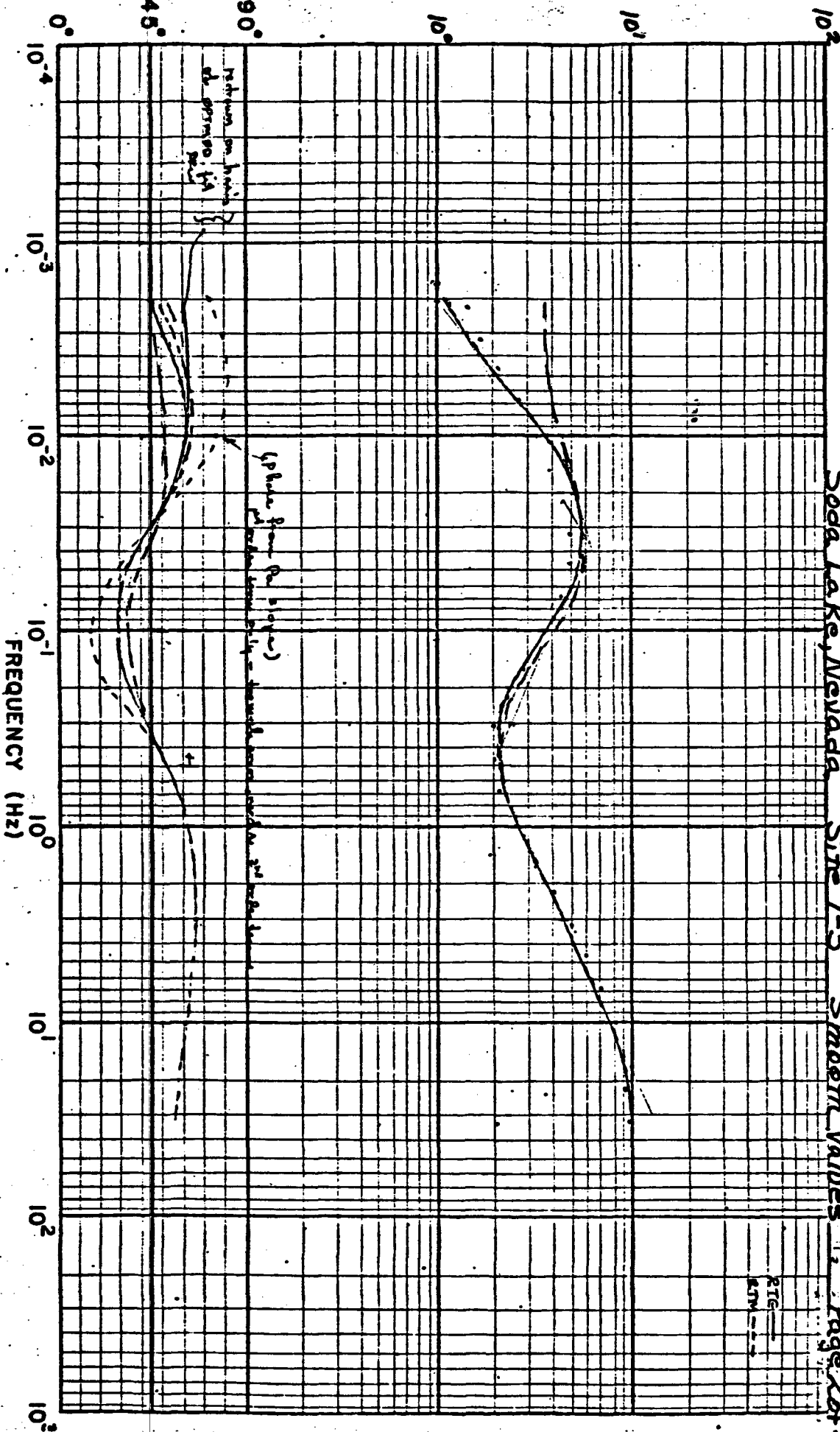
Soda Lake, Nevada Site 1-5

OPTIMOS 1-1

Figure II-5
Page 1 of 4

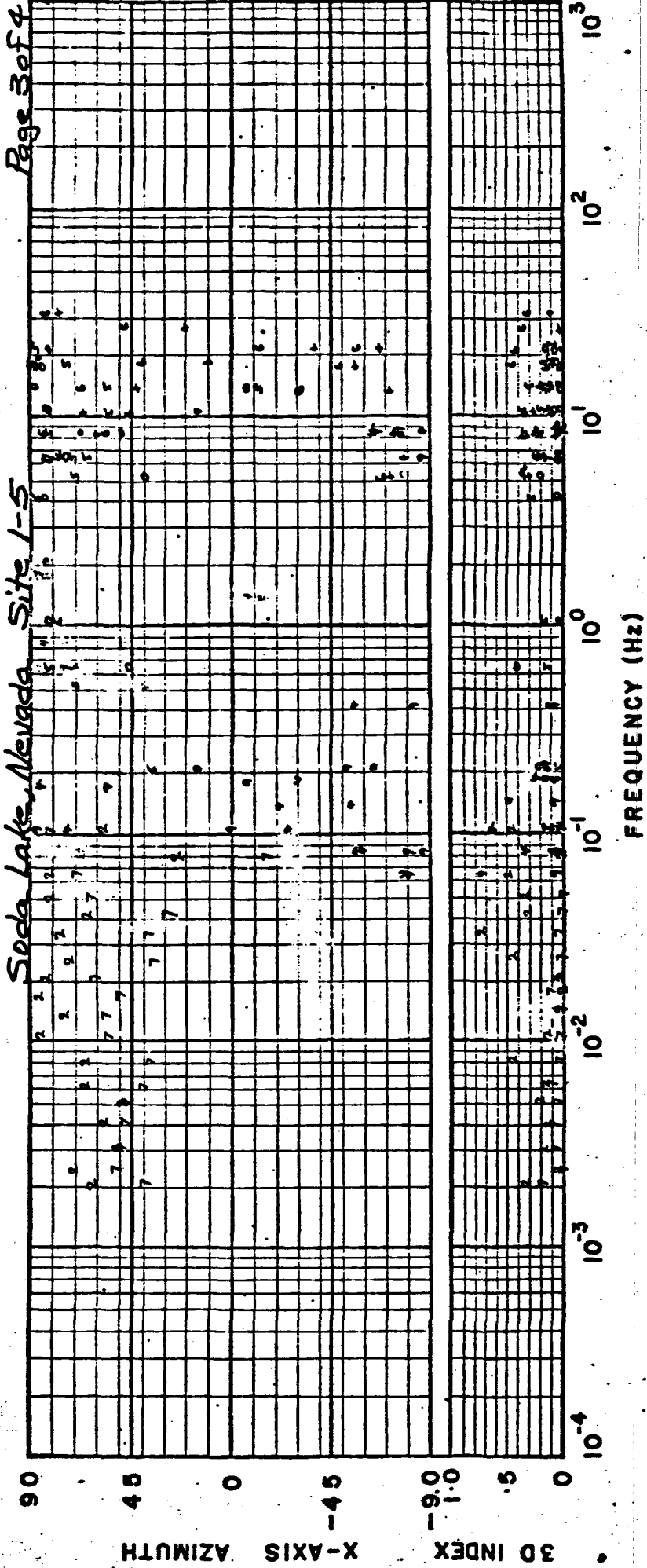
PHASE

APPARENT RESISTIVITY (Ω -m)



Soda Lake, Nevada Site 1-5 Smooth Values Page 2 of 4

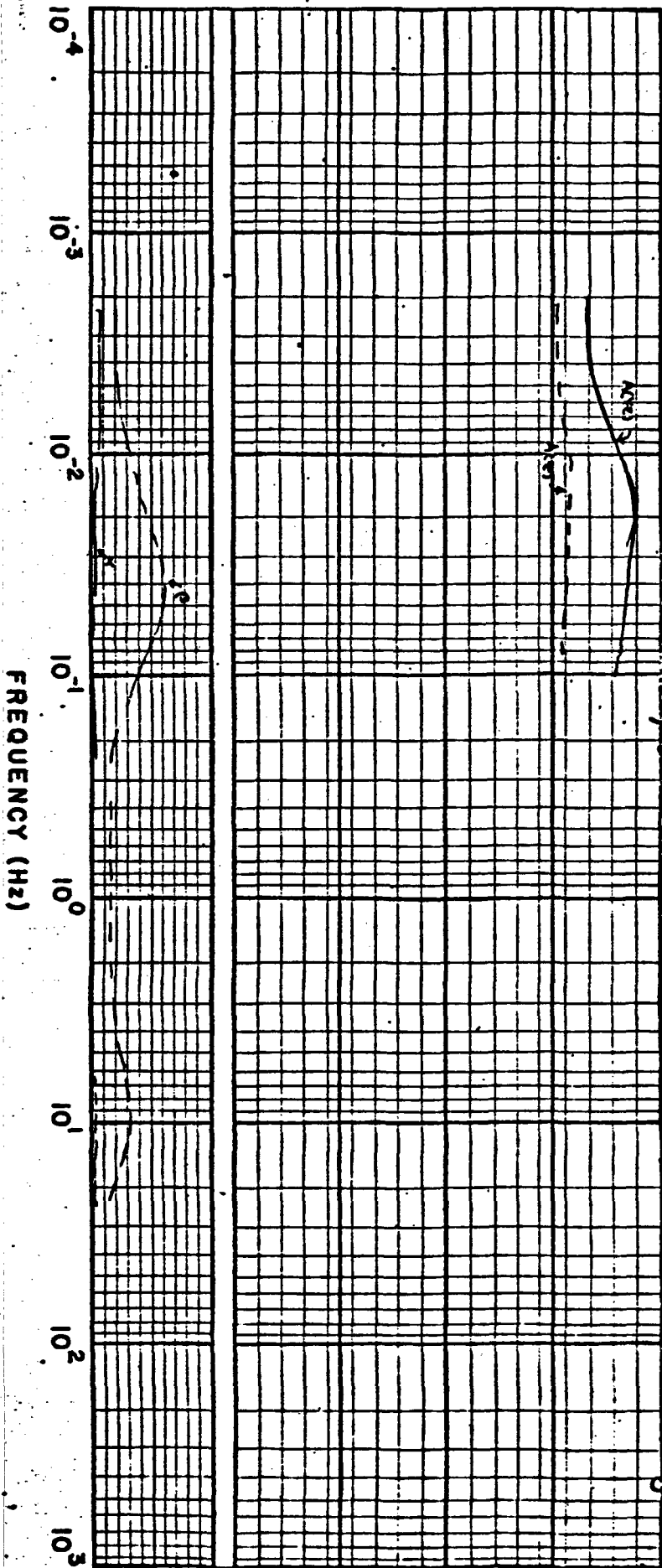
Lo ha - (P, ACYB)
US wo - (A, ACS)

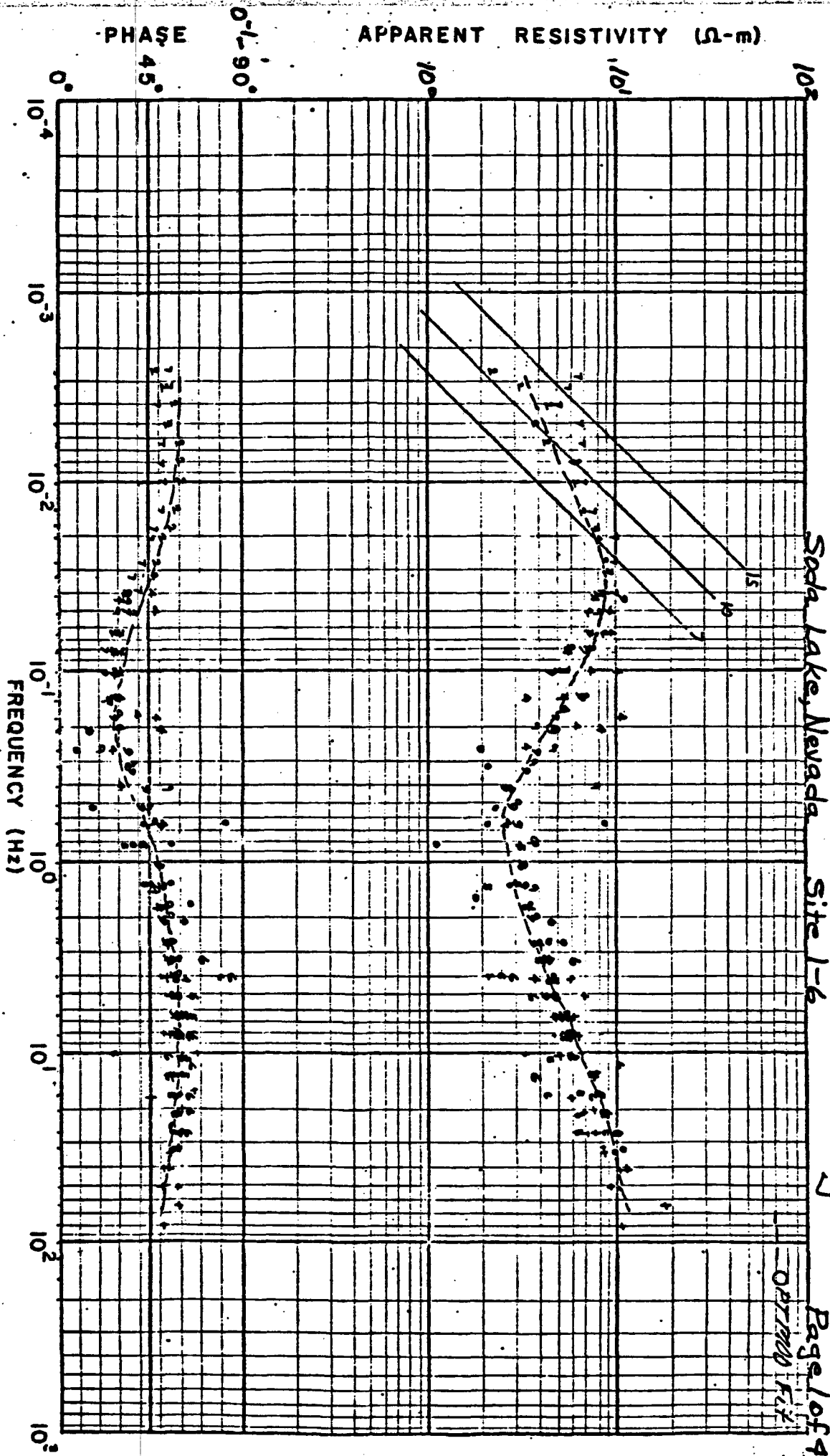


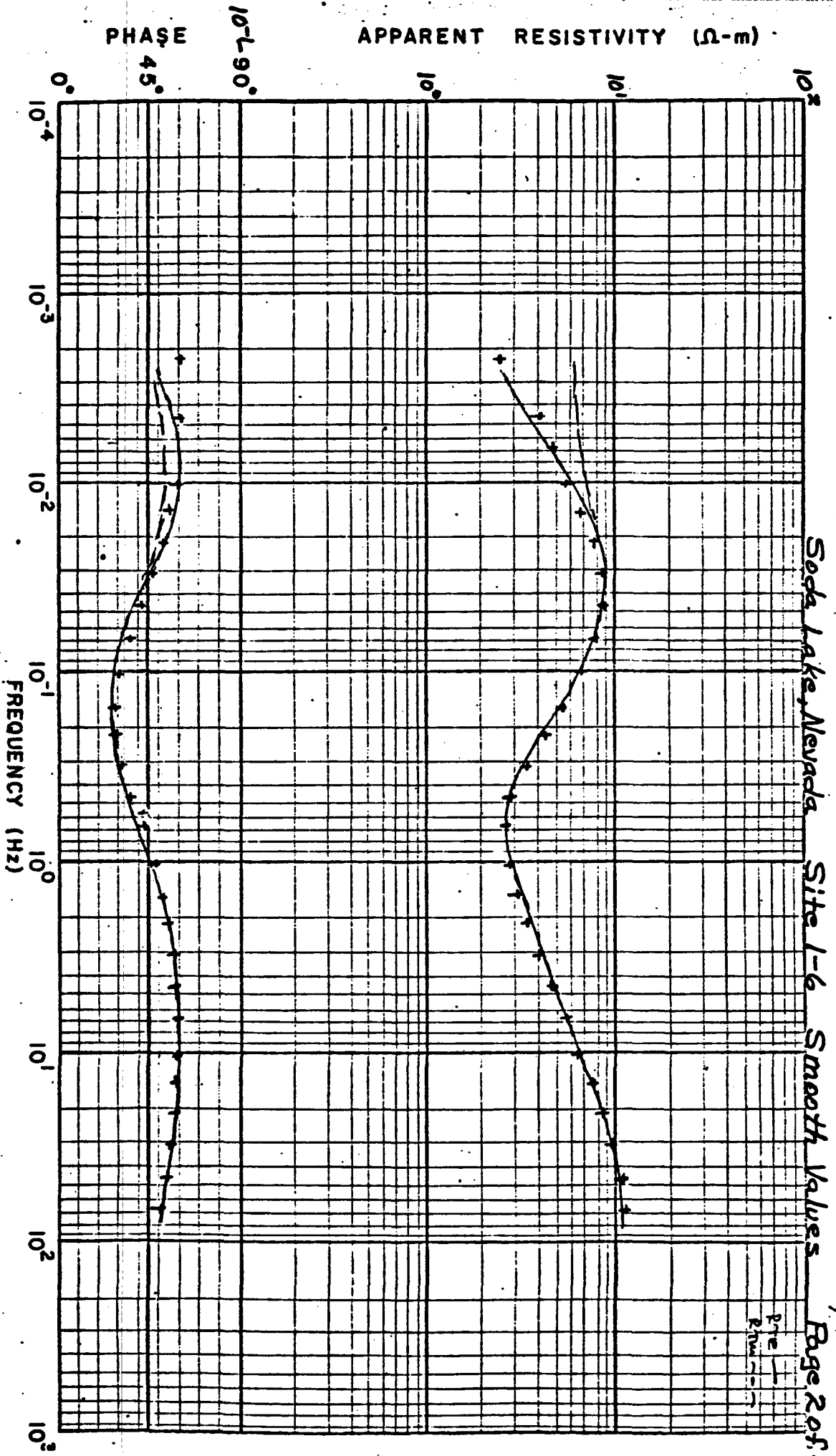
3D INDEX X-AXIS AZIMUTH

90
45
0
-45
-90

0 .5 1.0







Soda Lake, Nevada

Site L-6

Smooth Values

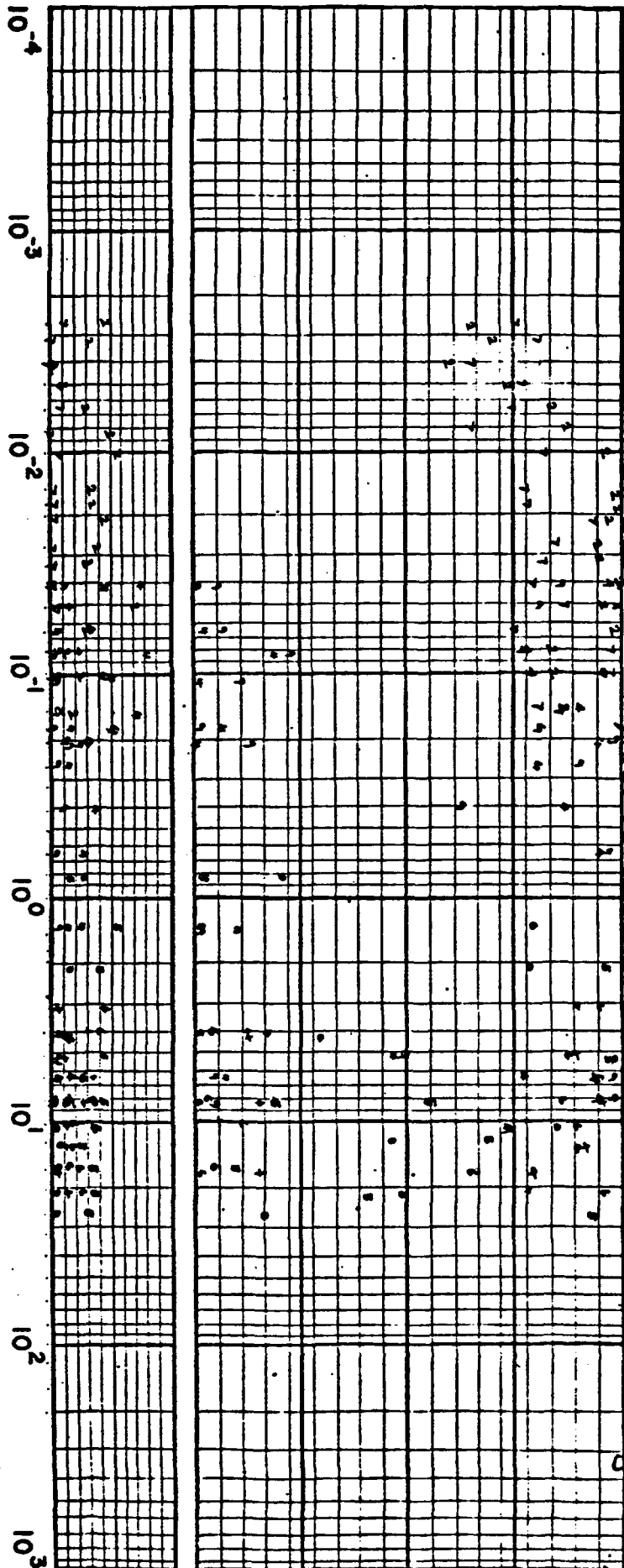
Page 2 of 4

Pre-
Phase

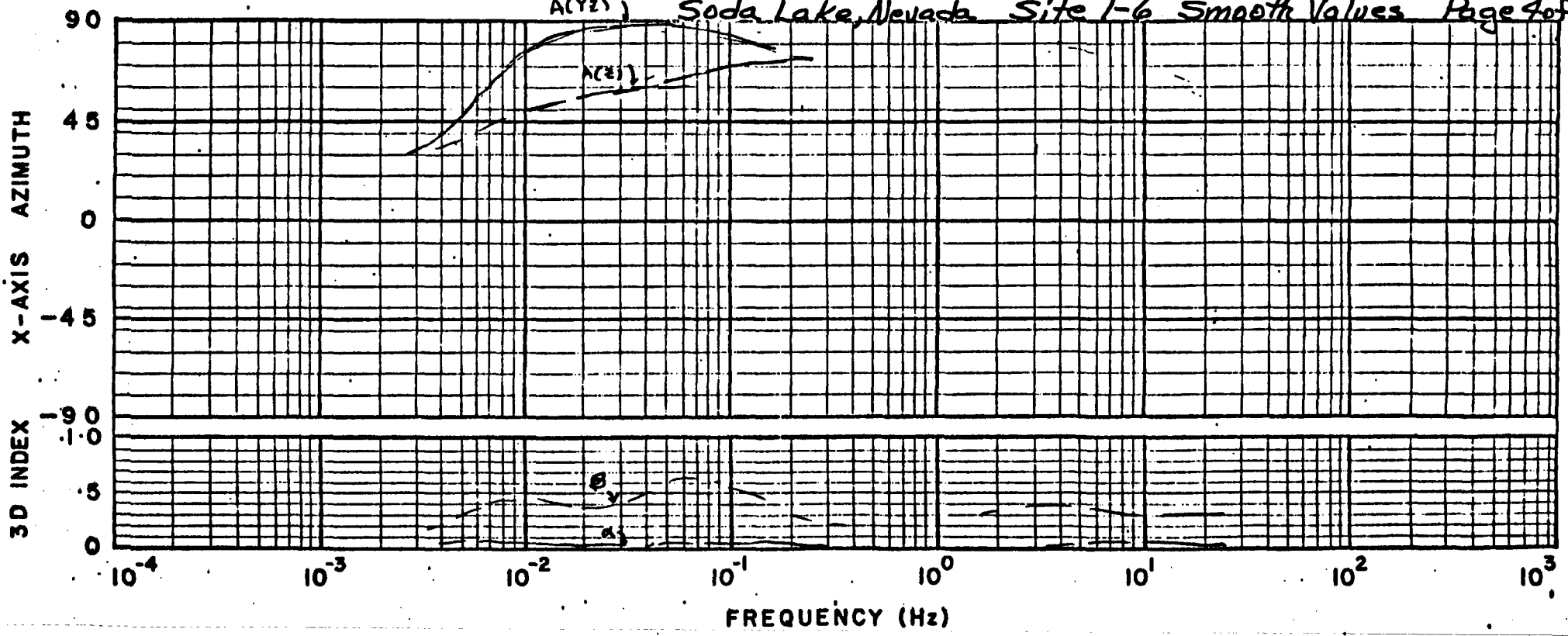
3D INDEX X-AXIS AZIMUTH

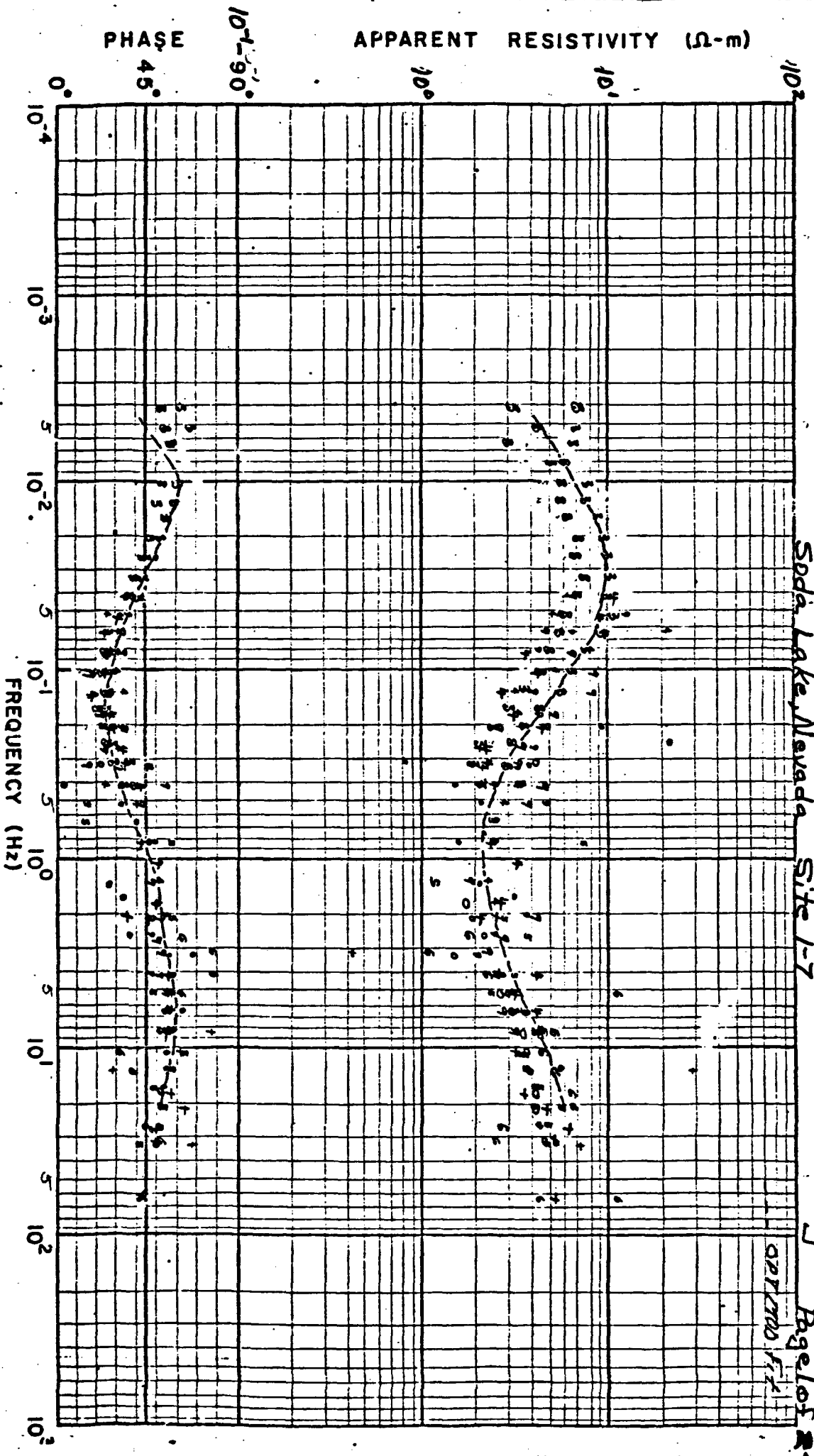
90
45
0
-45
-90

1.0
.5
0



A(YZ) Soda Lake, Nevada Site 1-6 Smooth Values Page 4 of 4

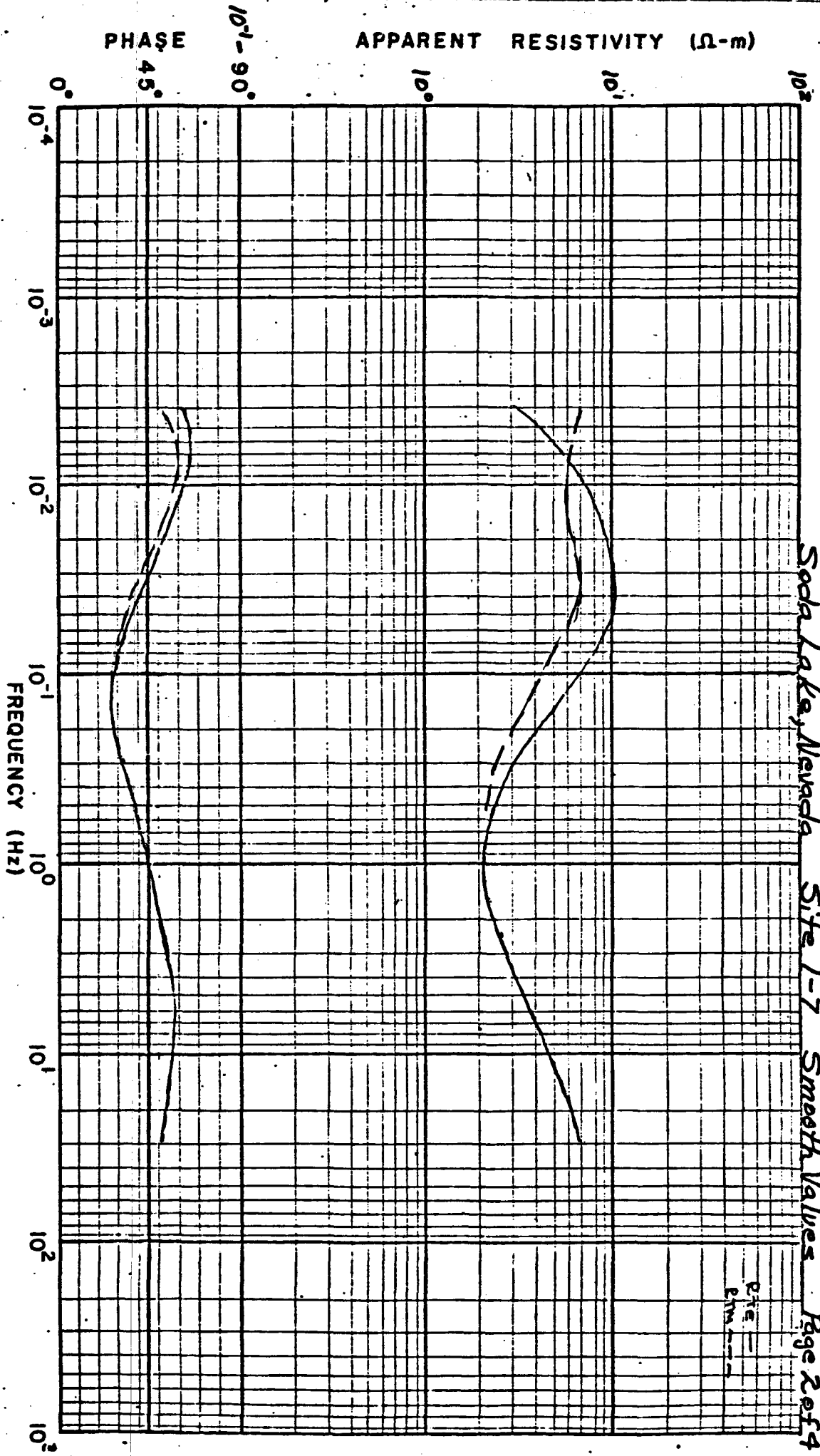


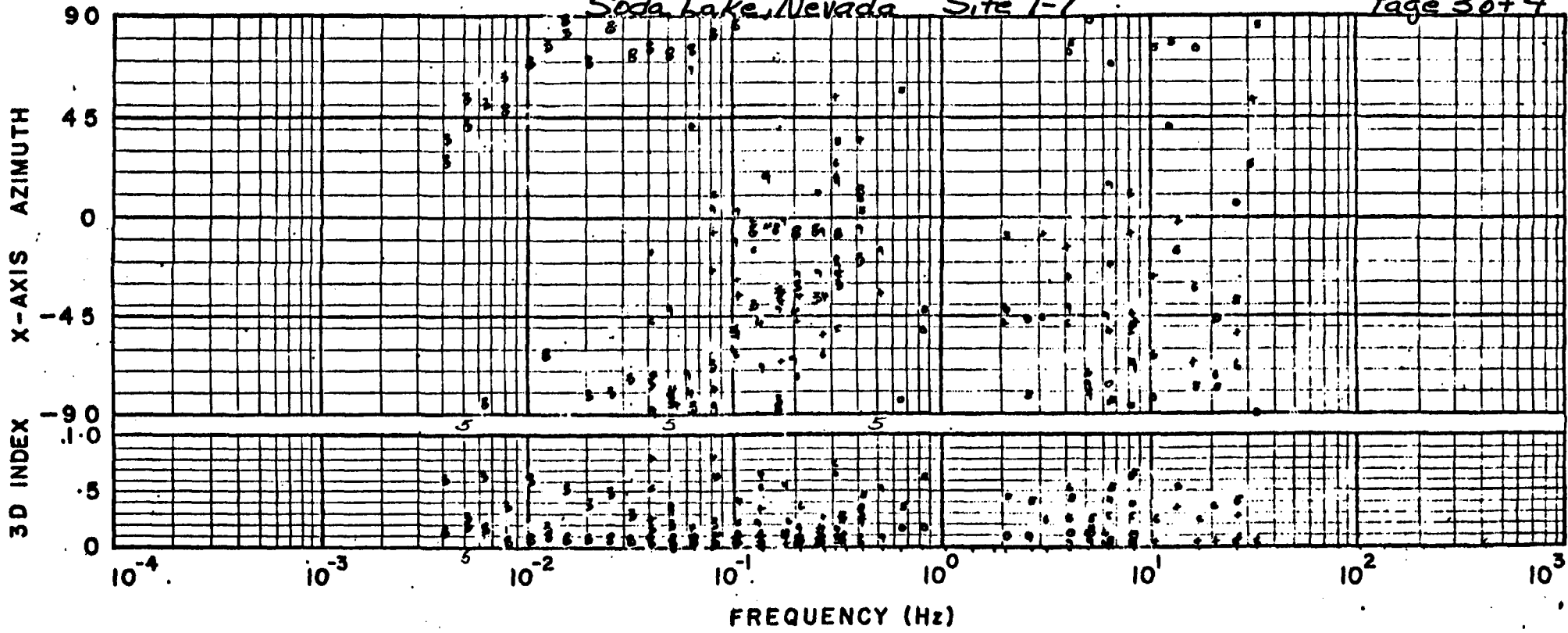


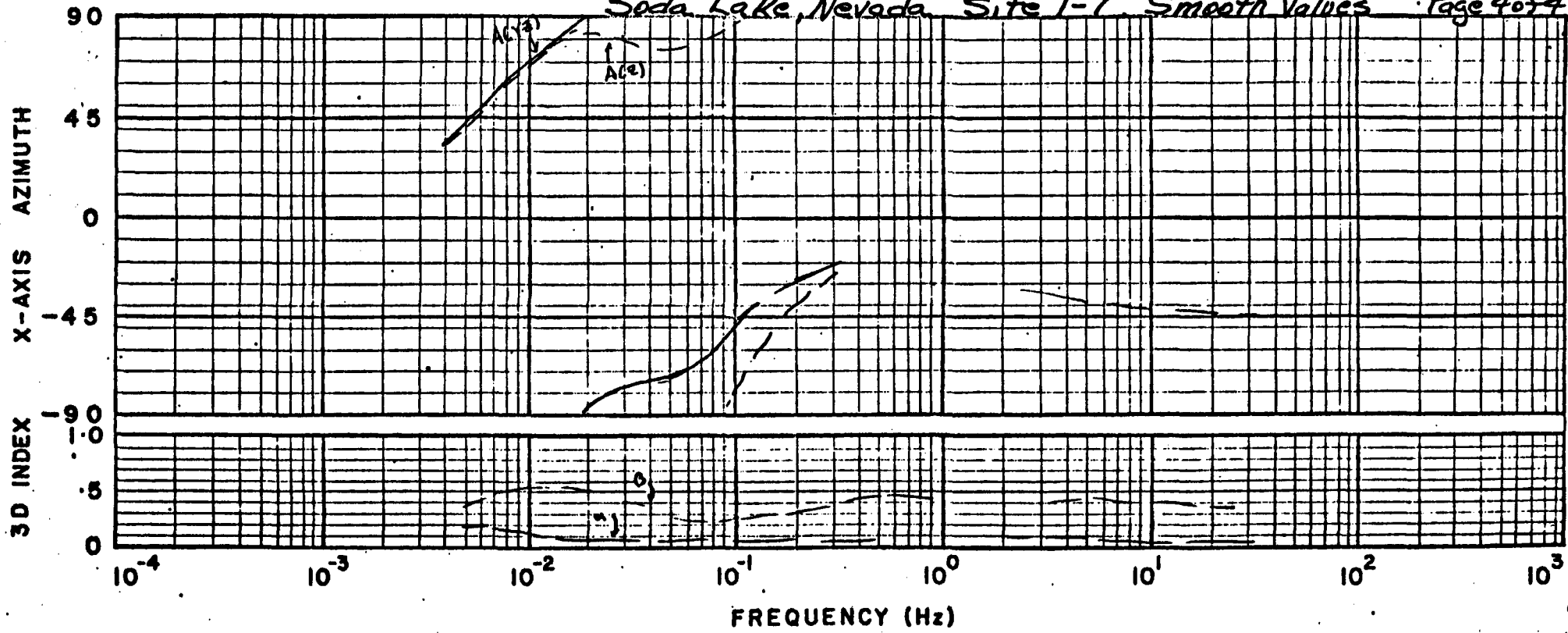
Soda Lake, Nevada Site 1-7

FIGURE II-7

Byelor
 APPENDIX I







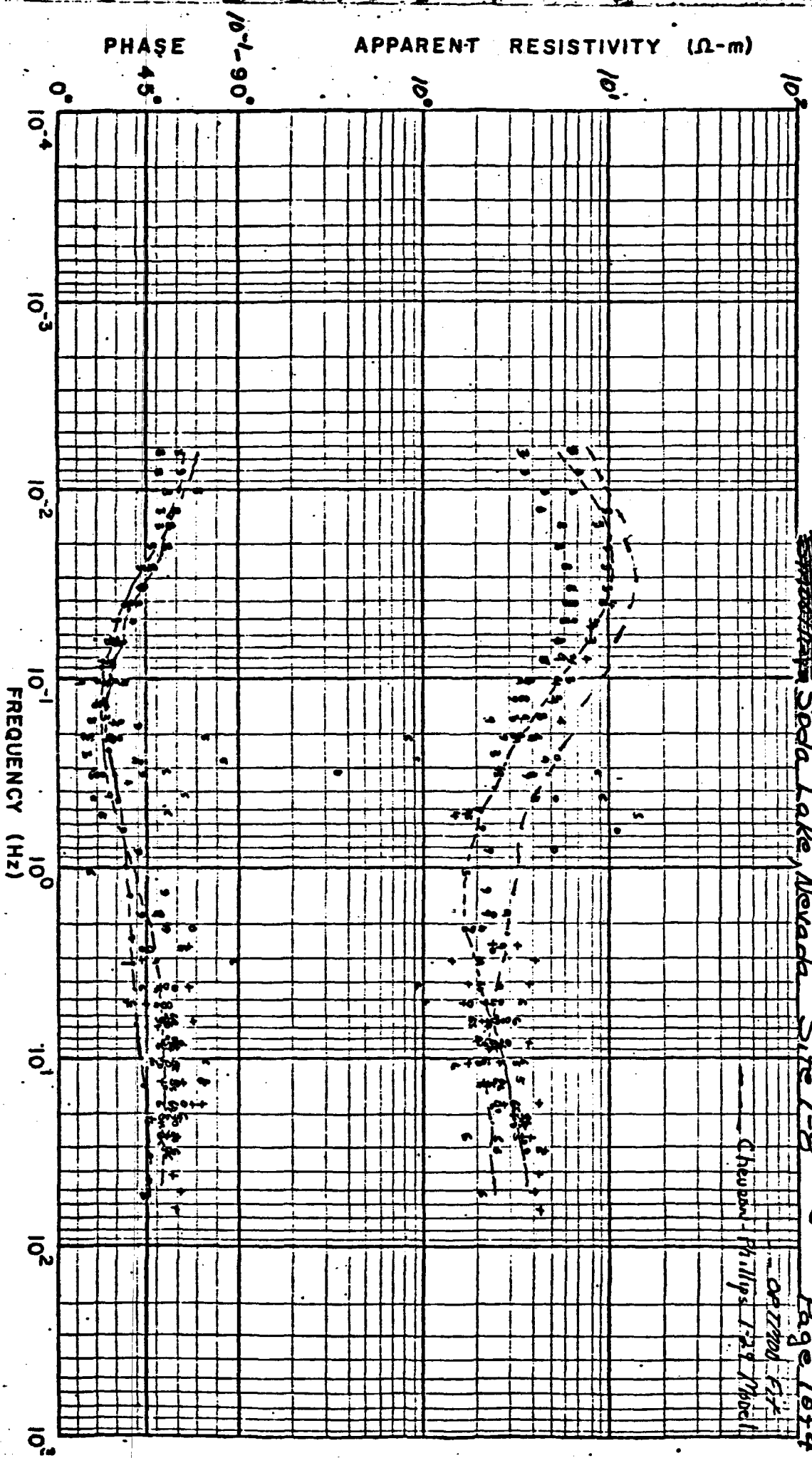
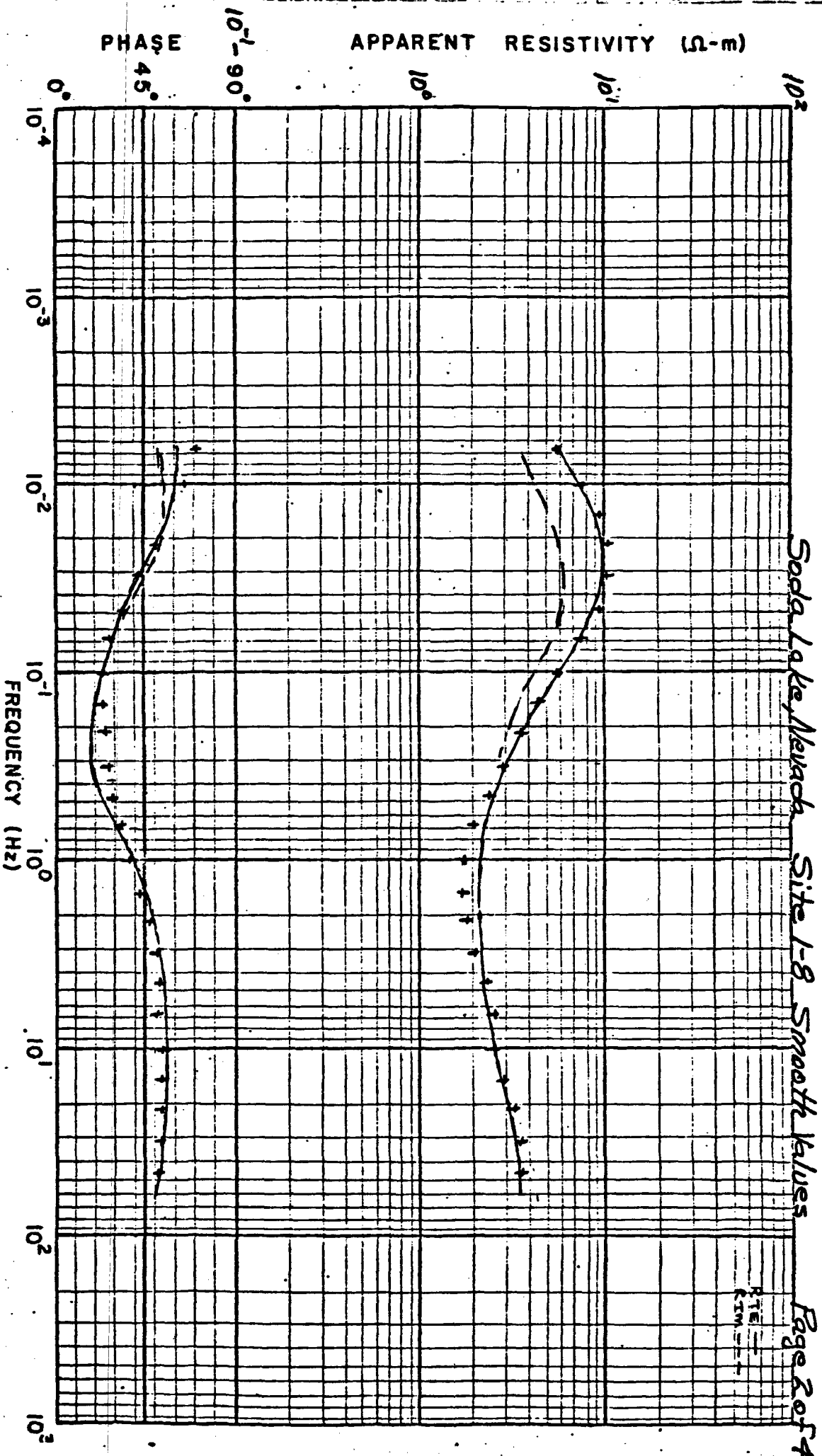
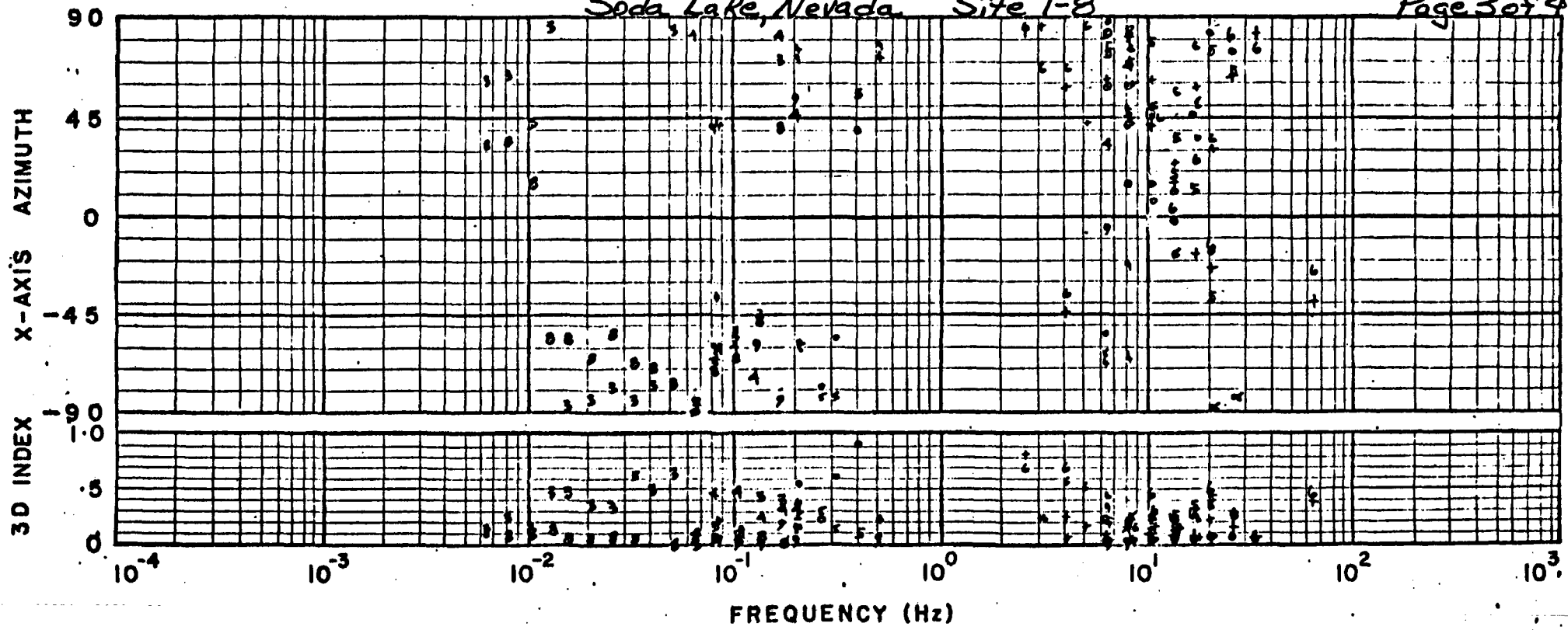


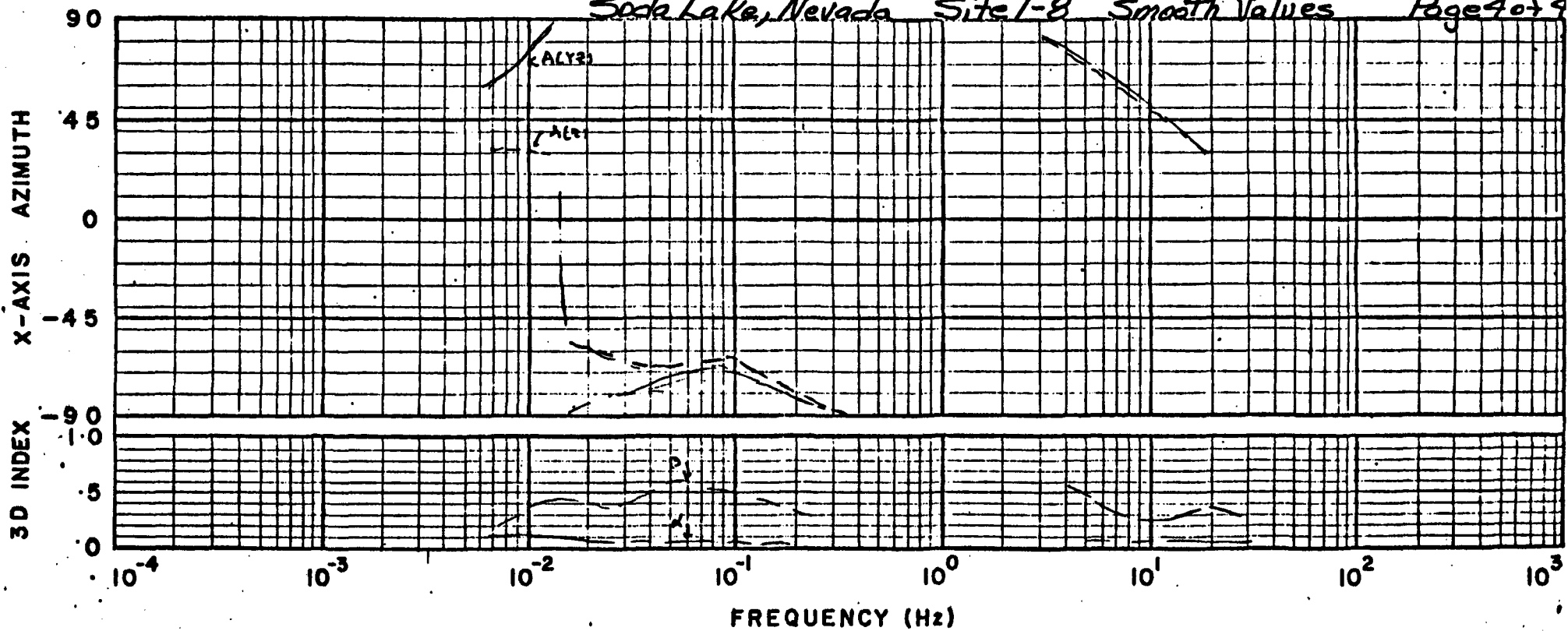
Figure II-8
Page 1044

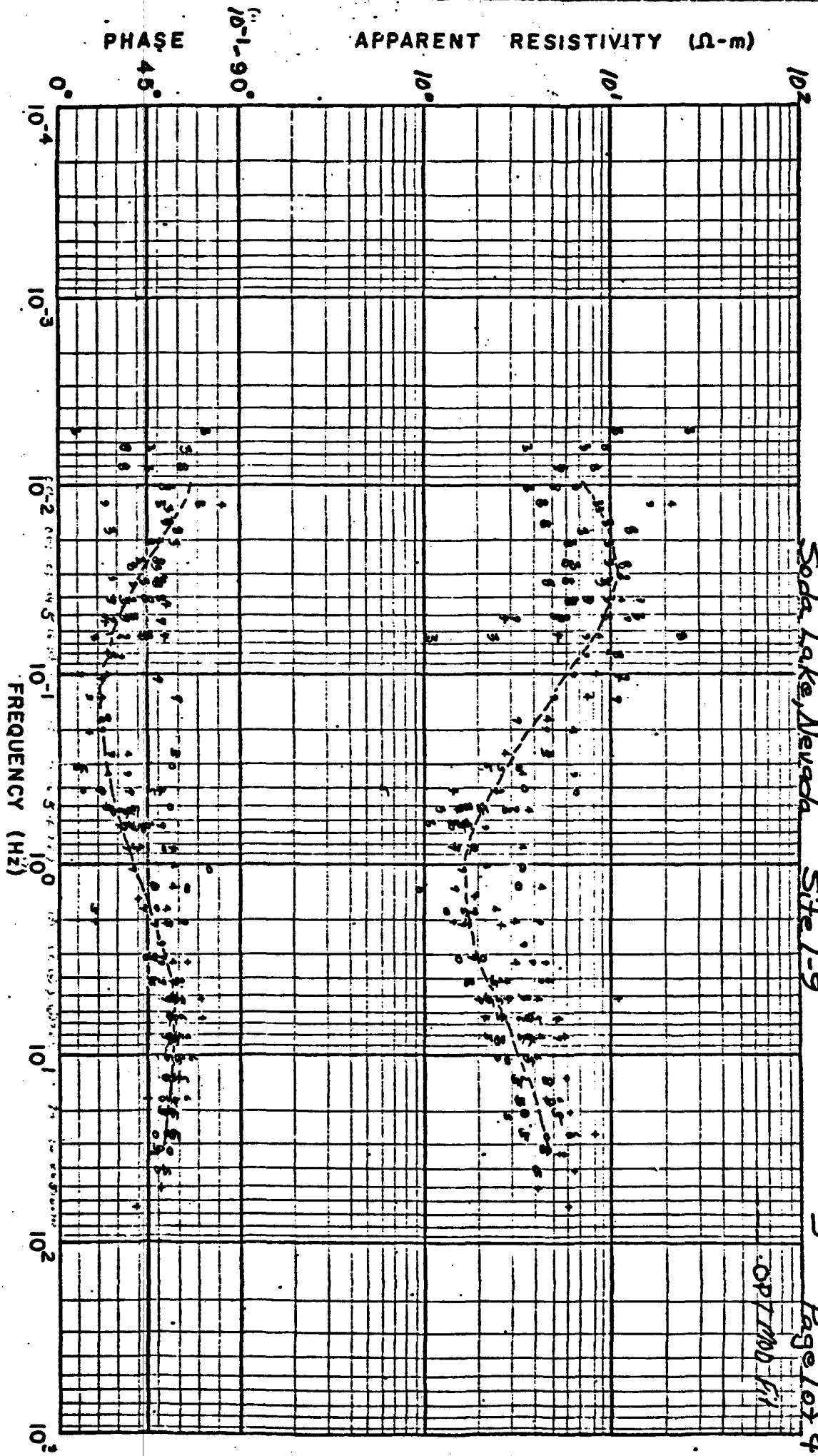


Soda Lake, Nevada Site 1-8

Page 3 of 4



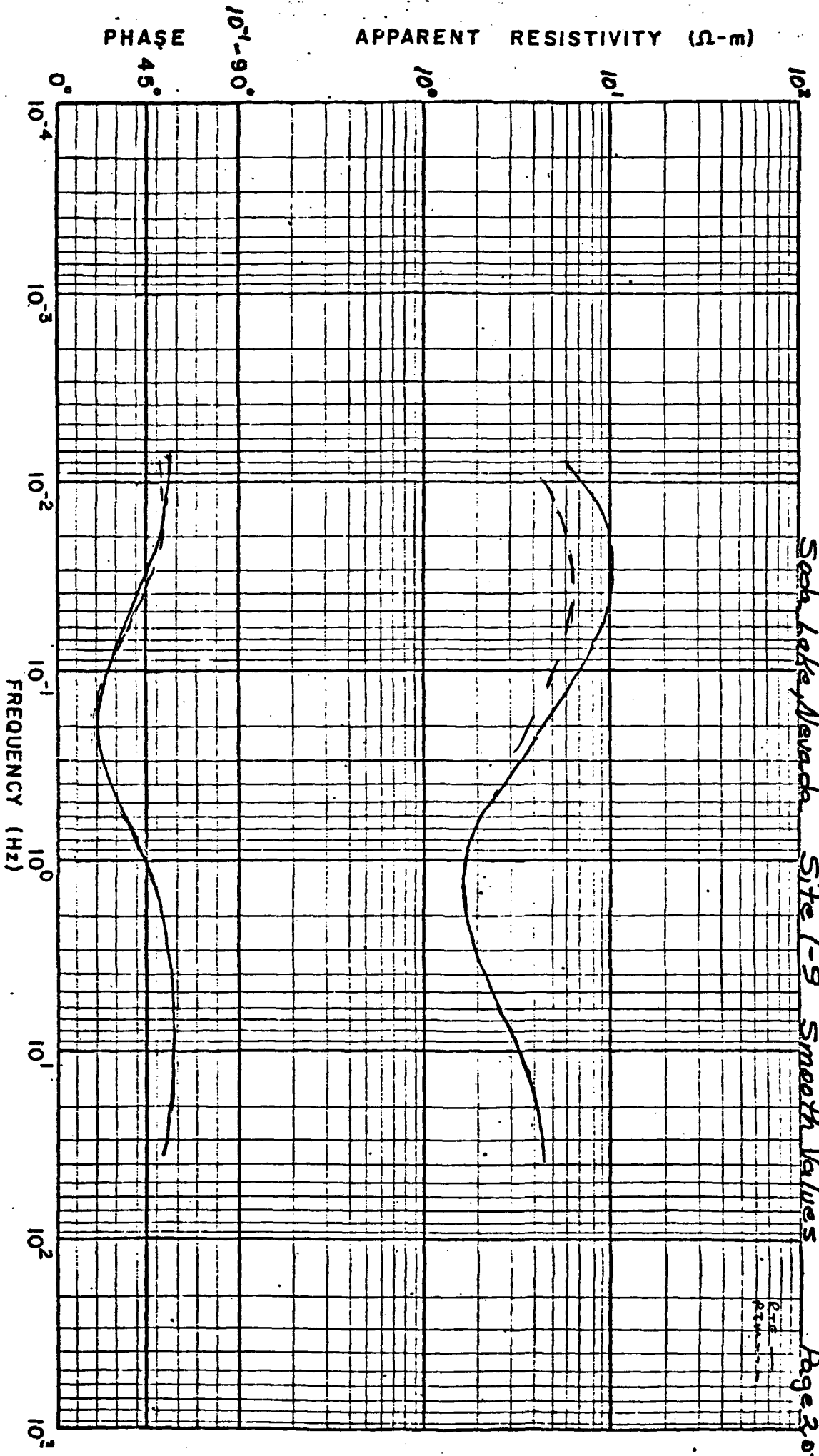




Soda Lake, Nevada Site L-9

OPT MOD FIT

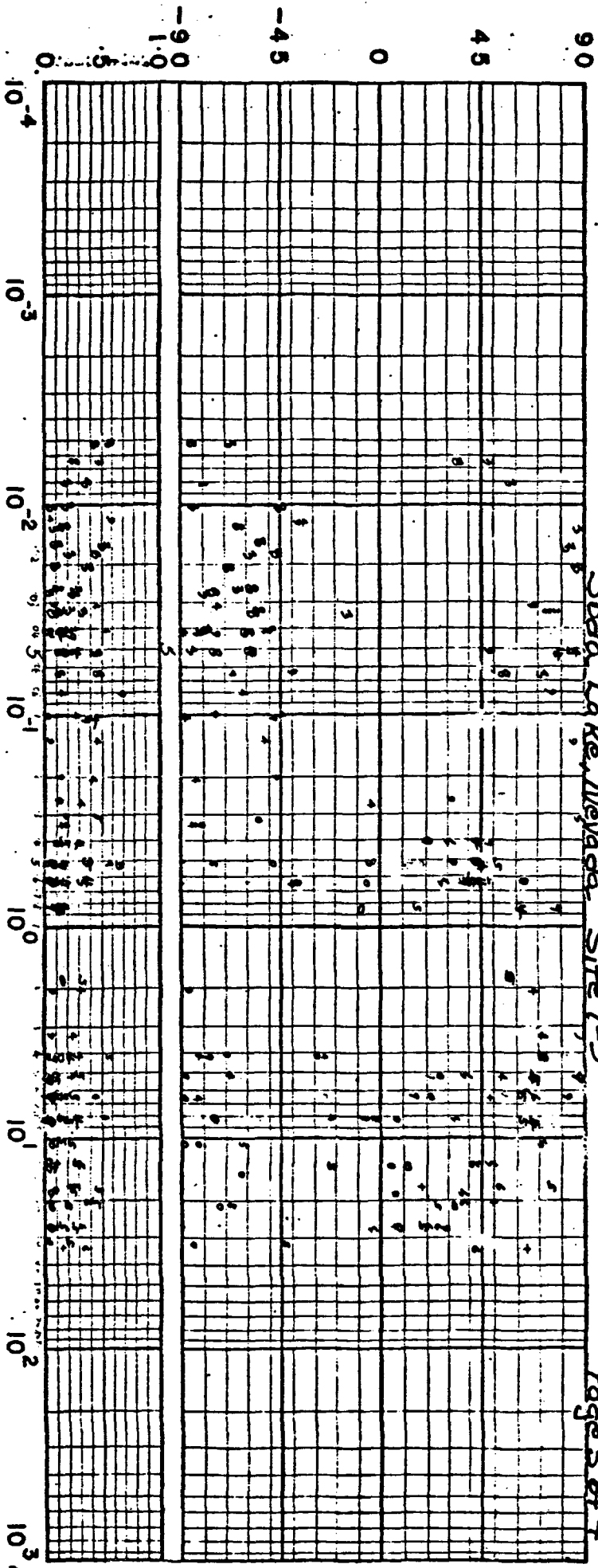
FIGURE II-9



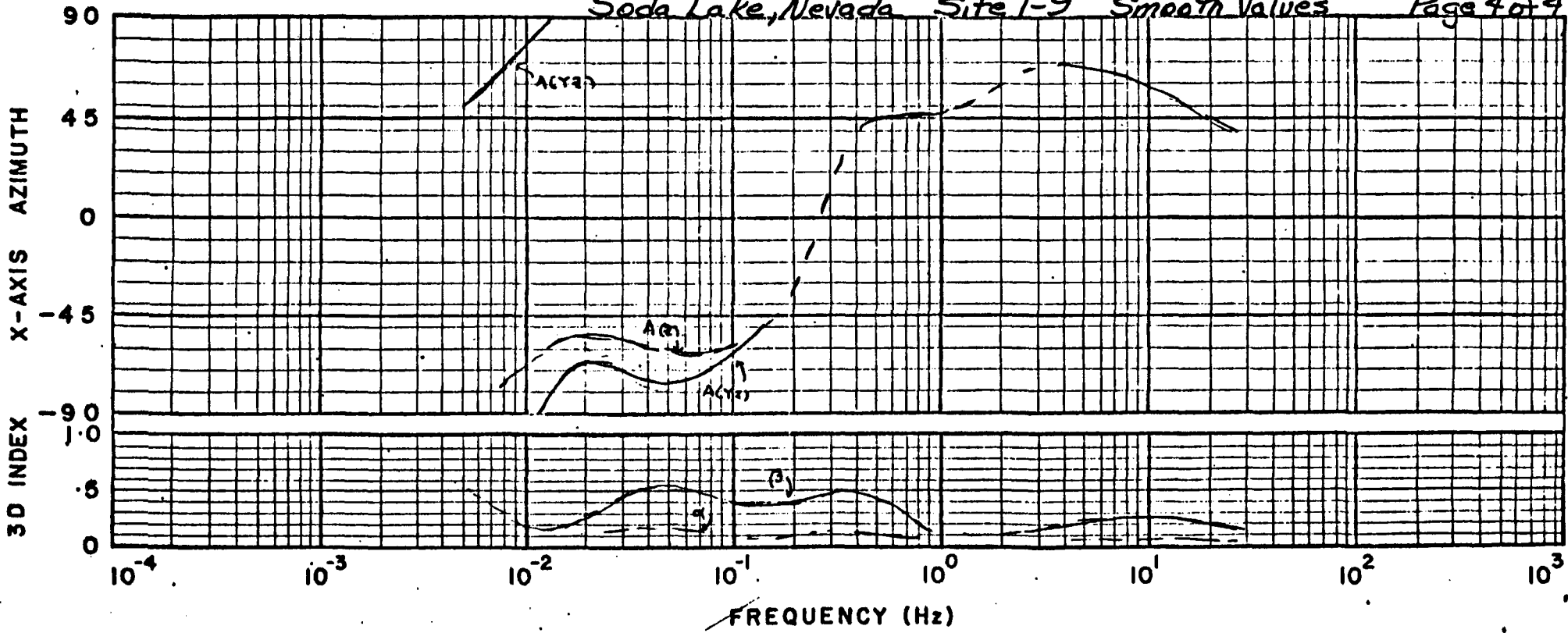
Seah Lake Nevada Site 1-9 Smooth Values

Page 3 of 4

3D INDEX X-AXIS AZIMUTH



DE 6/4/75



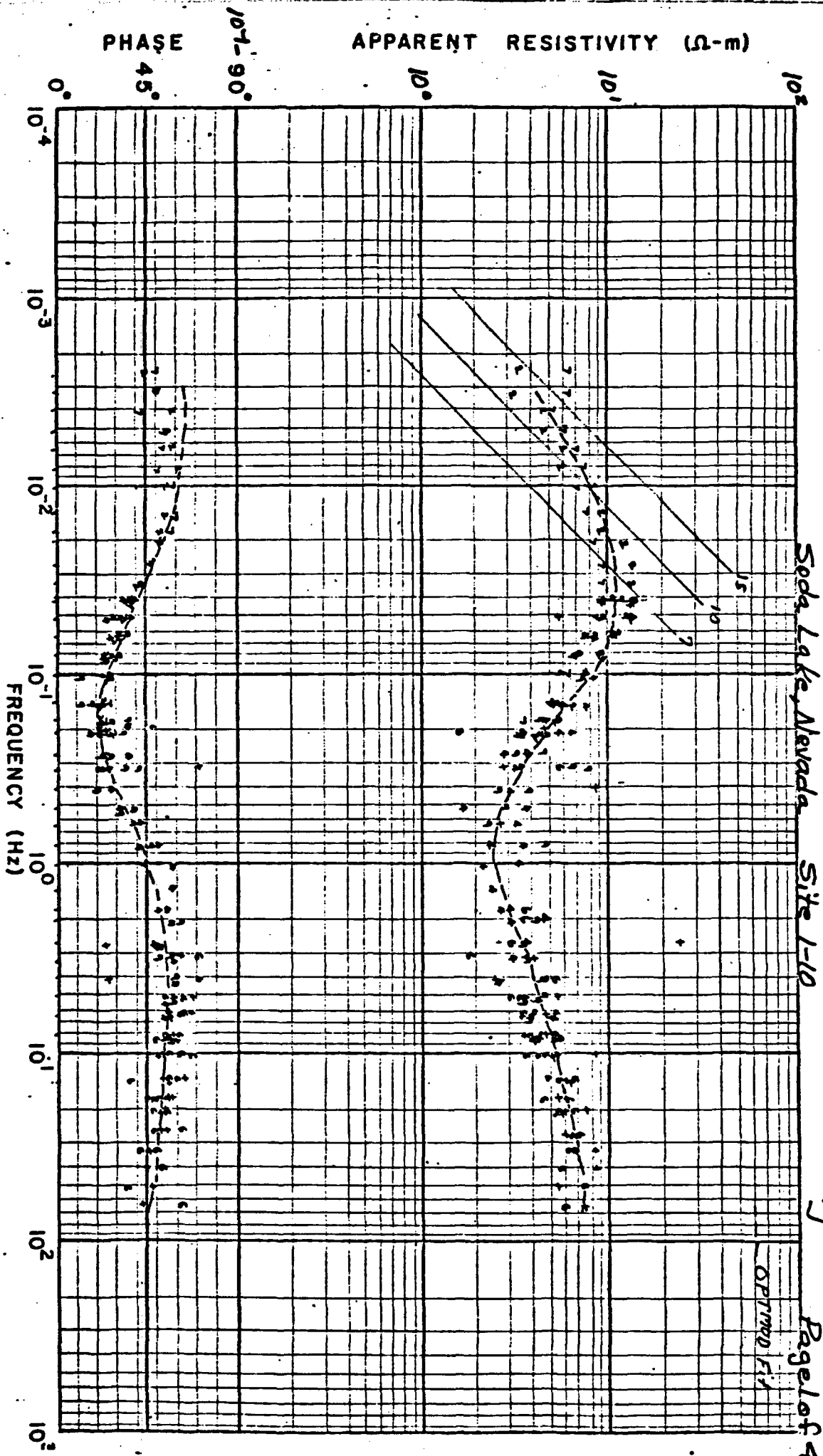
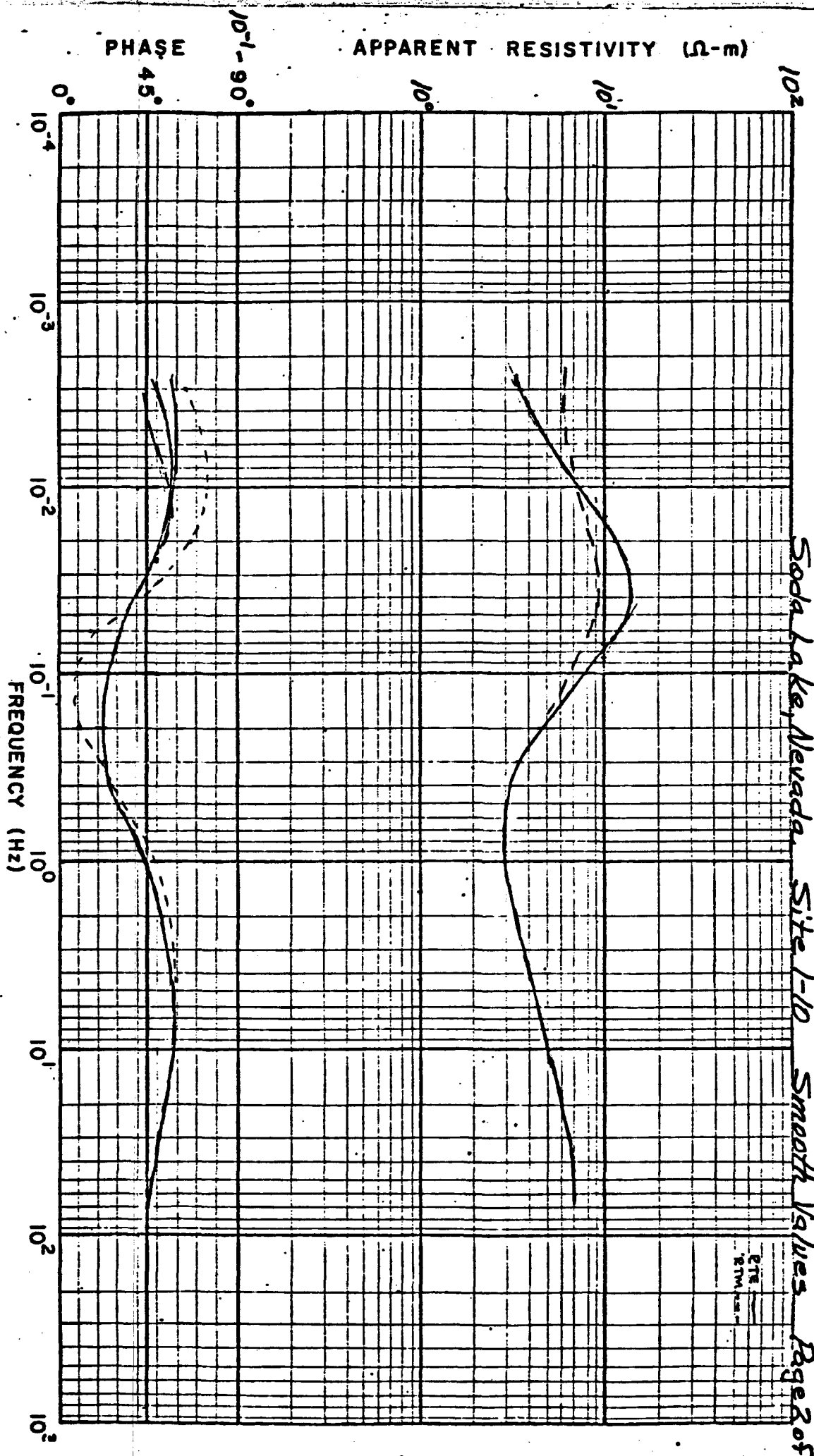


Figure - II - 10

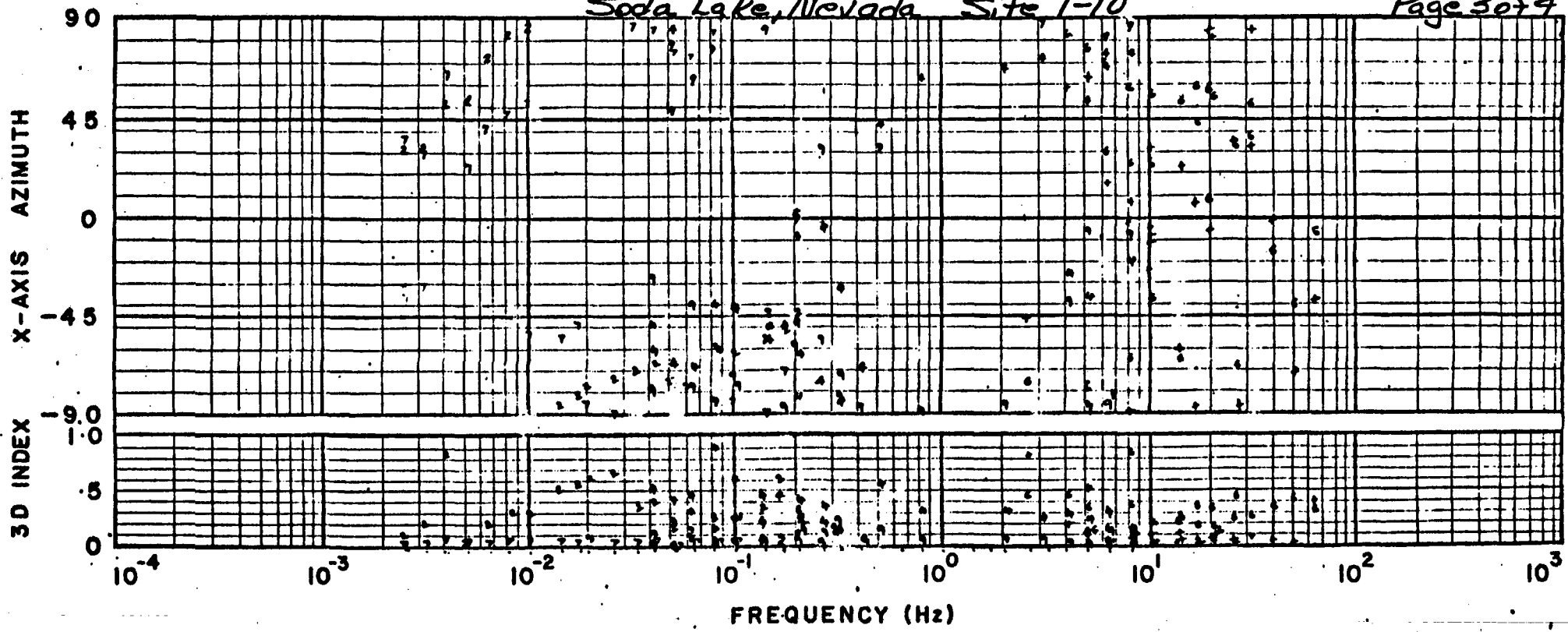


Soda Lake, Nevada Site 1-10 Smooth Values Page 2 of 4

ETC
ETM

Soda Lake, Nevada Site 1-10

Page 3 of 4



Soda Lake, Nevada Site 1-10 Smooth Values Page 4 of 9

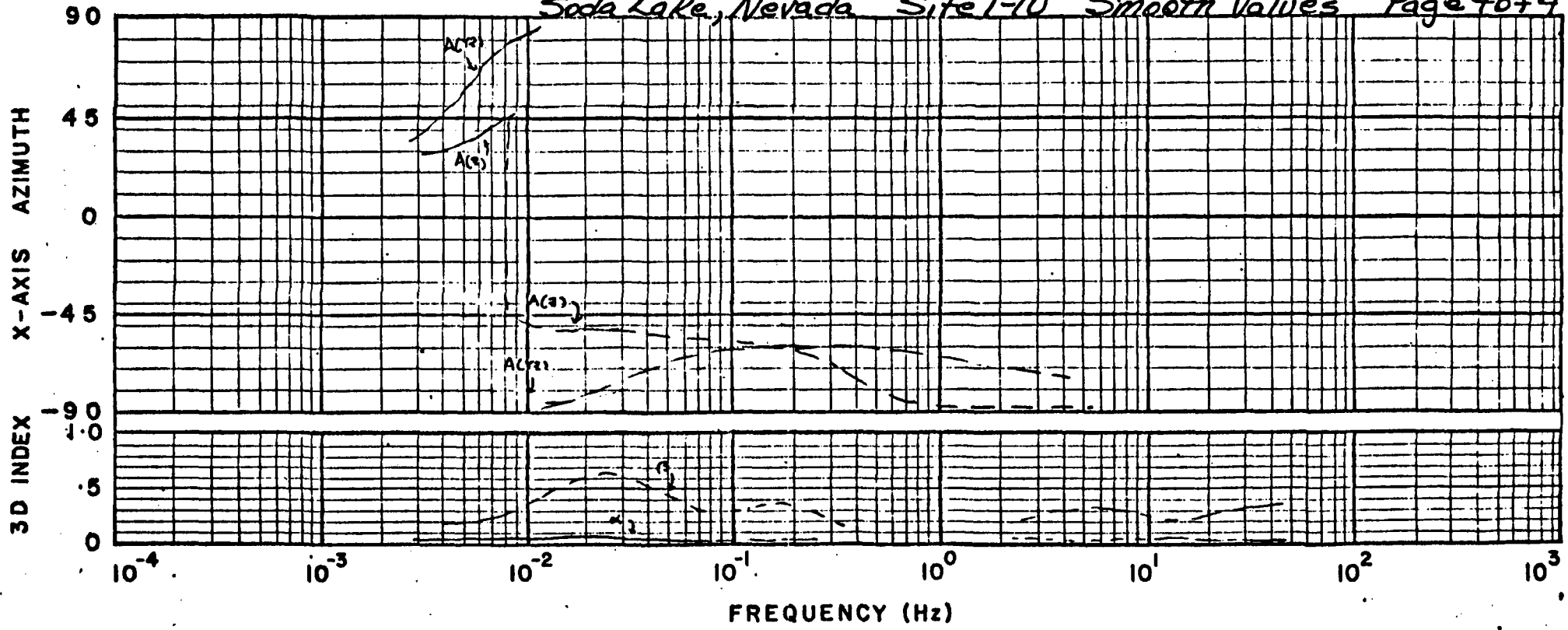


Figure II-11. Soda Lake, Nevada Area ~~Site 1-1~~
SITE 1-1

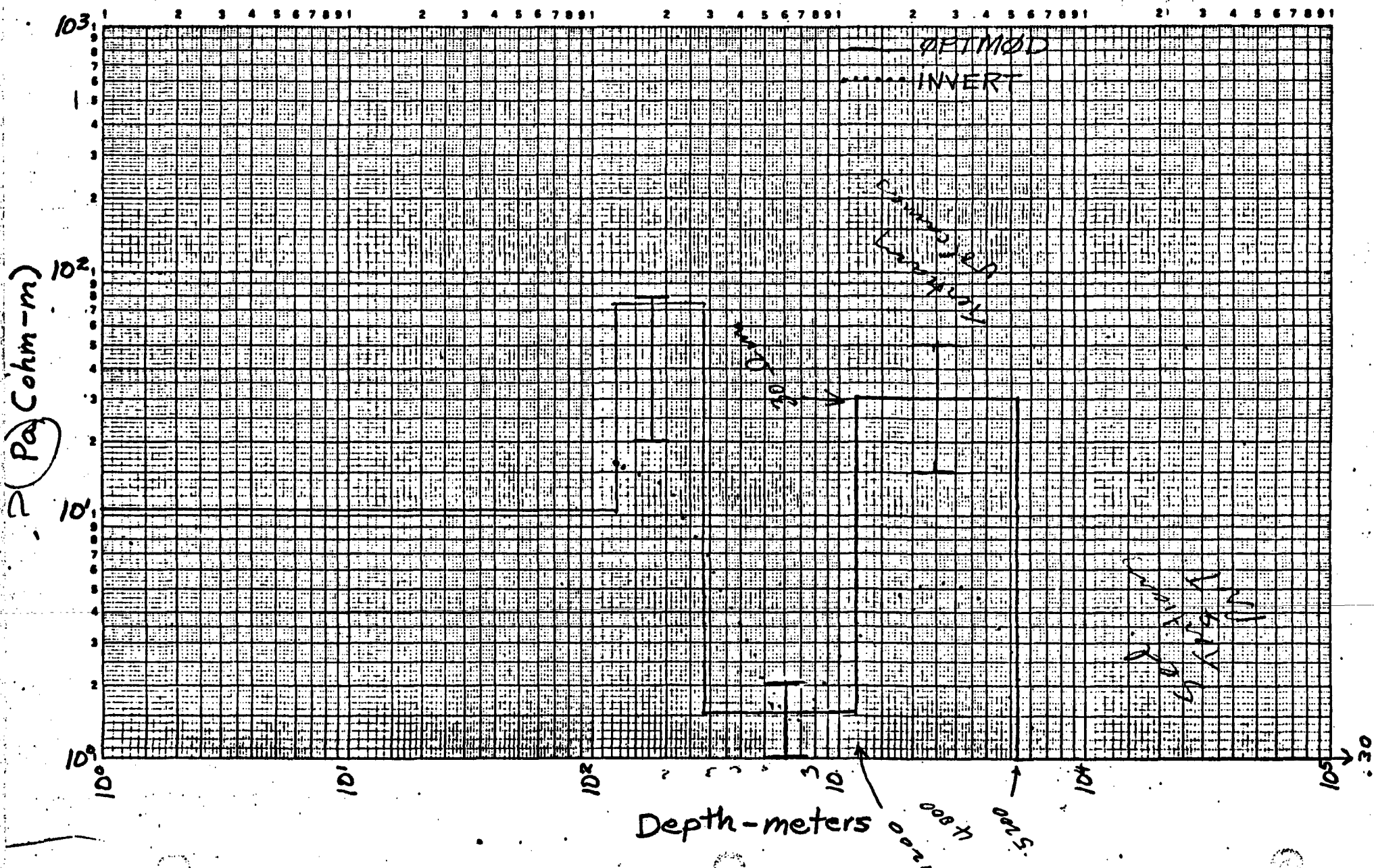


Figure II-12. Soda Lake, Nevada SITE 1-2

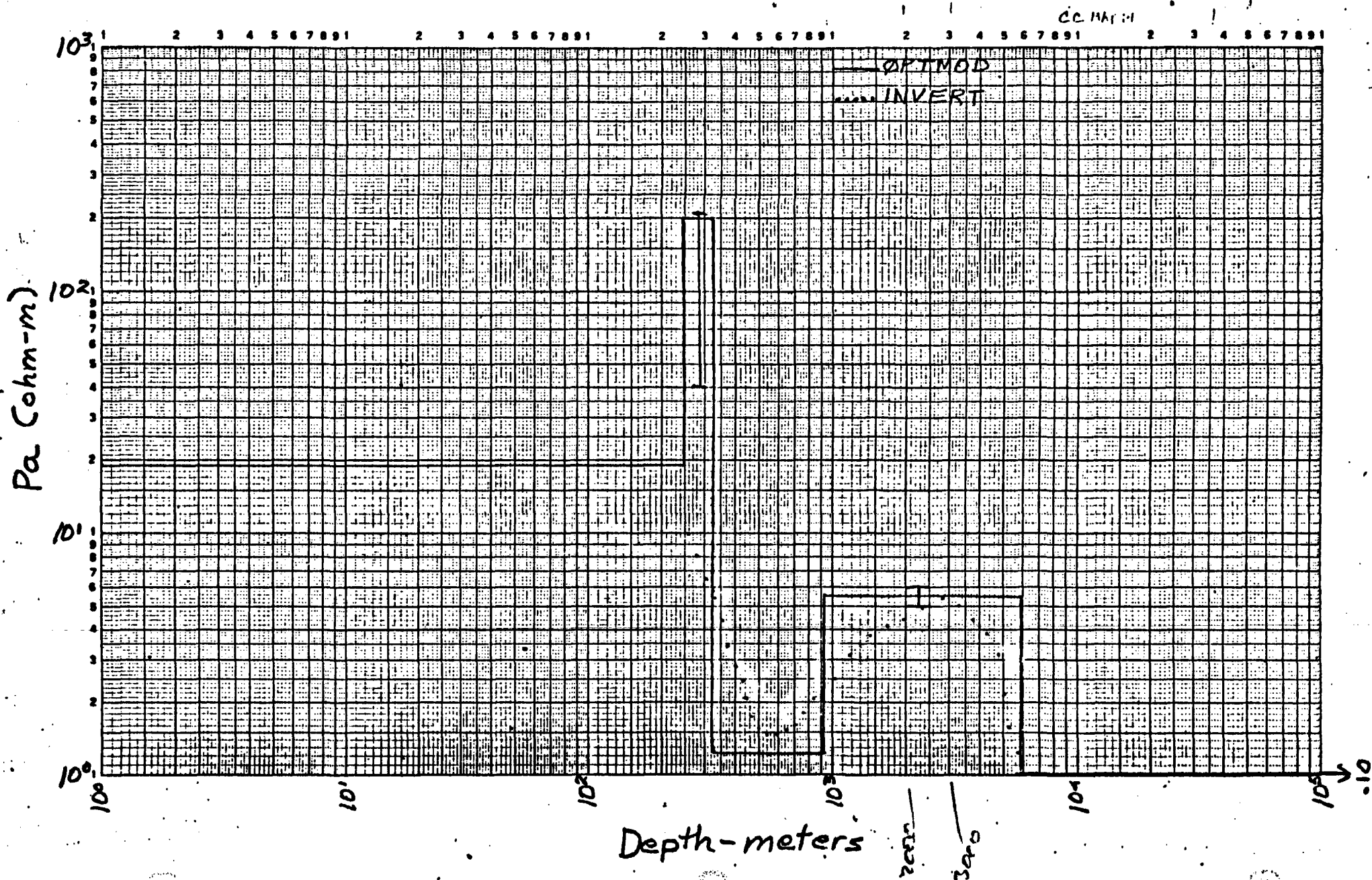


Figure II-13. Soda Lake, Nevada Site I-3

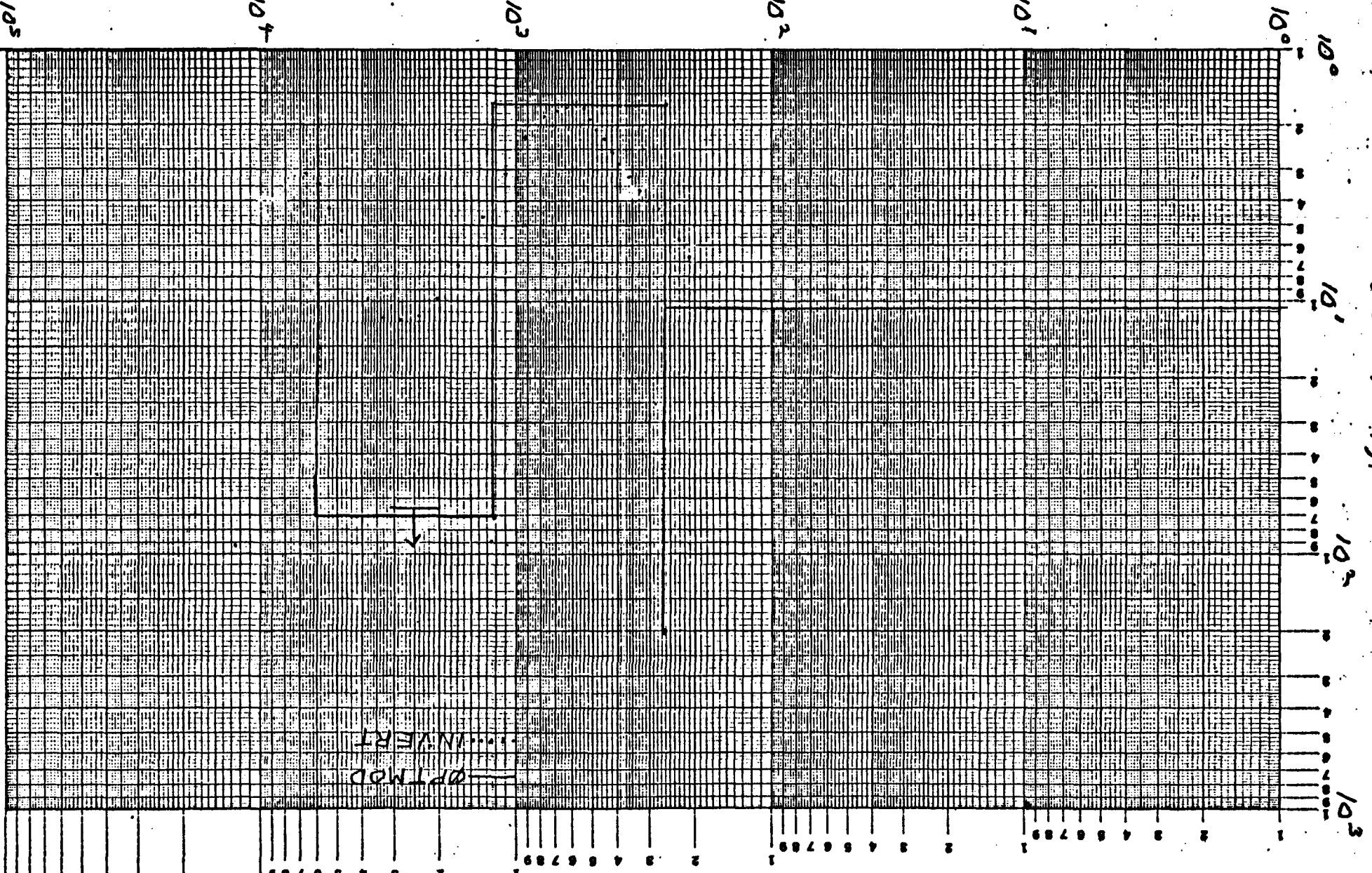


Figure II-14 Soda Lake, Nevada SITE 1-4

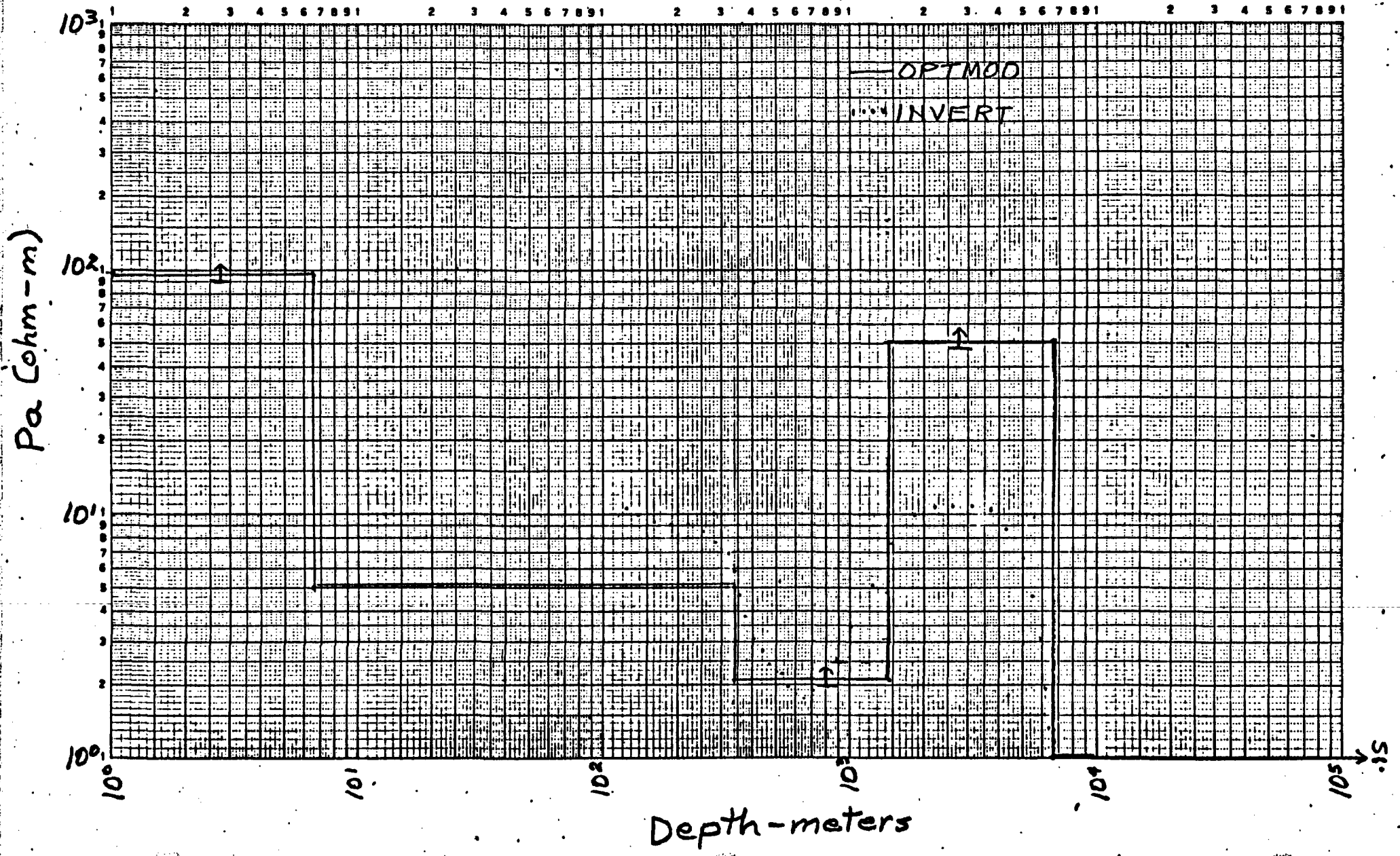


Figure II-15. Soda Lake, Nevada SITE 1-75

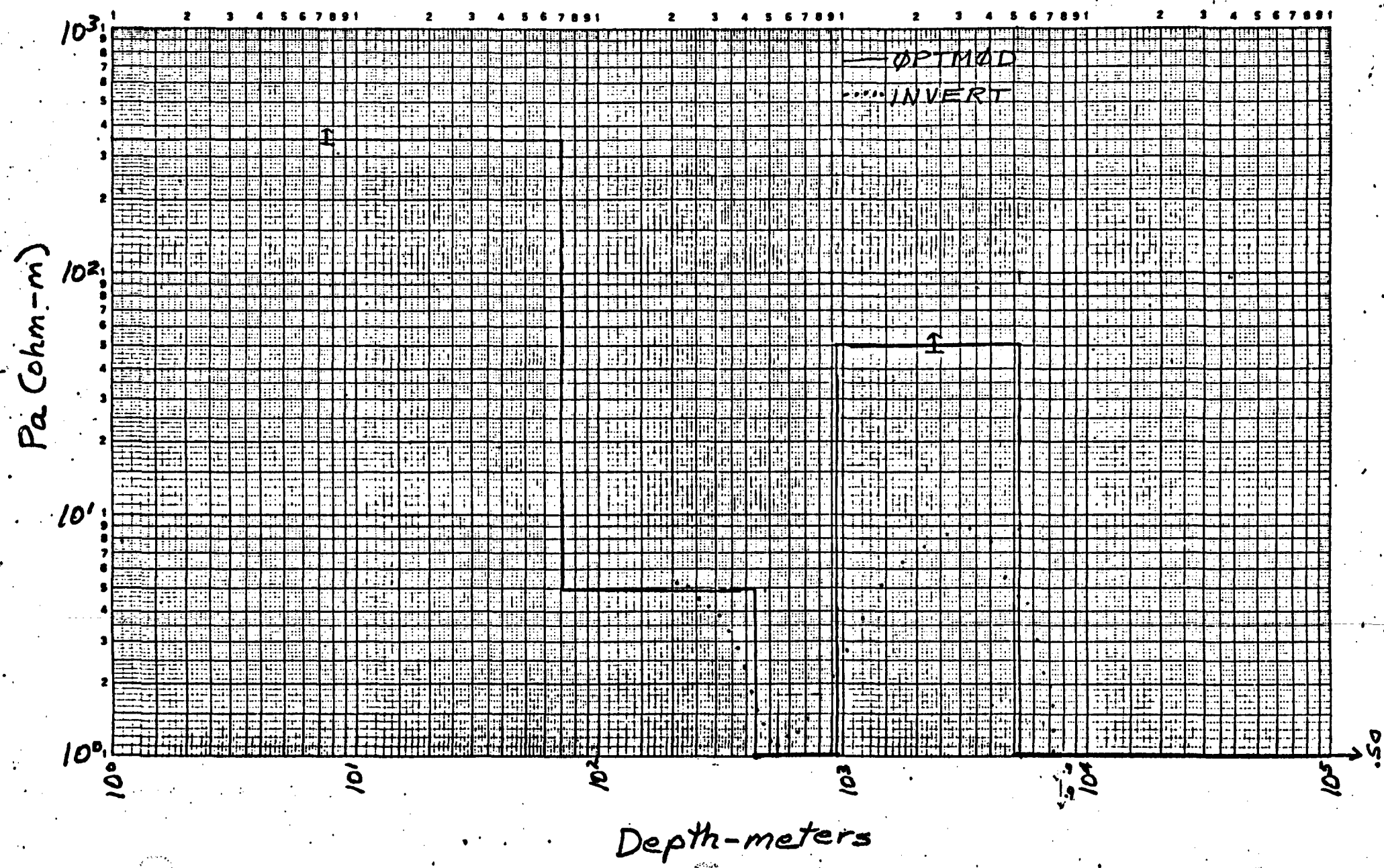


Figure II-16 Soda Lake, Nevada SITE 1-6

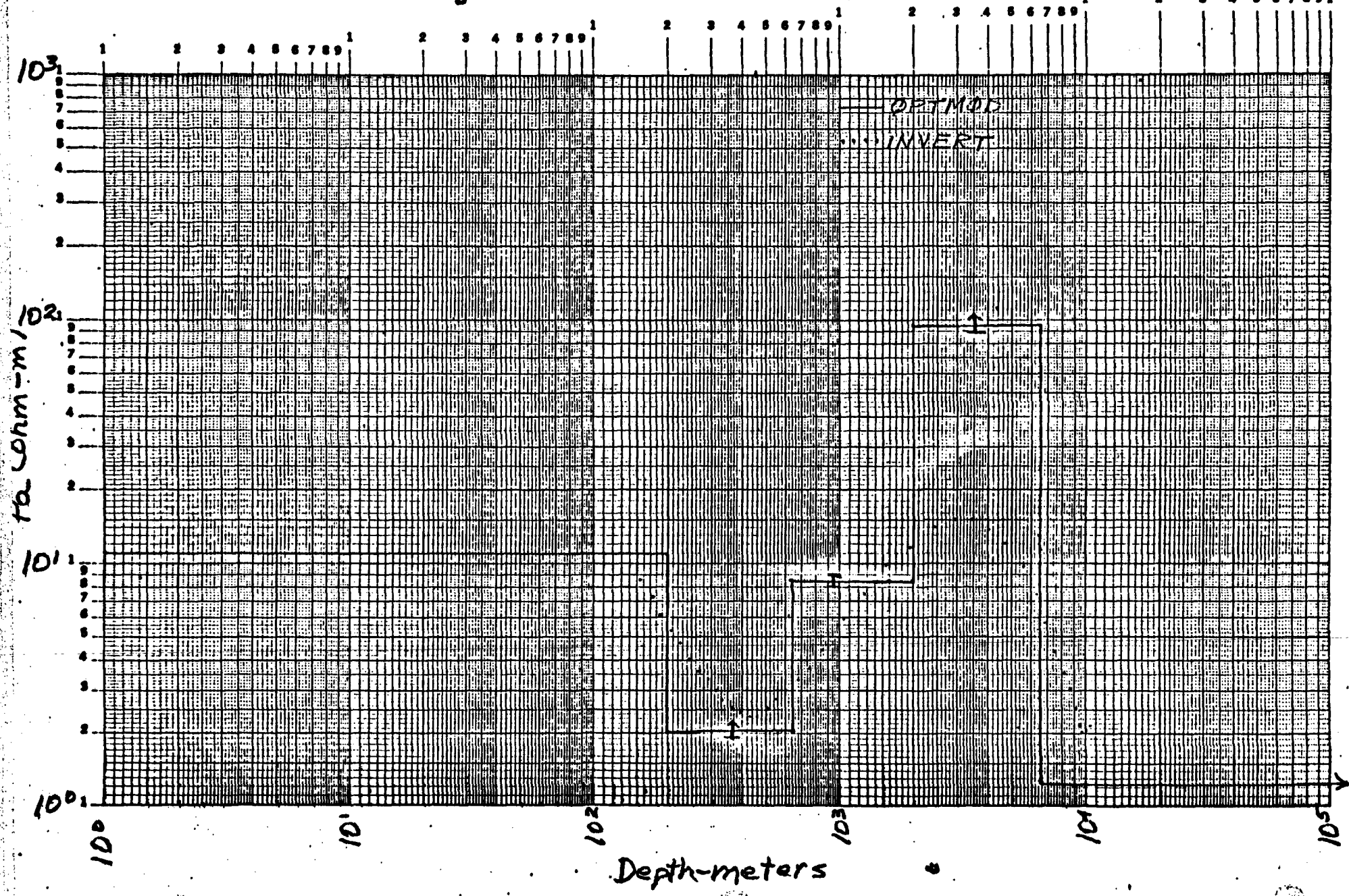
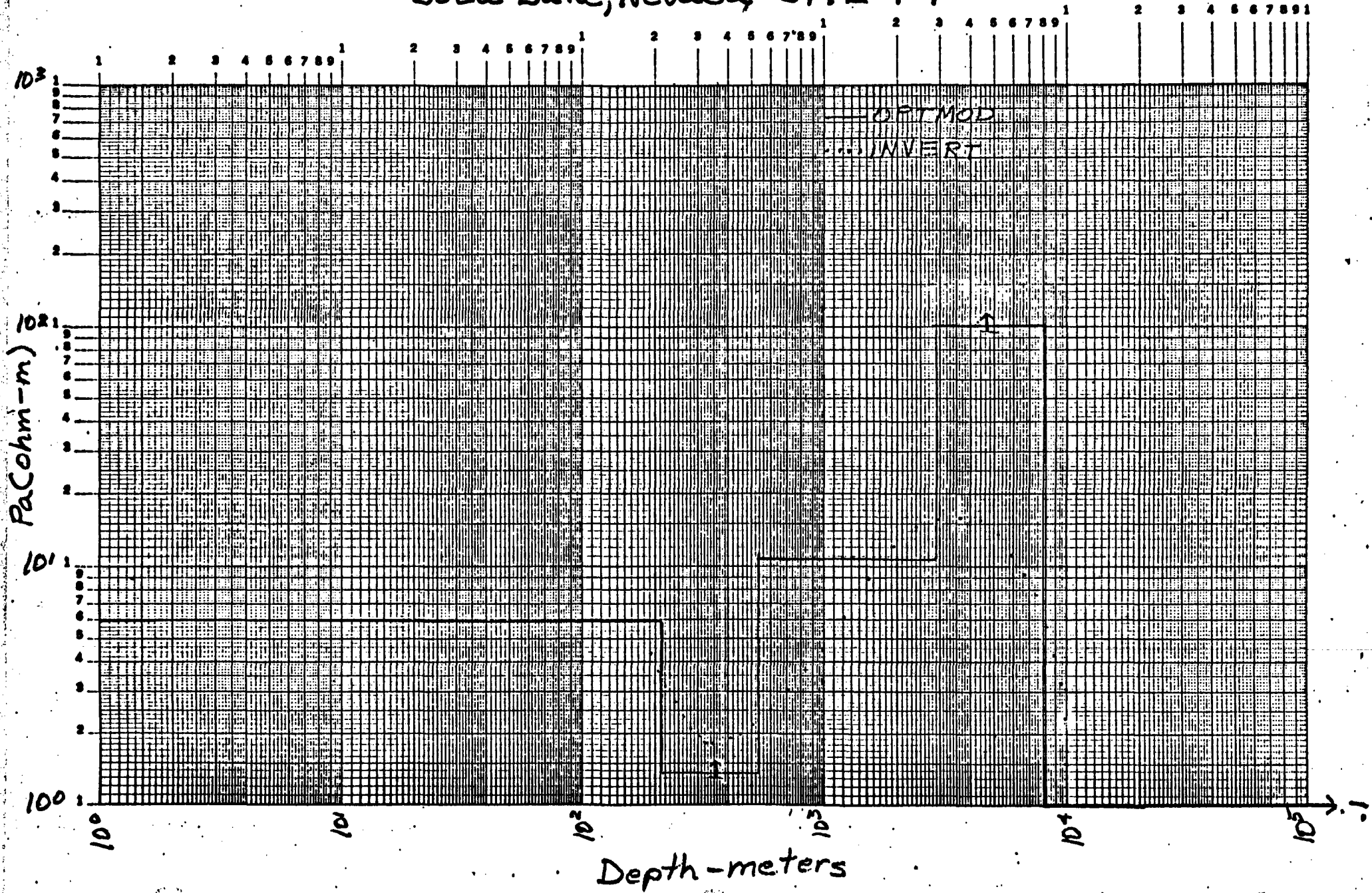


FIGURE II-17

Soda Lake, Nevada, SITE 1-7



800'
aquifer }
400'

Fundamental distribution
in the aquifer

Figure II-18. Soda Lake, Nevada SITE 1-8

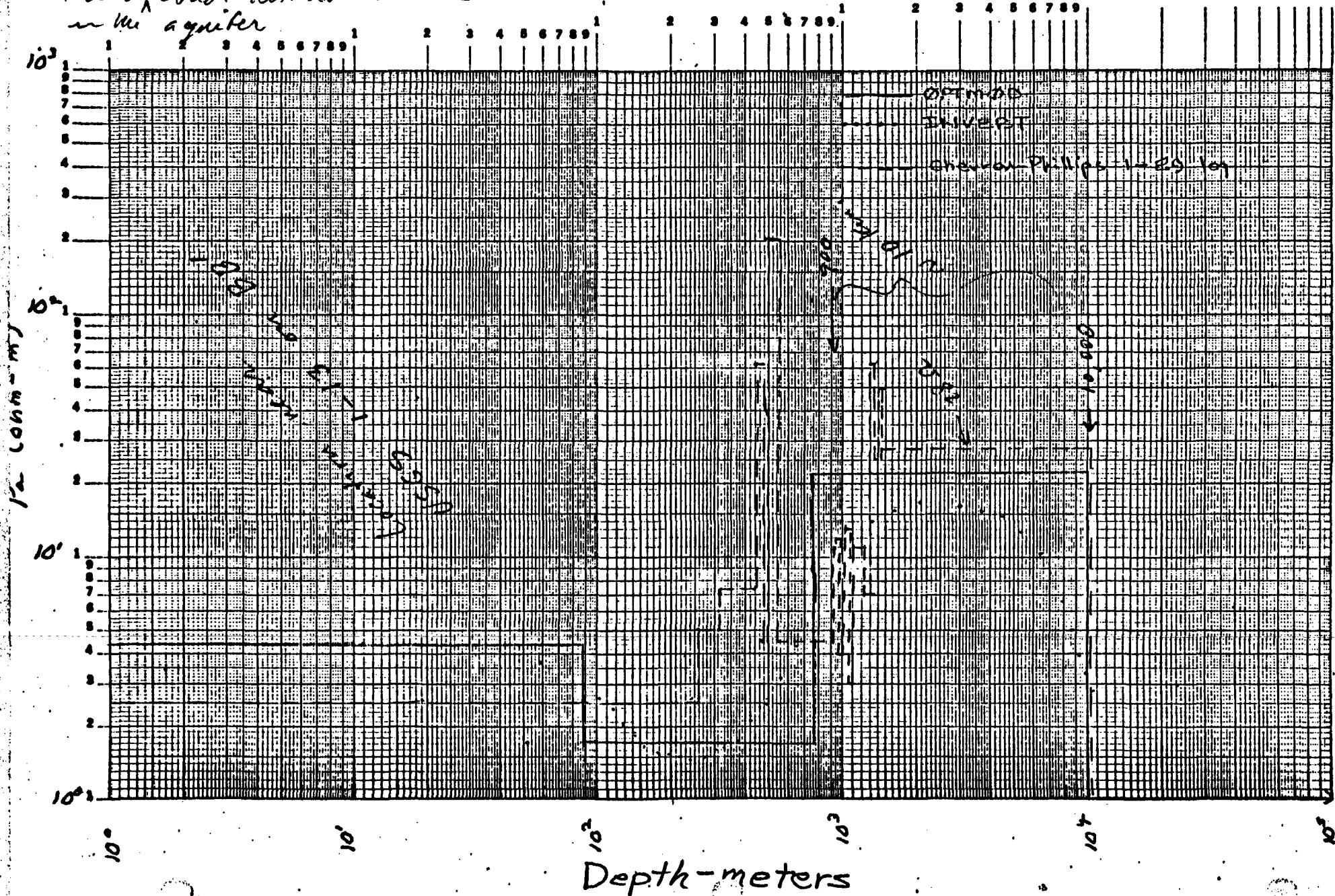


Figure. II-19 Soda Lake, Nevada SITE I-9

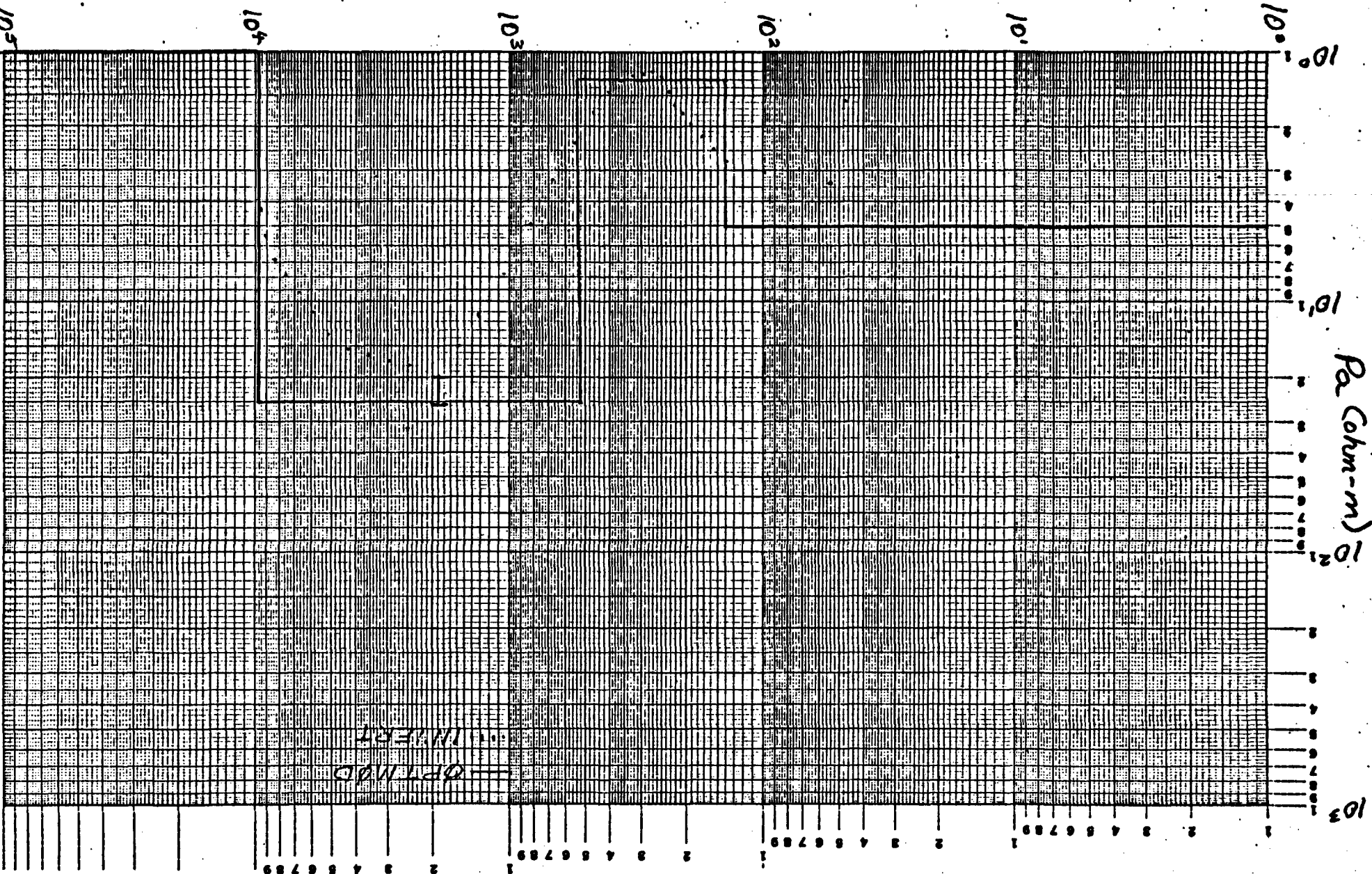
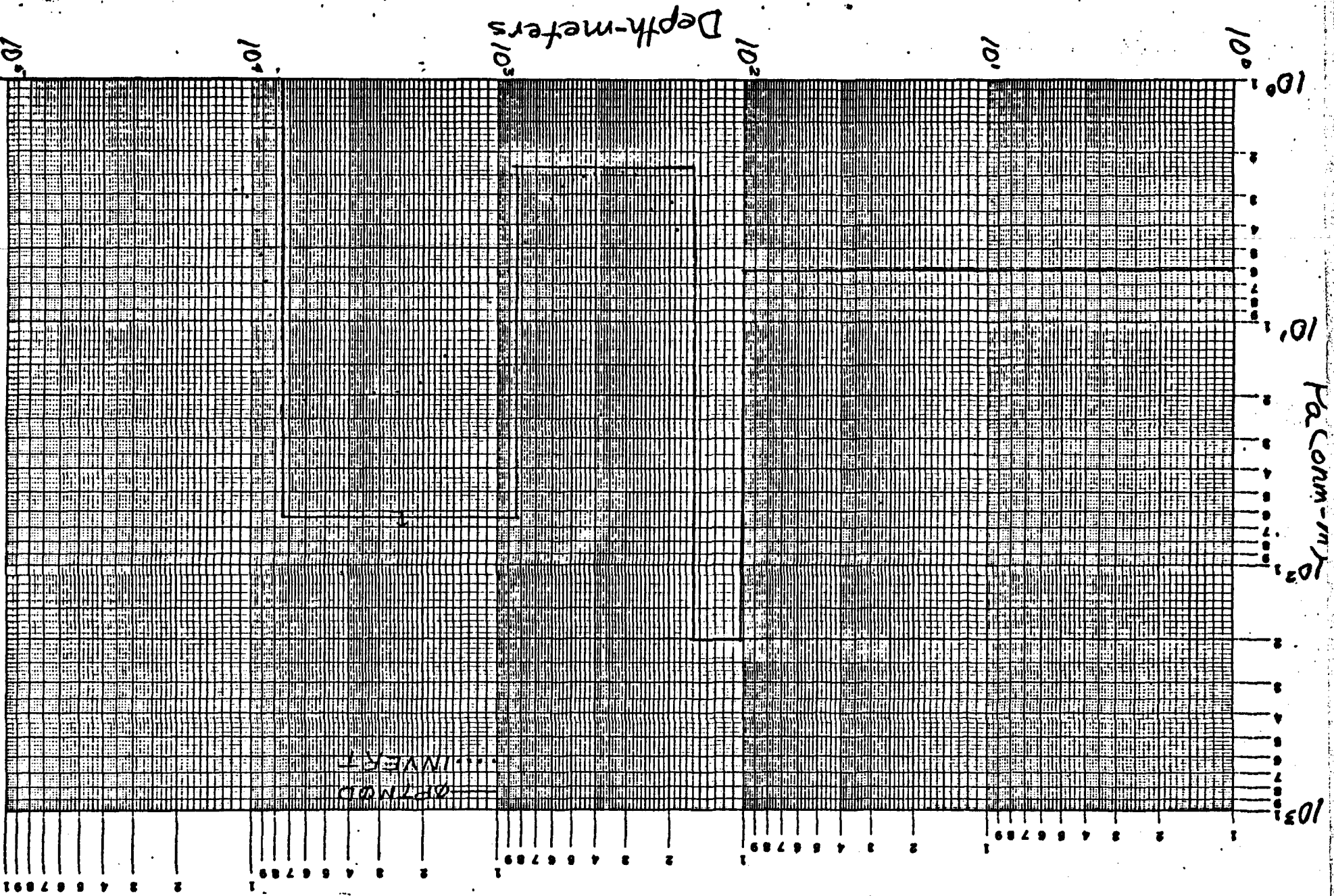


Figure II-20 Soda Lake, Nevada SITE I-10



10⁰

10¹

Depth-meters
10²

10²

10¹

10⁰

10⁰

10¹

Pa (cm-m)
10²

10³

INVERT

Chart No. 1-5

FIGURE III-1

COMPOSIT RESISTIVITY CROSS SECTION

: PLOTTED FROM THE RESULTS OF THE

MAGNETO TELLURIC SURVEY

OF THE
SODA LAKE NEVADA AREA

BY

GEOTRONICS CORPORATION

FOR

SOCAL MINERALS

MAY, 1975

LEGEND

APPARENT RESISTIVITIES IN OHM-METERS
 CONTOUR INTERVALS: 1, 1.5, 2, 5, 7.5, 10 Ω -m
 HORIZONTAL SCALE: 1" = 2000'
 HORIZONTAL/VERTICAL RATIO: 0.61
 PROGRAM: INVERT INVERSION
 USING AMPLITUDE AND PHASE

Handwritten:
 in resist.
 continuous

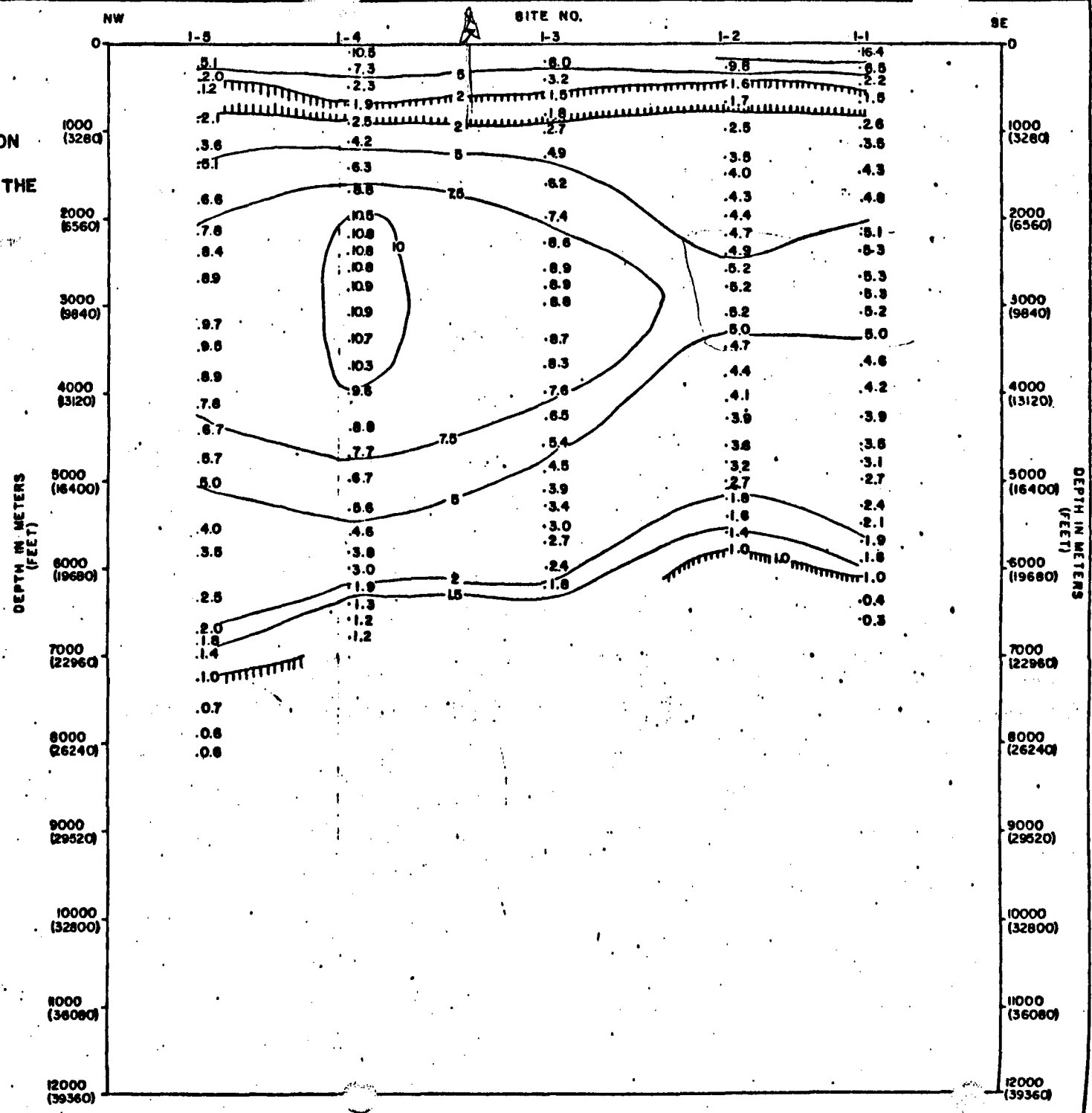


FIGURE III-2

COMPOSIT RESISTIVITY CROSS SECTION
 PLOTTED FROM THE RESULTS OF THE
 MAGNETO TELLURIC SURVEY
 OF THE
 SODA LAKE NEVADA AREA
 BY
 GEOTRONICS CORPORATION
 FOR
 SOCIAL MINERALS
 MAY, 1975

LEGEND

APPARENT RESISTIVITIES IN OHM-METERS
 CONTOUR INTERVALS: 1, 1.5, 2.5, 5, 7.5, 10 Ω-m
 HORIZONTAL SCALE: 1" = 2000'
 HORIZONTAL/VERTICAL RATIO: 0.61
 PROGRAM: INVERT INVERSION
 USING AMPLITUDE AND PHASE

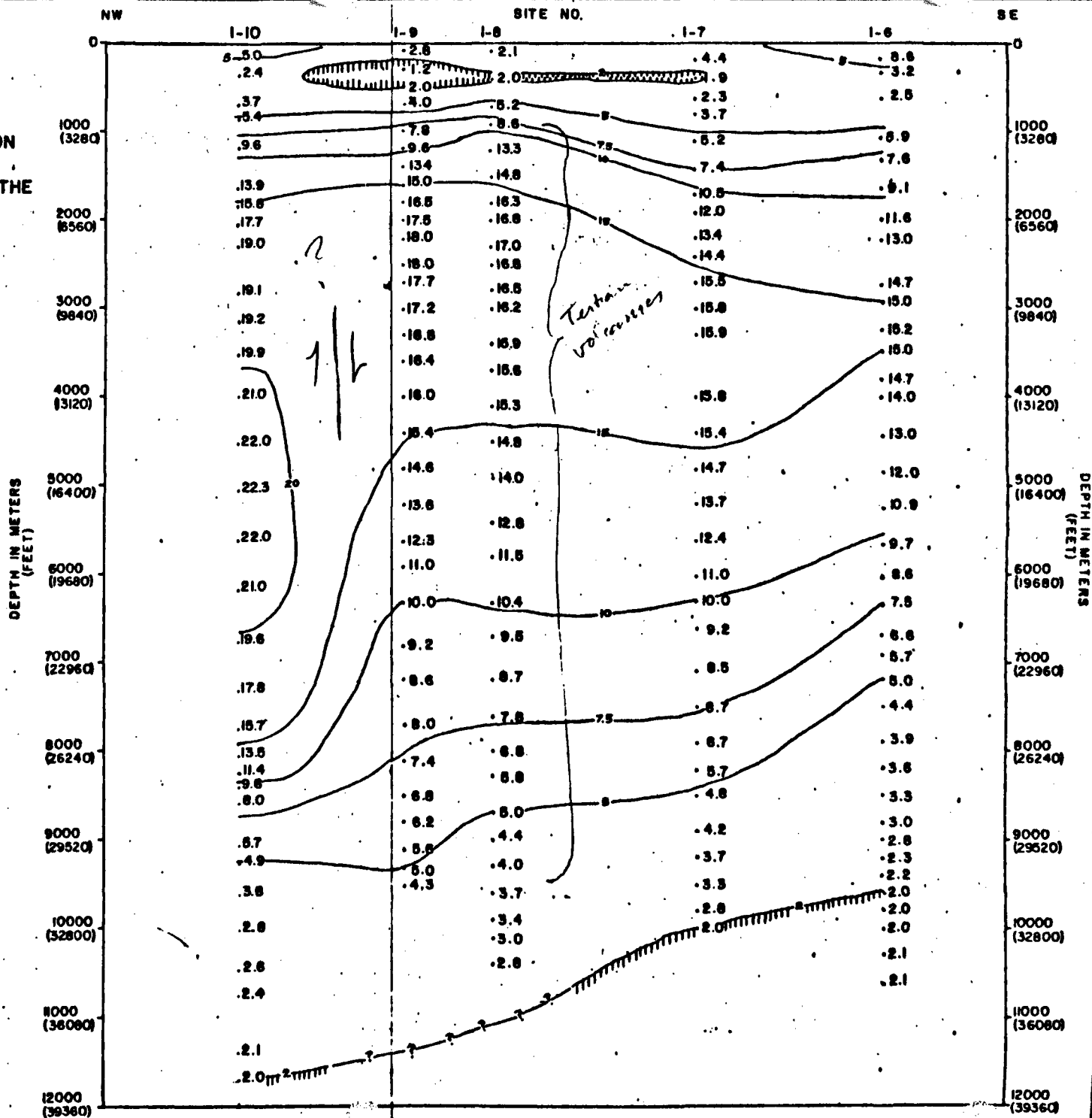


FIGURE III-3A

COMPOSIT RESISTIVITY CROSS SECTION
PLOTTED FROM THE RESULTS OF THE
MAGNETO TELLURIC SURVEY
OF THE
SODA LAKE NEVADA AREA
BY
GEOTRONICS CORPORATION
FOR
SOCAL MINERALS
APRIL, 1975.

Correlation of the 1-D discrete layer models

LEGEND

APPARENT RESISTIVITIES IN OHM-METERS
 CONTOUR INTERVALS:
 HORIZONTAL SCALE: 1" = 2000'
 HORIZONTAL/VERTICAL RATIO: 0.61

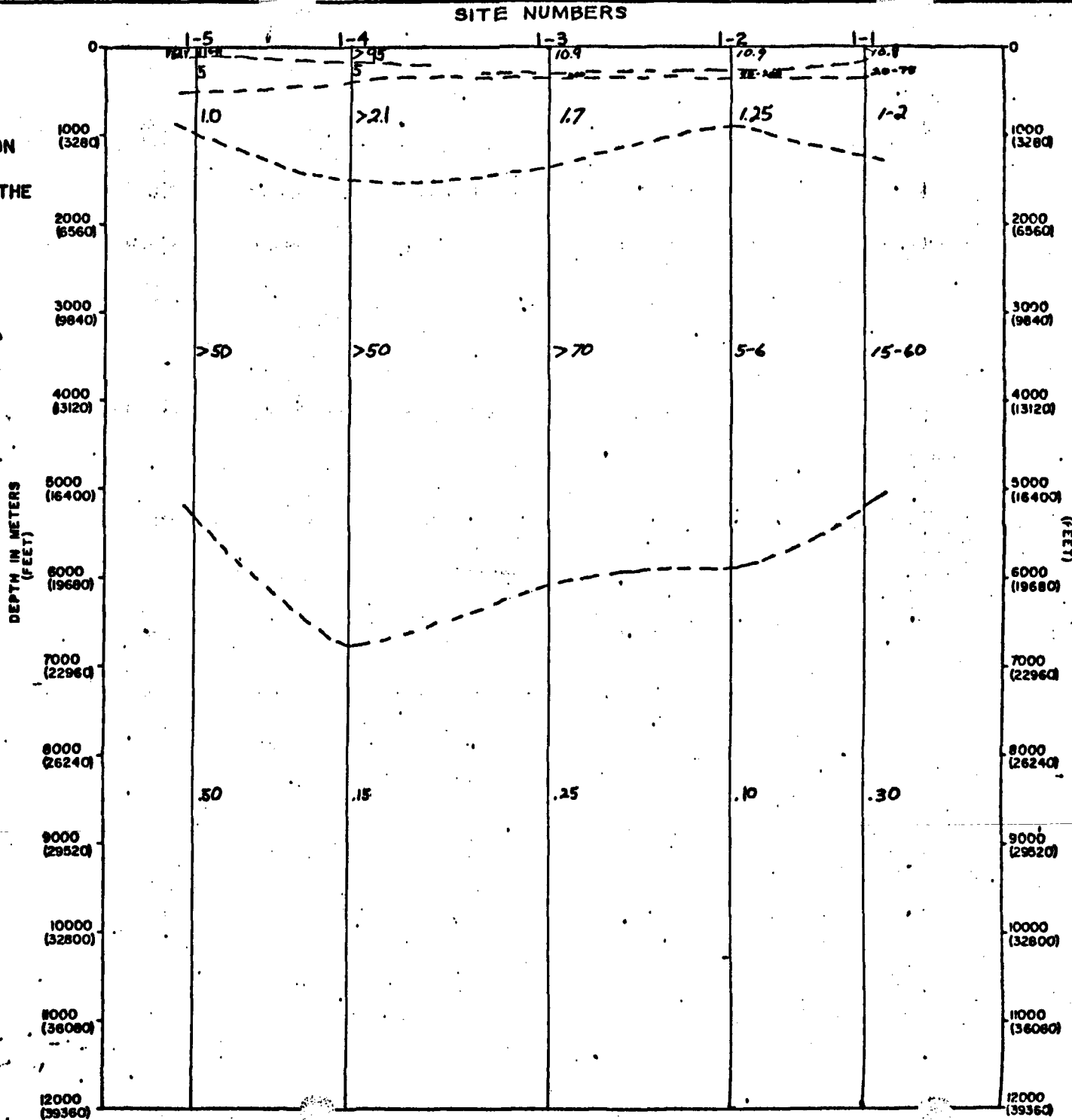


FIGURE III-3B

COMPOSIT RESISTIVITY CROSS SECTION
 PLOTTED FROM THE RESULTS OF THE
 MAGNETO TELLURIC SURVEY
 OF THE
 SODA LAKE NEVADA AREA
 BY
 GEOTRONICS CORPORATION
 FOR
 SOCAL MINERALS
 APRIL, 1975.

LEGEND

APPARENT RESISTIVITIES IN OHM-METERS
 CONTOUR INTERVALS:
 HORIZONTAL SCALE: 1" = 2000'
 HORIZONTAL/VERTICAL RATIO: 0.61

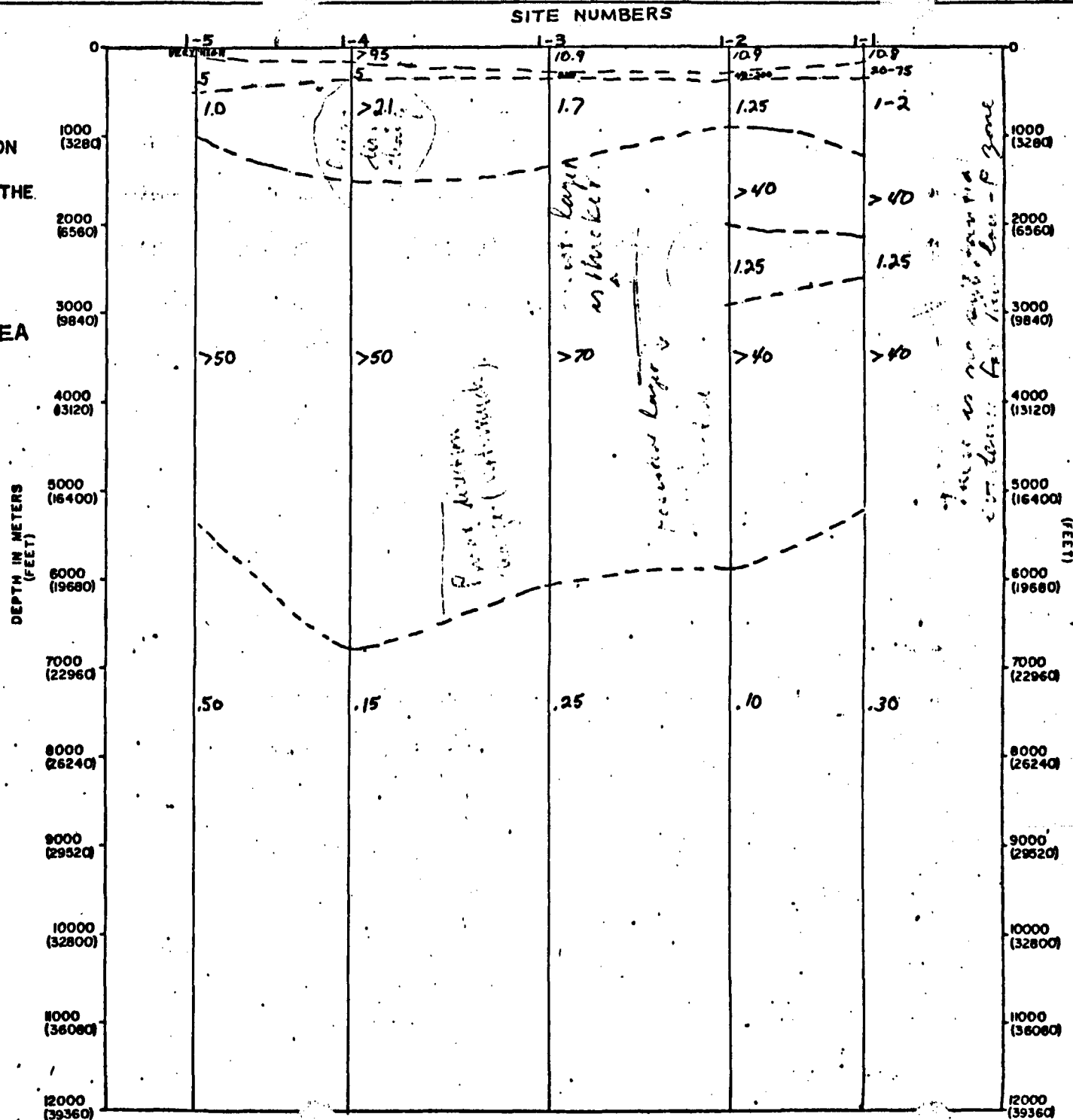


FIGURE III-4

COMPOSIT RESISTIVITY CROSS SECTION
 PLOTTED FROM THE RESULTS OF THE
 MAGNETO TELLURIC SURVEY
 OF THE
 SODA LAKE NEVADA AREA
 BY
 GEOTRONICS CORPORATION
 FOR
 SOCAL MINERALS
 APRIL, 1975

LEGEND

APPARENT RESISTIVITIES IN OHM-METERS
 CONTOUR INTERVALS:
 HORIZONTAL SCALE: 1" = 2000'
 HORIZONTAL/VERTICAL RATIO: 0.61

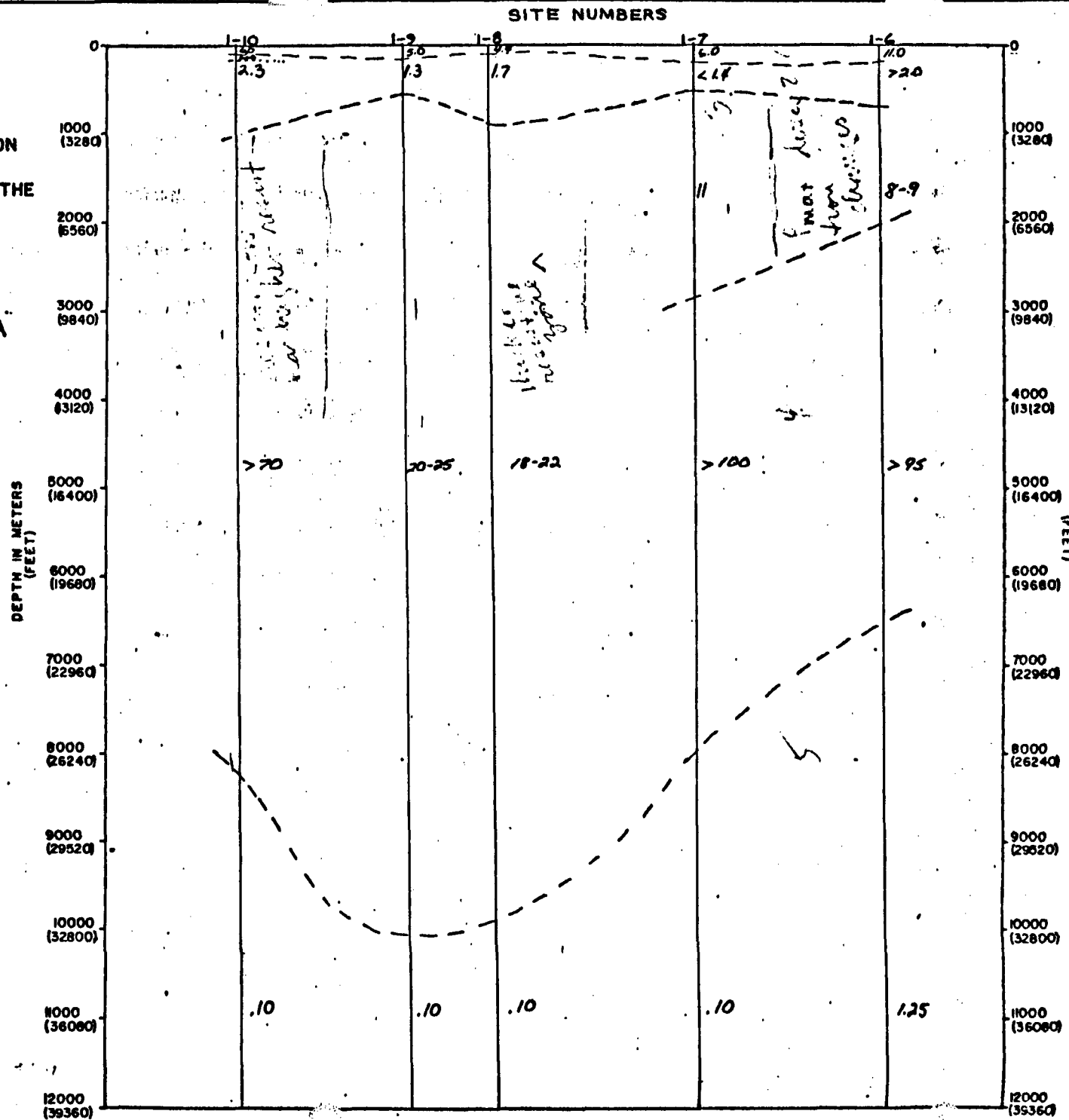


Figure III-5 OPTMOD Depth to Top Surface of Deep conductor
 (in meters) AND Maximum Impedance Direction at that Depth
 (Text. & pro-1271 sediment)

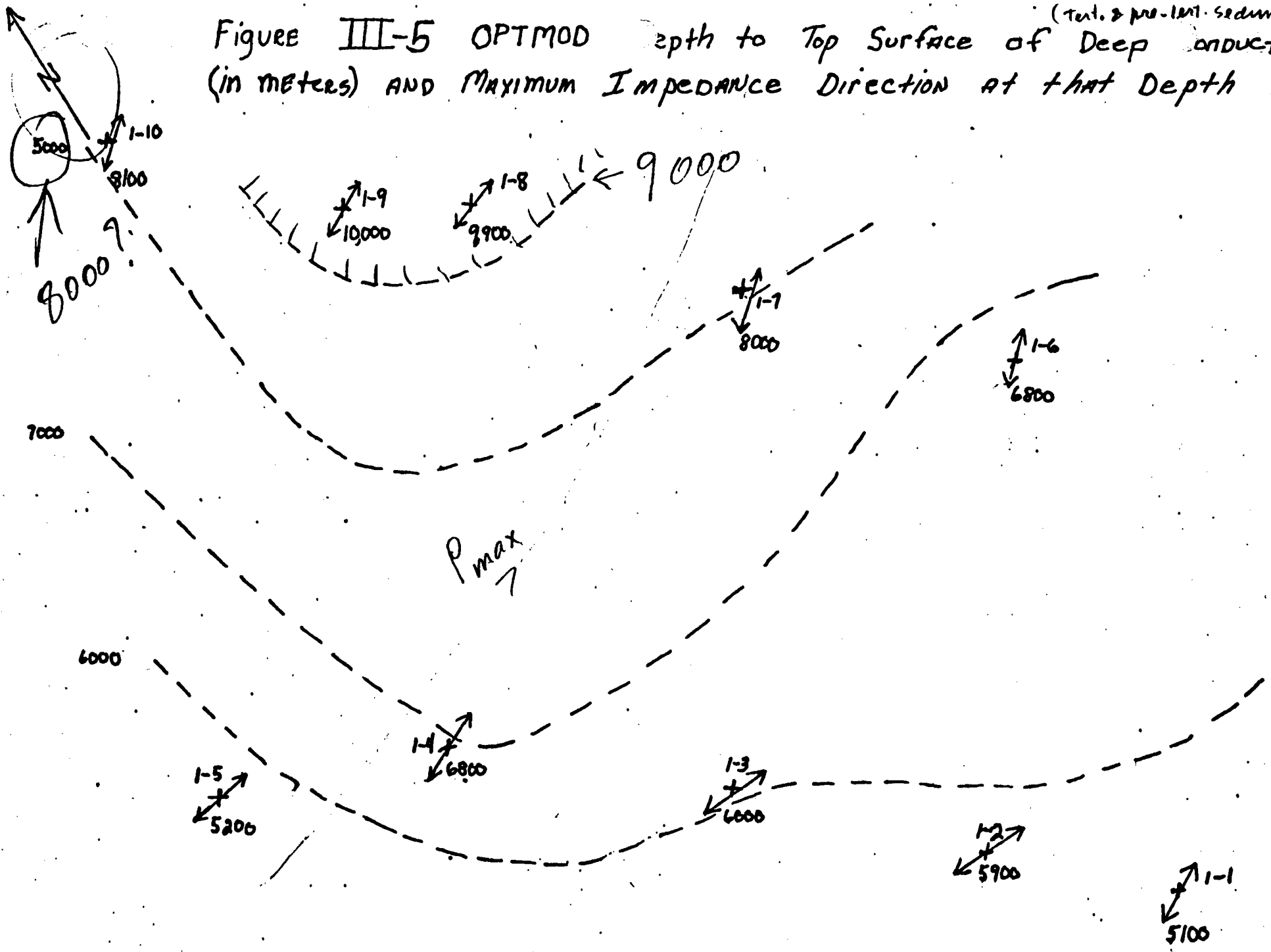


Figure III-6 OPTMOD depth to Resistive "Basemen" (ie, base of aquifer w/ hot water) (in meters) AND Maximum Impedance Direction AT 3 Kilometers.

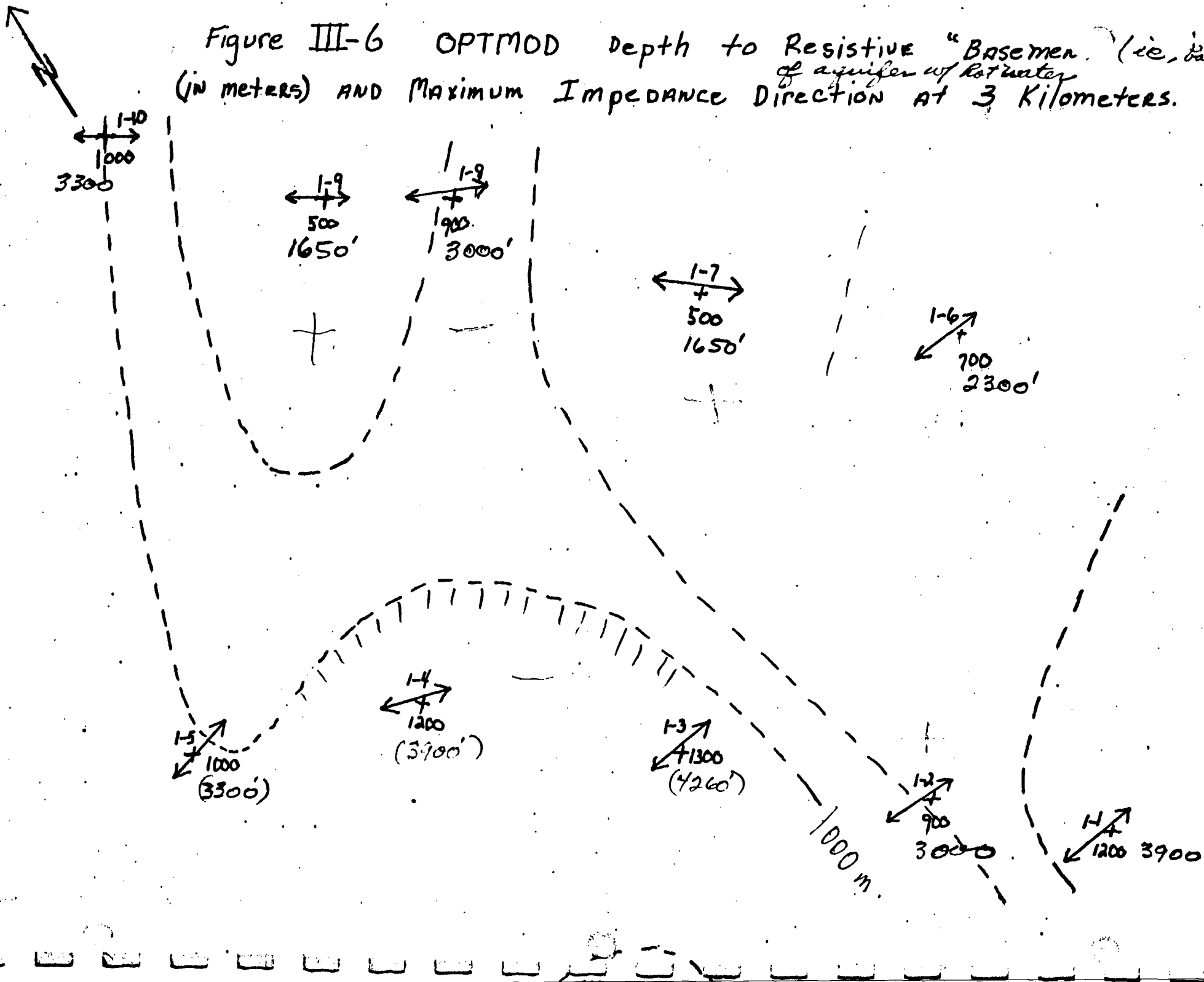
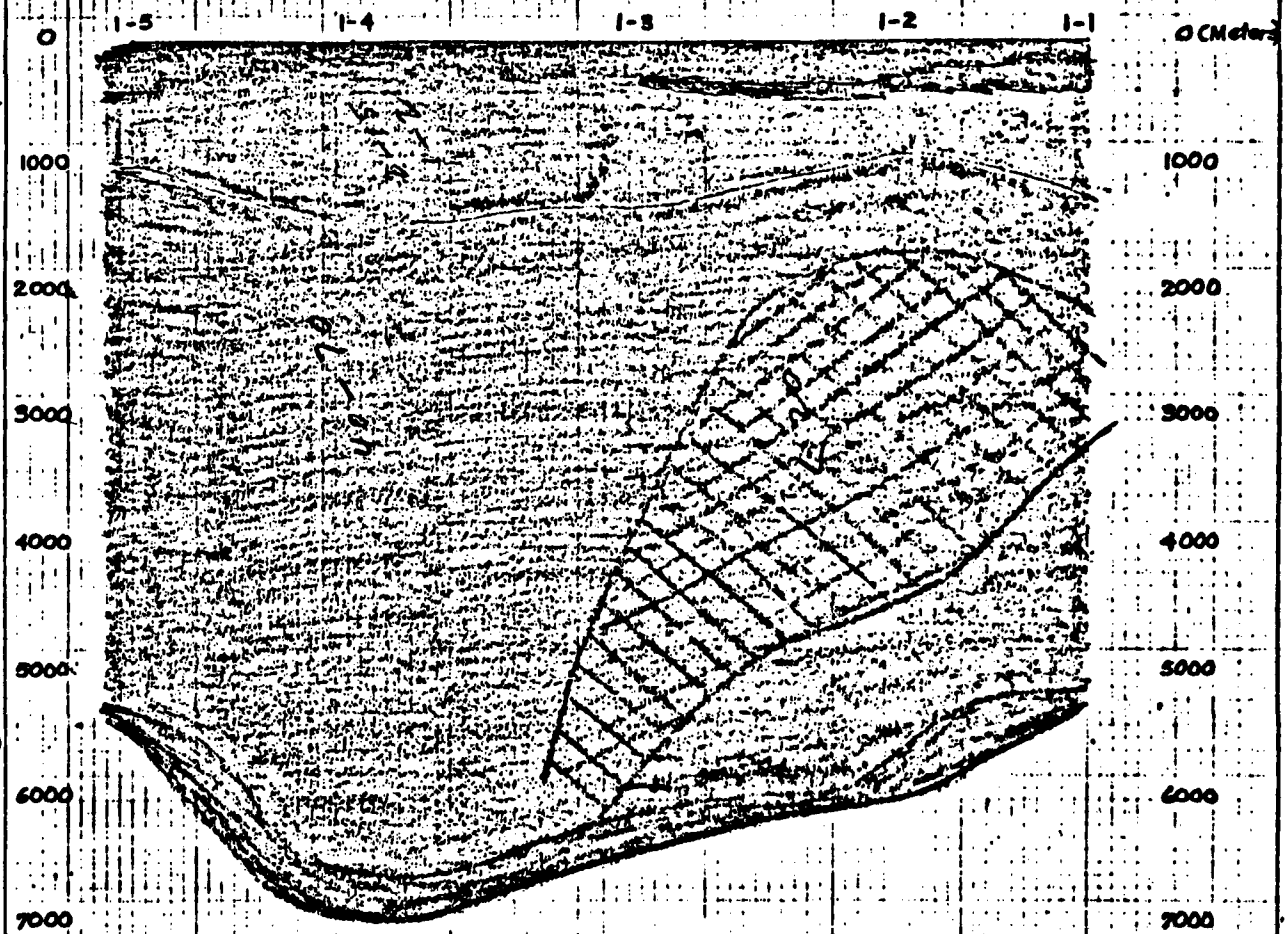


FIGURE IV-14 - LINE A-ALTERATION MODEL

PROPOSED LITHOLOGIC UNIT	PROBABLE RESISTIVITY RANGE - OHM-METERS
Upper Lahontan Valley Group (Schoof?)	5-15
Lower Lahontan Valley Group (Wemaha?)	2-15 (Unsaturated) 1-2 (Saturated)
Volcanics (Age Unspecified)	70+ (Probably Quite Variable)
Truckee Formation T A B C	1-2 (Saturated)
Tertiary (Rhyolites And Volcanics)	A) 40-70 (Unaltered) B) 20-25 (Moderate Alteration) C) <20 (Intense Alteration)
Magma Chamber	<1 (Probable)



Horizontal Scale: 1" = 2000'
Horizontal/Vertical Ratio: 0.61

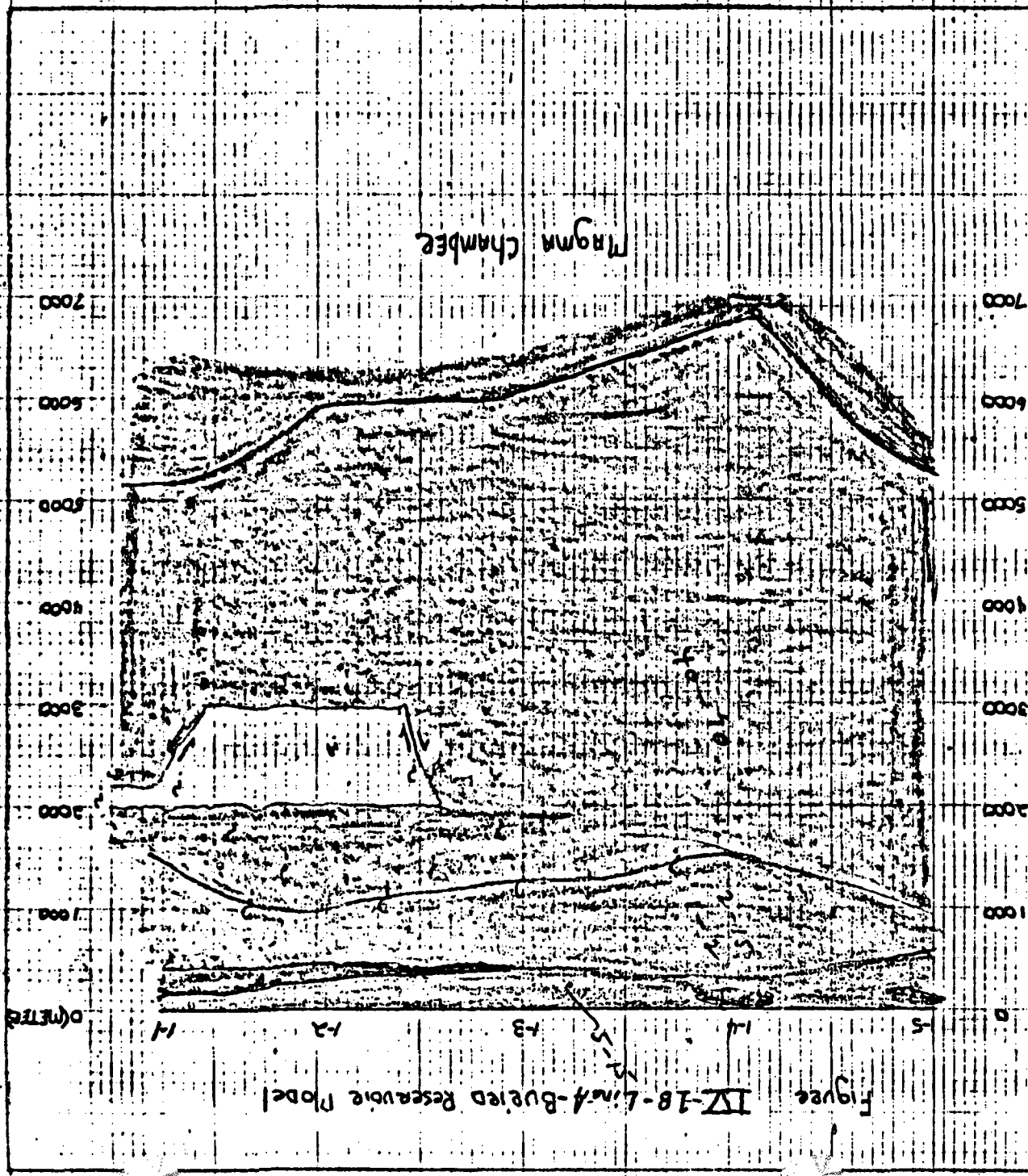


Figure IV-18-Linch-Buied Reservoir Model

Horizontal Scale: 1" = 2000'
 Horizontal/Vertical Ratio: 0.61

proposed Lithologic Unit
 range, John-meters
 5-15

Usee (hounan
 valley group (Gard?)

Lower Linton
 Valley group (Wymh?)

Volcanics
 (Age unspecified)
 70% probably
 quite variable

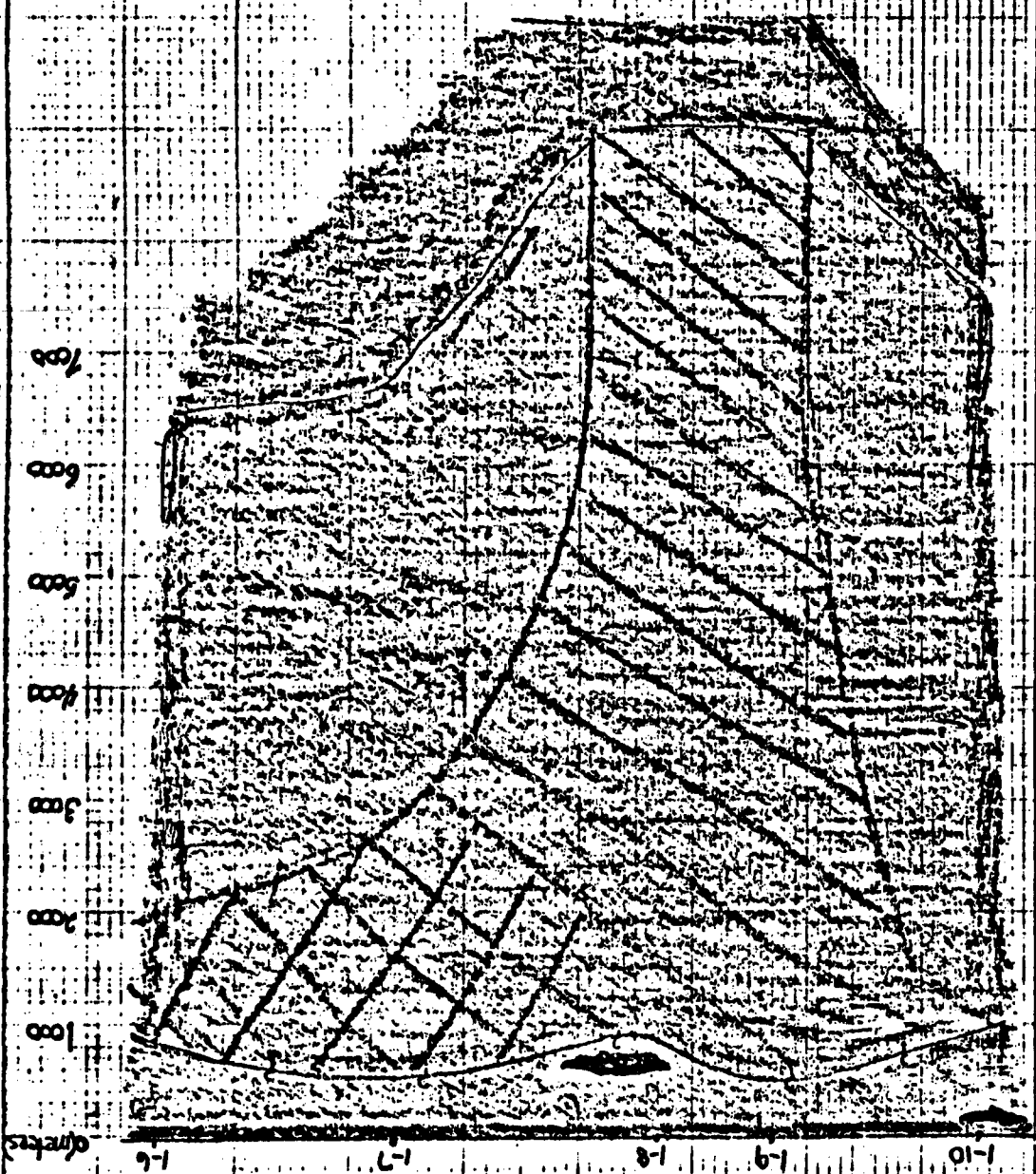
1-2 (unstratified)
 2-15 (unstratified)

Teuclce formation?
 1-2 (stratified)

H) 40-70' (unstratified)
 B) 20-25' (moderate)
 (alteration)
 C) < 20' (intense)
 (alteration)

Tertiary (Rhyolites
 and volcanics)

Magma Chamber
 < 1 (probable)



Magma Chamber

Figure IV-2 - Line B

probable restivity range, ohm-meters

Lithologic Unit

5-15

Upper Lihouan Valley-group (Seno?)

2-5 (unsaturated)

Lower Lihouan Valley-group (Wymah?)

1-2 (saturated)

Volcanics not, probably quite variable (Age unspecified)

1-2 (saturated)

Tucsee formation?

A) 40-70 (unsaturated) B) 20-25 (moderate alteration) C) 250 (intense alteration)

Tertiary (Rhyolites and volcanics)

Magma Chamber

< 1 (probable)

Horizontal Scale: 1" = 2000'

Horizontal/Vertical Ratio: 0.61